Environmental Measurements in the Beaufort Sea, Spring 1992

by T. Wen, F. Karig, and W. Felton

Technical Report
APL-UW TR9213
September 1992

Applied Physics Laboratory University of Washington
1013 NE 40th Street Seattle, Washington 98105-6698

SPAWARSYSCOM Contract N00039-91-C-0072

Acknowledgments

The research presented in this report was sponsored by the organizations participating in the ICEX 1-92 APLIS ice camp. Funding was provided by the Naval Sea Systems Command, Naval Undersea Warfare Center (New London) and the Naval Research Laboratory (Stennis Space Center). The authors express their sincere thanks to John Newton of Polar Associates Inc, Santa Barbara, California, for his help in interpreting the CTD data, to Robert Anderson of the Arctic Submarine Laboratory, Naval Undersea Warfare Center, for contributing side-scan records of the under-ice surface, and to Diane Bentley of the Arctic Submarine Laboratory for contributing ice core data.

The purpose of this report is simply to present the environmental data obtained during the camp. The data analysis is very limited. All the data presented here are stored in digital format and are available for further analysis. Requests for data should be forwarded to

Director
Applied Physics Laboratory
1013 N.E. 40th Street
Seattle, WA 98105-6698

TABLE OF CONTENTS

LIST OF FIGURES

LIST OF TABLES

ABSTRACT

This report presents environmental and underwater ambient noise data obtained by the Applied Physics Laboratory of the University of Washington (APL-UW) and the Arctic Submarine Laboratory of the Naval Undersea Warfare Center (ASL/NUWC) at APLIS 92, an ice camp established in the Beaufort Sea in Spring 1992 to support Navy-sponsored tests and research during ICEX 1-92. The purpose of this report is to provide field data to ice camp participants, so data analysis is limited here. The data were collected to document the meteorological and oceanographic conditions that existed during camp activities. The main data sets are weather, floe drift, STD profiles, currents, ice properties, and underwater ambient noise.

I. INTRODUCTION

This report presents environmental data taken in the spring of 1992 at APLIS 92 in the Beaufort Sea. The ice camp was established and maintained by personnel from the Applied Physics Laboratory, University of Washington, to support Navy-sponsored research and test activities conducted by the organizations participating in ICEX 1-92. The environmental data — weather, floe drift, STD profiles, currents, ice properties, and underwater noise — were gathered primarily by APL-UW personnel and are intended to support the analysis of experimental data obtained by ICEX 1-92 participants. In addition to the APL data, this report contains data on the physical properties of the ice determined from ice cores obtained by ASL/NUWC.

The ice camp was established on a multiyear floe approximately 350 km north of Prudhoe Bay, Alaska (see Figure 1). The floe (2 km × 2 km) was selected on 10 March after a 2-day search. Buildings were set up, and hydroholes were melted out for deploying instruments and sensors. Collection of environmental data started on 21 March and lasted until 4 April, when the tests and research of the APLIS portion of ICEX 1-92 were completed. Most personnel were evacuated on 6 April, and the camp was turned over to the Naval Research Laboratory (Stennis Space Center Detachment) and renamed GATOR for subsequent tests.

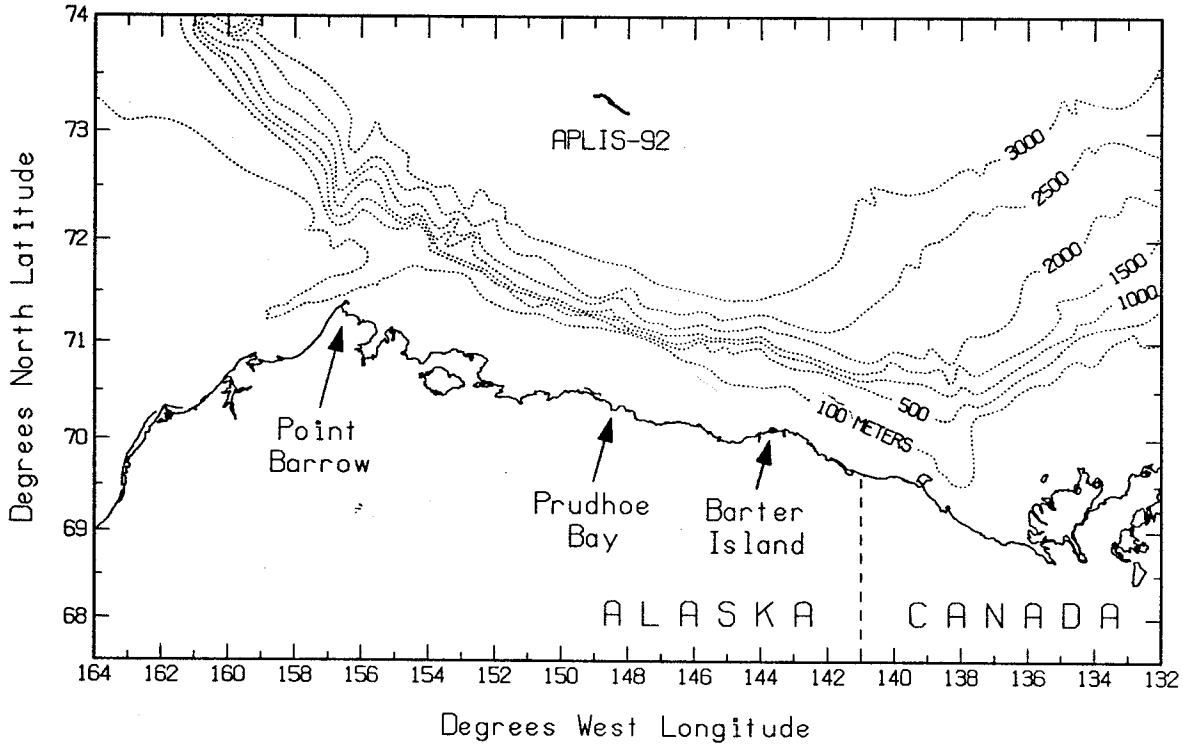

Figure 1. Position of APLIS 92.

The camp was located at the edge of the floe next to a refrozen lead. The thicker multiyear ice provided support for buildings, and the flat lead, with some leveling of the snow cover, made a good runway. There were active leads on three sides of the floe and the far side of the refrozen lead. A large, old pressure ridge approximately 7 m high (called the ice mine) provided nearly salt-free ice for making potable water.

Air temperature and pressure and wind speed and direction were recorded automatically at 10-minute intervals. The weather was generally calm, except for a 36-hour period when high winds built up snow drifts in and around the camp. Precipitation in the form of light snow was frequent, an unusual occurrence at that time of year.

CTD casts were made often to determine the properties of the water column down to 350 m. Sound speed profiles were then derived from the measured temperature and salinity and were used to predict the real-time performance of acoustic equipment.

Sources of underwater ambient noise included thermal cracking of the ice, ridging, wind-generated waves at open leads, and marine organisms. Only a few measurements of opportunity were made, some coincident with acoustic tests. The ambient noise data are useful in interpreting the acoustic data.

Some data presented here are tagged "L" for local time, while others are tagged "UTC" for Universal Coordinated Time. Local time = UTC – 9 hours.

Because the purpose of this report is simply to present environmental data from the camp, analysis is very limited. All data presented here are stored in digital format and are available for further analysis.

II. THE FLOE

Selection of an ice floe suitable for a camp was based on several requirements. First, we needed a refrozen lead long enough and thick enough (at least 1.2 m) to serve as a runway, since transportation to and from the camp depended entirely on aircraft. Second, the floe had to be over water with good acoustic propagation characteristics, i.e., a minimal shadow zone and the longest possible propagation range. This required that the camp be located north of 72° latitude, where the warm subsurface intrusion (a remnant of the summer Alaskan Coastal Current that produces complex sound speed structure) is less pronounced and the deeper water helps reduce acoustic interference from the bottom. The third criterion was that the initial site had to be far enough east to allow for the westerly drift that would (historically) occur during the period of camp occupancy. As in previous years, the first criterion usually narrowed down the usable floes to those north of 72°N so the second criterion was fulfilled automatically. This year, a suitable floe was found at 73.12°N and 147.47°W after 5 hours of air search. Another 5 hours were spent the next day searching unsuccessfully for a bigger floe.

The camp was established at the edge of the floe, next to a refrozen lead (see Figure 2). The floe was surrounded by active leads. Ice in the floe was 2.5 m thick with a snow cover of 10 cm. Ice in the refrozen lead was 2.1 m thick with a snow cover of 5 cm. A 420-m runway was constructed on the lead by leveling off the undulating snow cover with a snowmobile-towed grader. Later, a second, longer runway was built closer to the camp.

Some of the ICEX 1-92 tests involved a submarine. To track the submarine during these tests, we set up an underwater tracking range with the imaginary XY coordinate system shown in Figure 3. The origin of the coordinate system was a 0.91-m-diameter hydrohole (marked "O" on the figure) beneath the control building. The true bearing of the +Y axis was, on average, 72°, as determined by sighting the sun. The magnetic variation at the general locale was 32.2°, calculated using GEOMAG, a PC program published by the Naval Oceanographic Office, Stennis Space Center, based on the World Magnetic Model for Epoch 1990 (WMM-90).

Figure 2. Ice Camp APLIS 92.

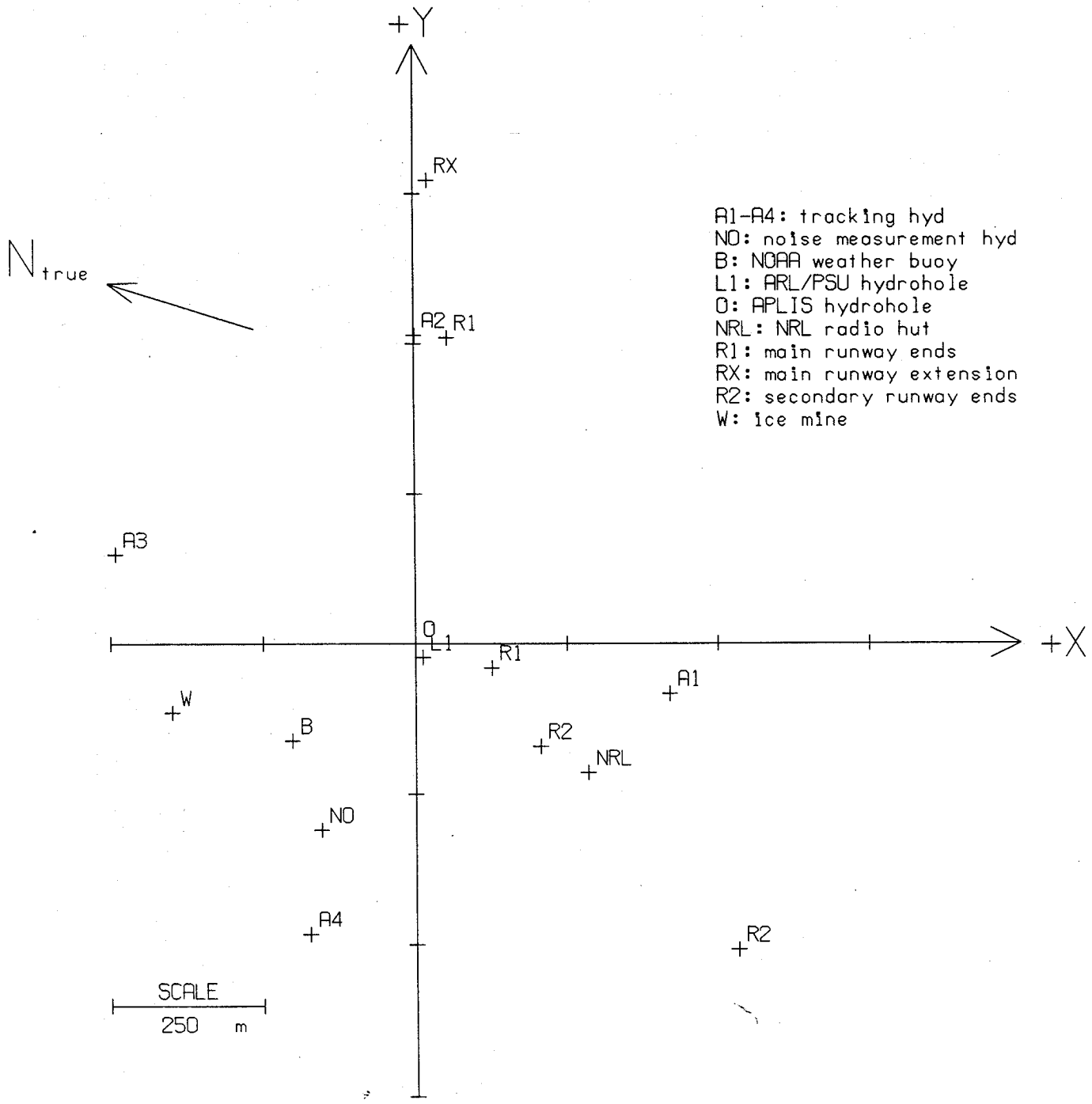

Figure 3. Tracking range X-Y coordinate system and locations of interest.

A modified Klein Model 595 side-scan sonar was deployed at 61-m depth through the hydrohole under the control building to profile the underside of the ice. The modification consisted of placing three regular transducers end-to-end to produce a narrow (0.3°) beam. Because of its length, the transducer head had to be lowered through the hole vertically and then pivoted to a horizontal position for scanning. The sonar was rotated through 370° while pinging at 100 kHz to obtain a gray-scale map/sonogram of the under-ice surface around the camp (Figure 4). The refrozen lead, actually straight, appears curved in the sonargram because of the plotting method. The underside of the lead was almost flat, as shown by the nearly constant intensity of the sonogram. (The sonar may have been unable to detect small undulations, approximately 4 cm in amplitude and 9 m in wavelength, that typically exist under flat ice because of uneven snow cover on top.[1]) Some small features of unknown draft are seen to the left of the keel marked B in the middle of the frozen lead. Most of the keels of the multiyear floe (left side and bottom of Figure 4) were well rounded, as shown by the gradual changes in intensity. On the other hand, the area indicated by the letter C on the neighboring floe contained many first-year keels composed of uneroded blocks which produced a higher contrast in the scanned image. The features marked A are bubble trails and pools left by divers. The large keel marked B was easily identifiable topside by a corresponding sail 2 m in height. Based on the length of the keel's shadow, in white in the sonogram, its draft is estimated at about 10 m.

Figure 5 is a polar display of the under-ice surface reconstructed from another side scan. The shading was inverted during processing so the white areas represent features with high reflections. The maximum range of this scan was 400 m. The under-ice features generally have corresponding surface counterparts, as shown by the aerial photographs of the camp in Figure 6.

In addition to the side-scan profiles, the submarine profiled the under-ice surface in the area of the camp with an upward-looking sonar, going back and forth along the X and Y directions. Because of an initial malfunction of the profiling sonar and later deployment of deep transducer arrays in the vicinity of the camp, submarine profiling data within a 400-m radius of the camp are sparse. The location of one such transect, at 120-m depth, is shown in Figure 5. Figure 7 shows the profile obtained. The deepest keel in this figure extends to 12 m.

Figure 4. A 360° side-scan record of the under-ice surface. The maximum range is 300 m. (Courtesy of Robert Anderson of ASL/NUWC)

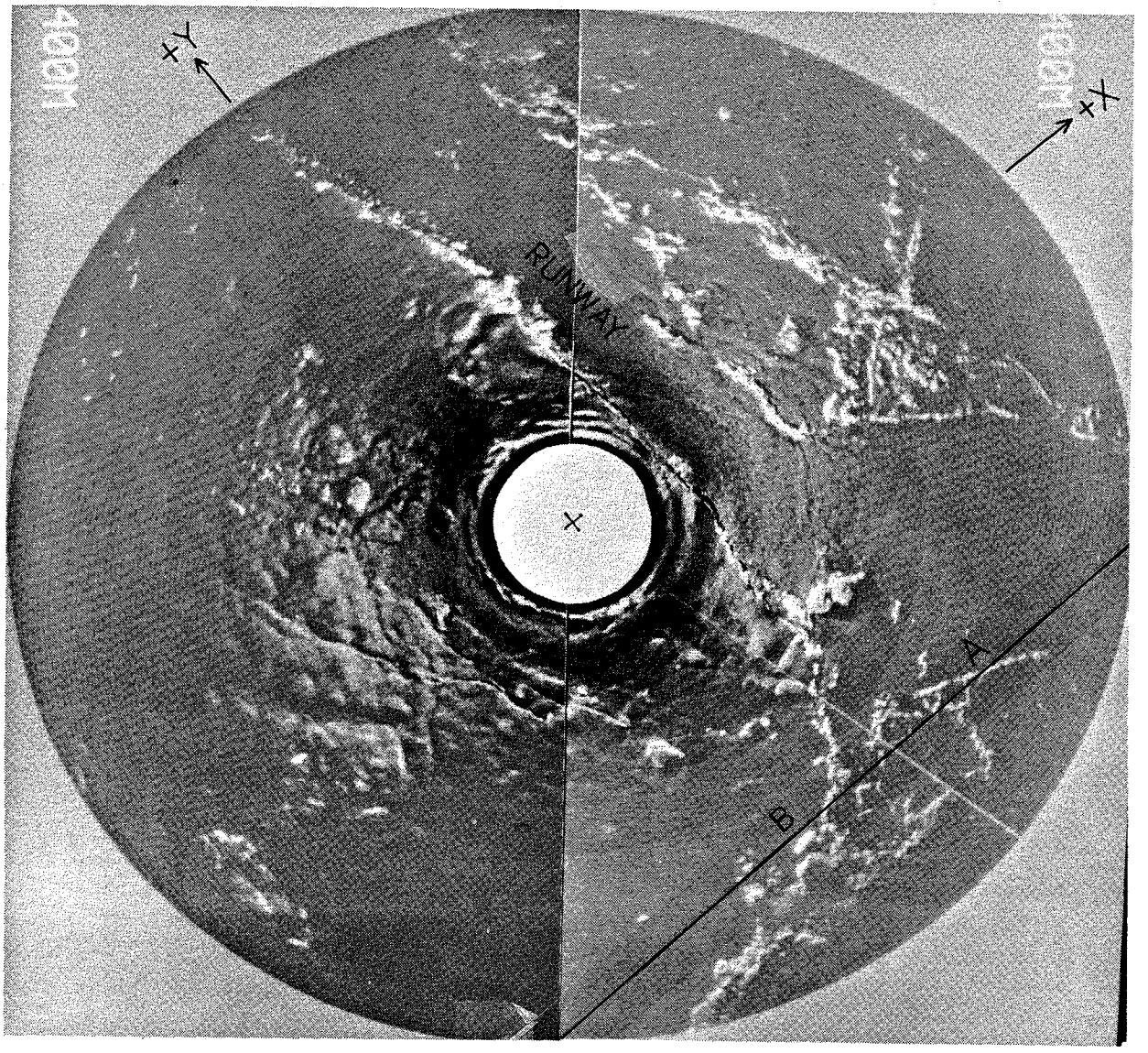

Figure 5. True polar representation of side-scan image. The maximum range is 400 m. Line indicates submarine profiling track. (Courtesy of Robert Anderson, ASL/NUWC)

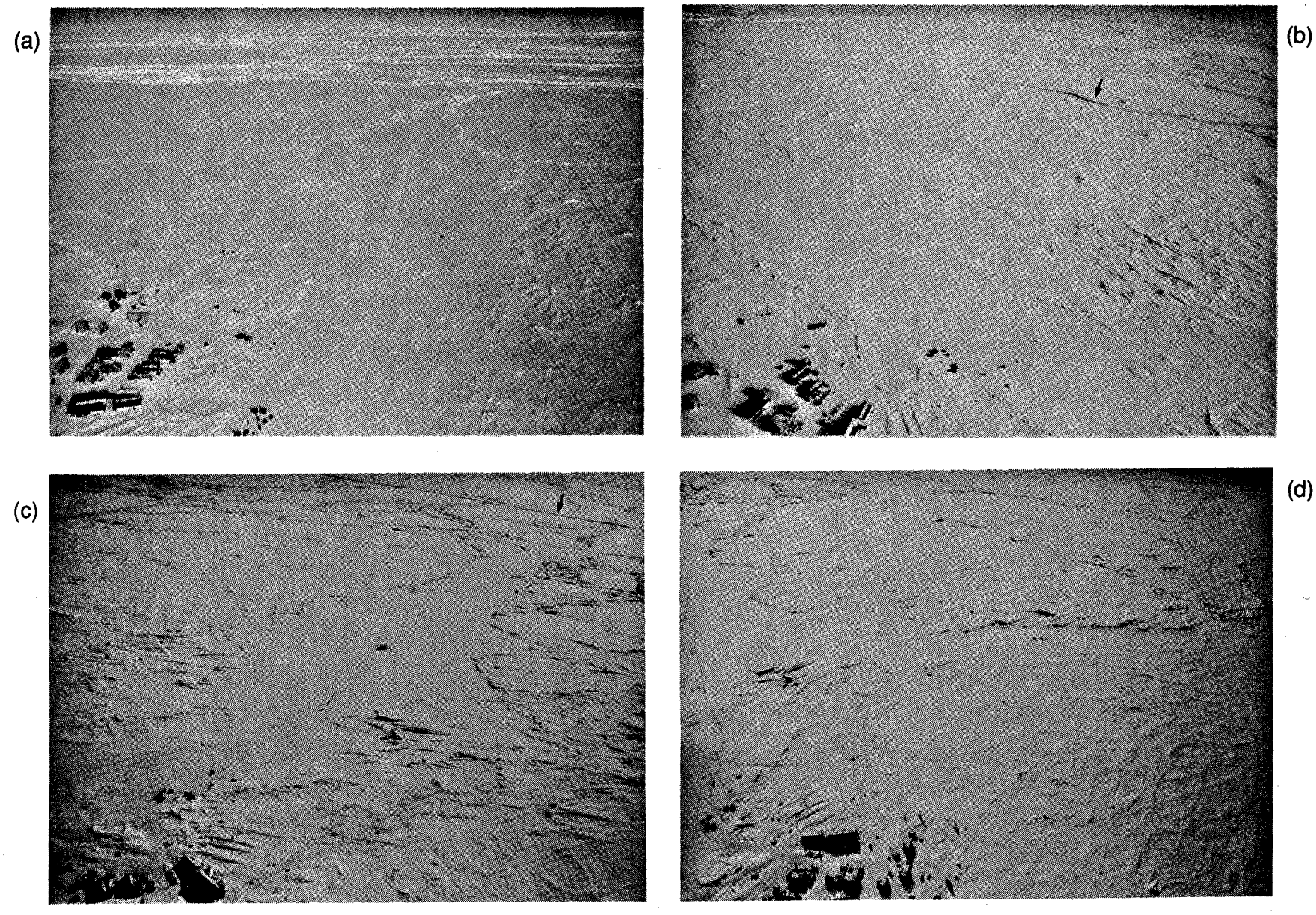

Figure 6. Views of the ice floe and its surroundings, taken clockwise at ~60° intervals from the Y axis. (a) shows the main runway, (c) the old runway, and (e) the drinking water ''ice mine'' (center). Active leads (arrows) can be seen in (b),(c),(e), and (f).

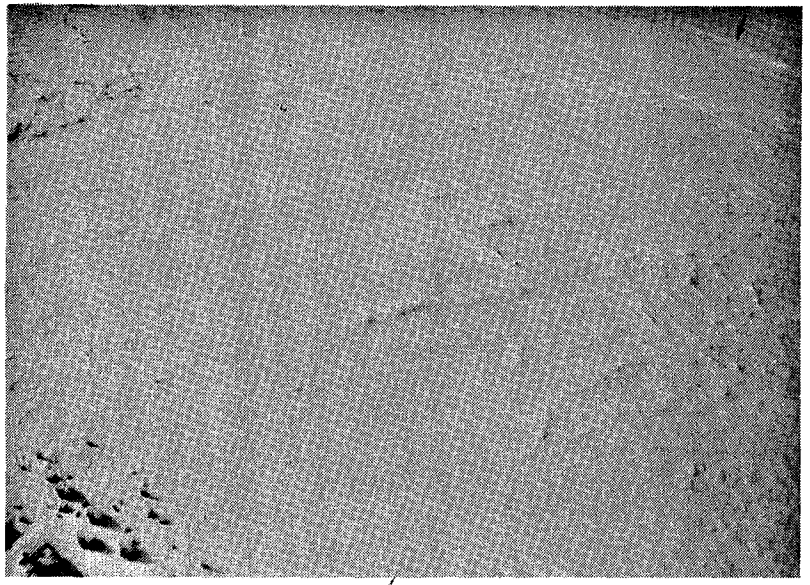

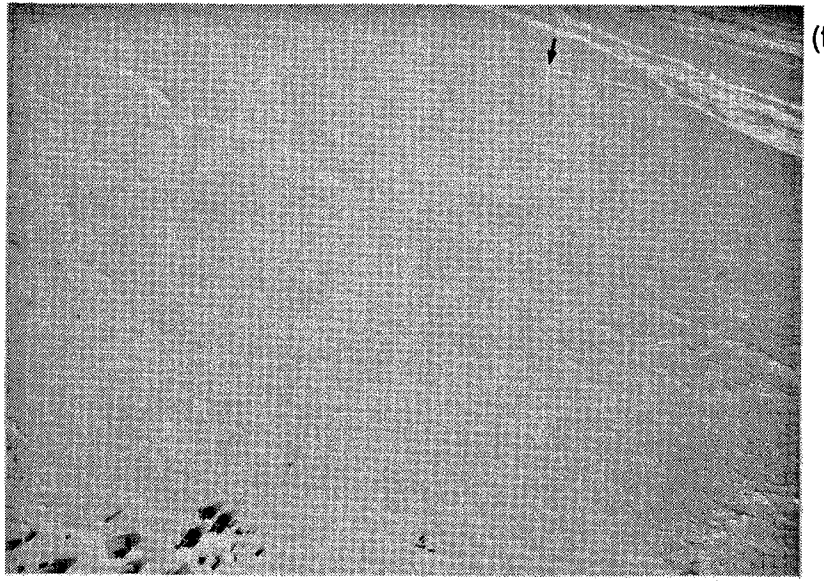

Figure 6, cont.

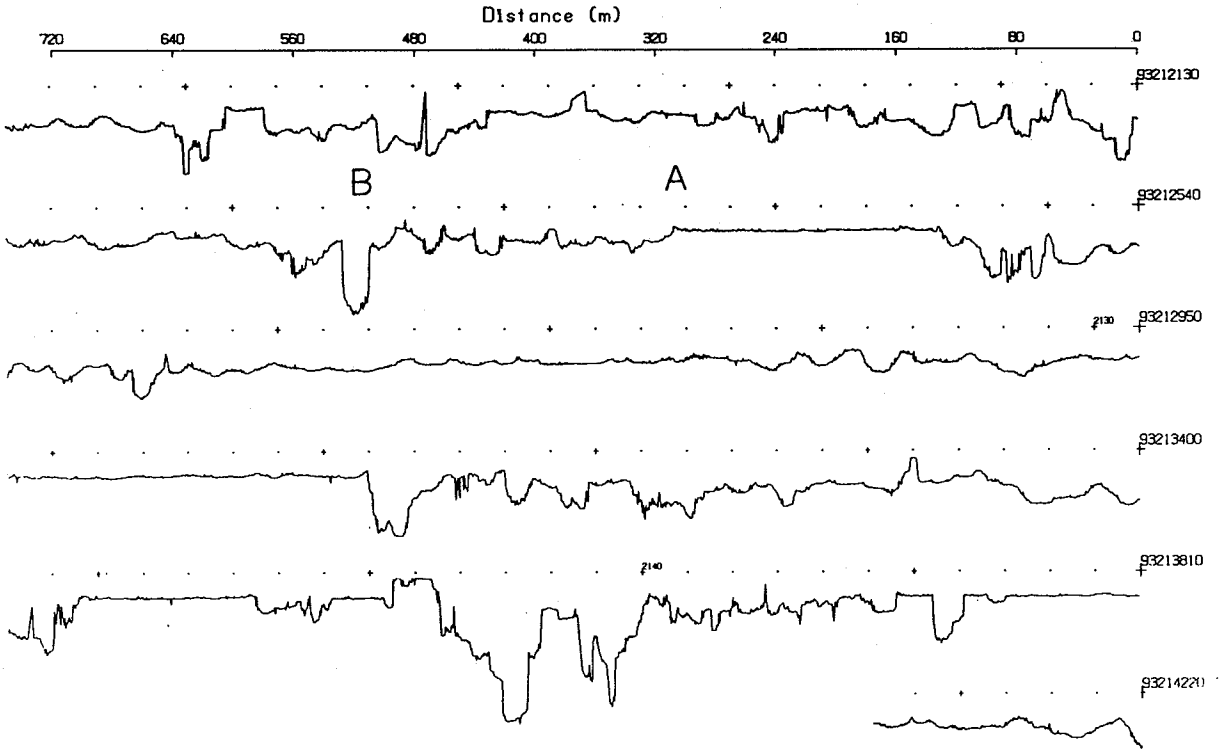

Figure 7. Sample under-ice profile. The dotted line marks 0 depth, and the vertical scale is 10 m between the dotted lines. Numbers at right are time-of-day in ddhhmmss format. Profile is continuous and reads from right to left and top to bottom. Letters A (edge of refrozen lead) and B (keel) correspond to the features marked in Figure 5.

III. FLOE MOVEMENT

The camp's position was determined using a Global Positioning System (GPS) receiver (Kinemetrics/Truetime GPS-DC) and displayed and logged on an HP85 computer via a GPIB bus. GPS fixes were read from the receiver every 30 minutes and stored on a tape cartridge. Figure 8 shows the drift track of the floe. Speed and direction of the drift are plotted in Figure 9 along with wind speed and direction (sense reversed); the plots show good correlation between the wind and drift. The offset in the two directions was caused by the Coriolis force. A listing of the floe's position and its drift speed and direction is given in Appendix A. At least four satellites were in view 99% of the time. Consequently, the geometric dilution of precision, an indicator of tracking precision, was usually 3 or less. Our GPS receiver also provided UTC signals accurate to within microseconds, which was crucial to the precision of our underwater tracking range.

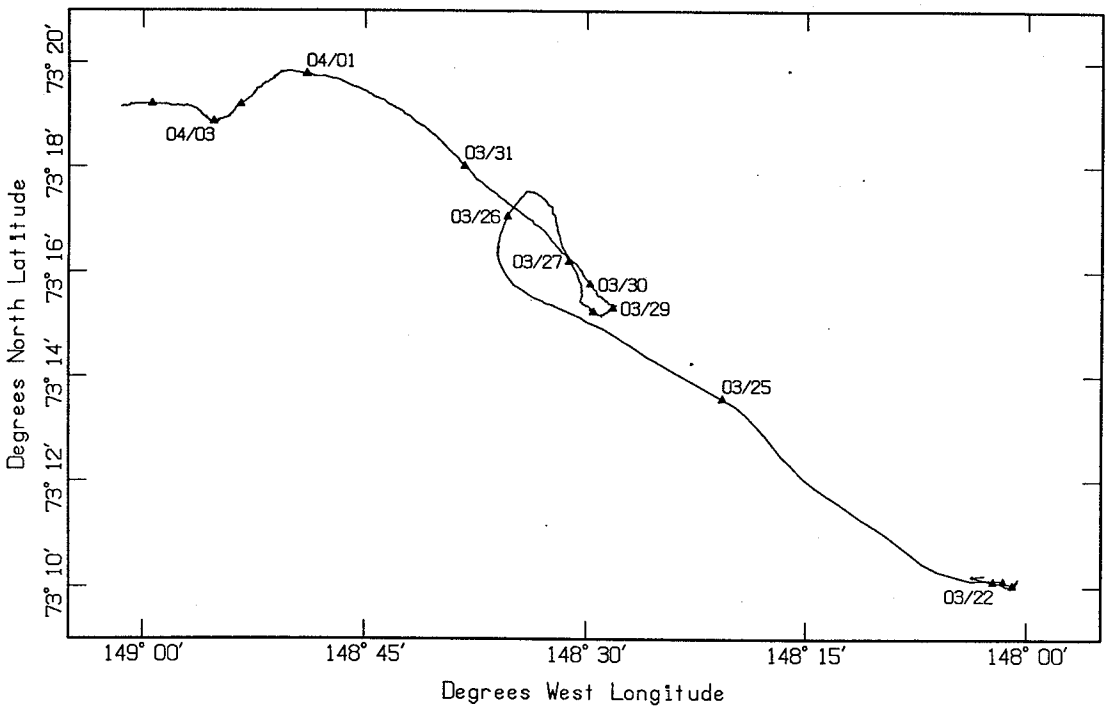

Figure 8. Drift track of the APLIS 92 floe. Net distance traversed was 10 km.

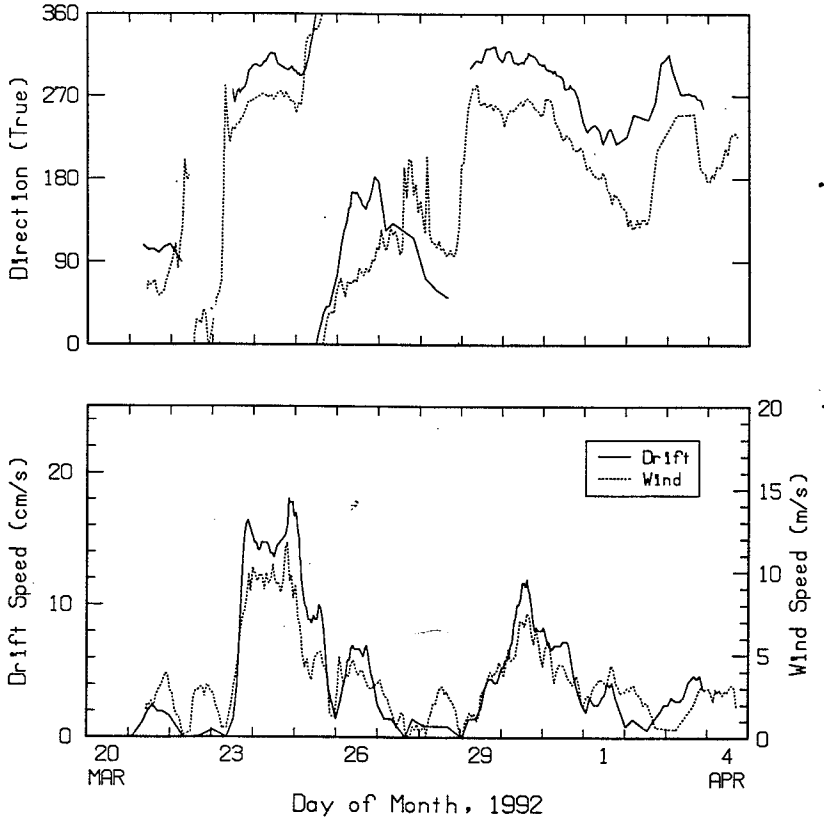

Figure 9.

Comparison of speed and direction of wind with speed and direction of floe drift.

The rotation of the floe was determined by measuring the true bearing of the +Y axis of the XY coordinate system. To obtain the true bearing of the +Y axis, the grid bearing of the sun was first read with a transit positioned atop the control building over the (0,0) hydrohole. Then the true bearing of the sun at the time of the transit sighting was calculated using a PC program "ICE" (Interactive Computer Ephemeris) published by the Naval Observatory, Washington, D.C. The difference between the grid and true bearings of the sun was considered the true bearing of the +Y axis. Because the sky was frequently overcast, only a few sun sightings were made, but they showed little rotation. The +Y axis of the coordinate system remained at around 72° True for the camp duration (see Table 1).

Table 1. Bearing of +Y axis of underwater tracking range.

Year Day	Time, UTC (hhmmss)	Latitude (N)	Longitude (W)	Grid Bearing of Sun	Azimuth of Sun	True Bearing of +Y Axis
85	003900	73°14.14′	148°24.37′	147.47	221.6	074.13
86	231037	73°16.25′	148°31.30′	126.75	198.8	072.05
86	231245			127.33	199.3	071.97
87	201446	73°15.30′	148°28.60′	080.29	152.5	072.21
87	201851			081.37	153.6	072.23
89	015211	73°15.34′	148°28.06′	168.43	240.3	071.87
89	015404			168.92	240.7	071.78
89	200336	73°15.66′	148°29.01′	077.38	149.6	072.22
89	200614			078.07	150.3	072.23
90	215001	73°17.70′	148°37.10′	105.05	177.7	072.65
90	215223			105.69	178.2	072.51
95	191851	73°18.85′	149°06.25′	065.70	137.5	071.80
95	192115			066.33	138.1	071.77

IV. WEATHER

A Weatherpak 100 weather station, manufactured by Coastal Climate Co. (Seattle), was mounted on a telescoping mast at a height of 8 m. The mast was guy-wired so that it would not sway in high winds and cause erroneous wind speed readings. Air temperature, atmospheric pressure, and wind speed and direction were recorded at regular intervals. The accuracy of the meteorological measurements is 0.5 m/s for wind speed, 2° for wind direction, 0.5 mbar for atmospheric pressure, and 0.2°C for temperature.

A laptop PC in the control building was used to control the weather station and to display meteorological data. Commands and data were sent over an RS-232C link. The Weatherpak was programmed to average the weather parameters for 5 seconds at 10-minute sample intervals. Sampled data were stored in the Weatherpak's internal memory and also downloaded to the PC for display. Weather parameters could also be read at any time by pressing a programmed menu key on the PC. Once a day, data collected in the previous 24 hours were downloaded to the PC and stored on floppy disk. Data for 3 April were lost because of a malfunction during downloading. Half-hour averages from a NOAA weather buoy deployed at APLIS 92 were used to fill the gap. The combined data are presented in Figure 10.

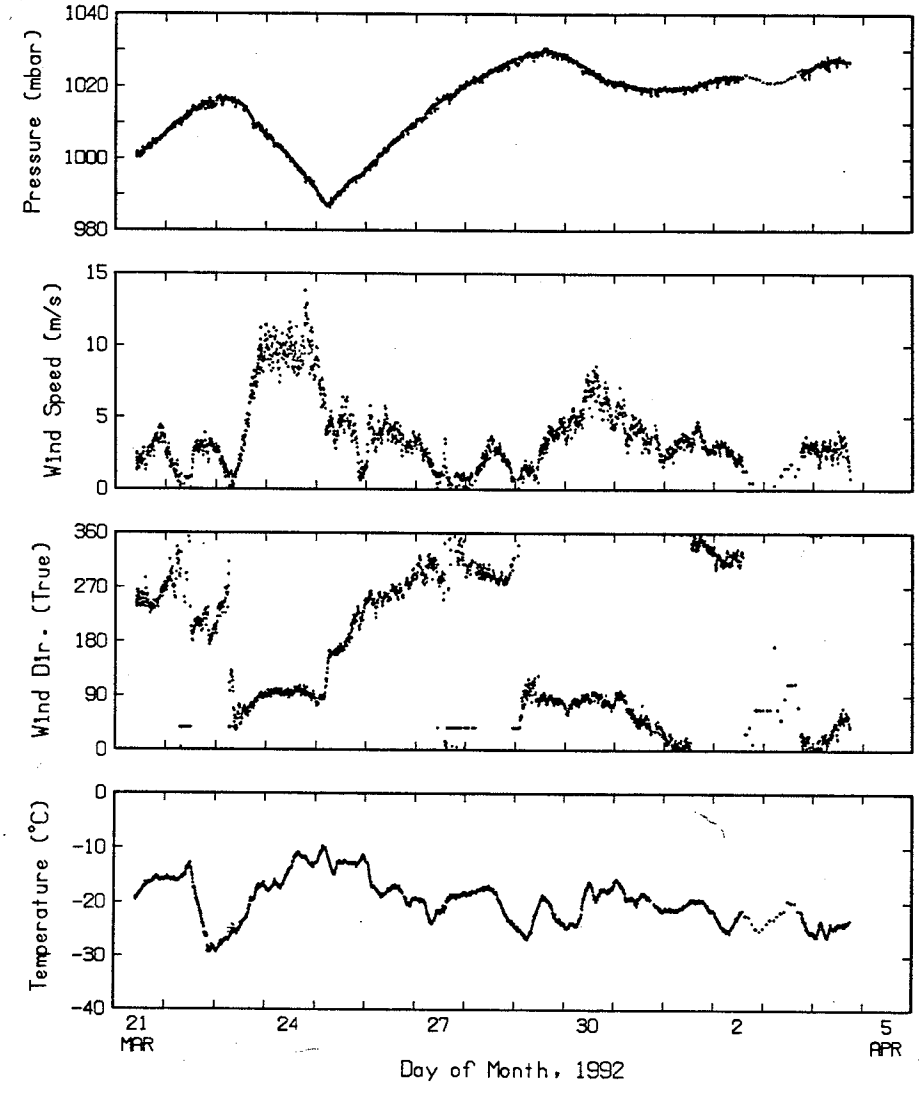

Figure 10. Meteorological record of APLIS 92.

The temperature data showed minor or no diurnal variations, compared with a historical variation of about 8° C in the spring.[1–4] Winds above 5 m/s were mostly from the east while lighter winds were from the west. The sky was often overcast. Light snow was frequent, probably owing to evaporation of water through the active leads around the floe.

V. CTD MEASUREMENTS

CTD casts were made several times daily to obtain the temperature and salinity properties of the water column. The components of the CTD profiler were a solid-state data logger (Sea-Bird), a thermistor (Sea-Bird), a conductivity cell (Sea-Bird), and a pressure sensor (Paroscientific Digiquartz). The profiler was attached to the end of a 6.4-mm-diameter nylon line and deployed with an ac-powered winch. To ensure adequate flushing of seawater through the conductivity cell, the profiler was lowered at a rate of ~1.3 m/s, the maximum speed of the winch motor. Because the sampling rate of the logger is 8 Hz, the water column was sampled at ~16 cm intervals, resulting in high-resolution temperature and salinity profiles. The casts were generally to only ~350 m or less because water properties at greater depths do not vary significantly from day to day. After each cast, the raw data were read out of the logger via an RS-232C link to an HP Integral Personal Computer for processing and plotting. The raw data were first converted to temperature, conductivity, and depth using sensor calibration constants. UNESCO '83 algorithms[5] were then used to compute salinity, sound speed, and σ_t (the density of the *in situ* water with the pressure reduced to atmospheric). The conductivity cells and the depth sensors were last calibrated a year before the field trip, and the thermistors 4 months before. Because these sensors are very stable according to the historical calibration data, we used the last calibration constants, which we consider accurate for all but the conductivity cells. For the measured properties, we suggest an accuracy of 0.002°C for temperature, 0.005 mS/cm for conductivity, and 0.1 m for depth; the computed properties should have an accuracy of 0.005 ppt for salinity, 0.008 m/s for sound speed, and 0.005 kg/m^3 for σ_t.

Table 2 lists the casts made at the camp. The STD plots from all casts are given in Appendix B. Figure 11 shows the STD profiles from a deep cast to 750 m. The corresponding temperature-salinity (T-S) diagram is shown in Figure 12. The well-mixed upper layer was 40 m deep, although it has extended as deep as 60 m in other years. An intrusion of warmer water from the Bering Sea lies under the mixed layer, creating a thermocline and a halocline (and therefore a pycnocline) between the two layers. This intrusion typically extends to a depth of 100 m. This year, however, we encountered more intrusions which varied from 100–200 m depth (see Figure 13). Below ~200 m (Figure 11) is Atlantic Water with a temperature maximum of 0.5°C. Between 260 and 380 m was a temperature staircase (Figure 14) with an average step change of ~2 m and ~0.007°C.

Table 2. CTD casts taken at APLIS 92.

Date	Time (UTC)	Cast No.	Latitude	Longitude	Comments
03-21-92	1236	01	73°10.1´N	148°02.6´W	
03-21-92	2102	02	73°10.0´N	148°01.3´W	
03-22-92	0657	03	73°10.0´N	148°01.1´W	Deep cast to 750 m
03-22-92	1232	04	73°10.0´N	148°00.9´W	
03-22-92	1410	05	73°10.0´N	148°00.8´W	
		06			Thermistor comparison test
03-22-92	2052	07			Aborted
03-22-92	2134	08	73°10.0´N	148°00.7´W	
03-23-92	0645	09	73°10.1´N	148°00.8´W	
03-23-92	1537	10	73°10.1´N	148°01.9´W	
03-23-92	2011	11	73°10.3´N	148°06.4´W	
03-24-92	0651	12	73°12.1´N	148°15.3´W	
03-24-92	1240	13	73°13.2´N	148°19.0´W	
03-24-92	2146	14	73°14.6´N	148°27.4´W	
03-25-92	0808	15	73°15.9´N	148°35.5´W	
03-25-92	1008	16	73°16.2´N	148°36.0´W	
03-25-92	1101	17	73°16.4´N	148°35.9´W	Deep cast to 610 m
03-25-92	1825	18	73°17.5´N	148°34.2´W	Deep cast to 600 m
03-26-92	0633	19	73°17.1´N	148°32.3´W	
03-26-99	1349	20	73°15.8´N	148°30.4´W	Temperature time series
03-26-92	2254	21	73°15.4´N	148°30.3´W	
03-27-92	0701	22	73°15.2´N	148°29.7´W	
03-27-92	1354	23	73°15.2´N	148°29.5´W	
03-27-92	1623	24	73°15.2´N	148°29.5´W	
03-27-92	2007	25	73°15.2´N	148°29.1´W	1-second averages
03-28-92	1218	26	73°15.3´N	148°28.3´W	
03-28-92	1754	27	73°15.4´N	148°28.0´W	
03-28-92	2049	28	73°15.4´N	148°28.0´W	
03-29-92	0740	29	73°15.5´N	148°28.8´W	
03-29-92	1824	30	73°16.0´N	148°30.4´W	
03-30-92	0627	31	73°16.9´N	148°33.7´W	
03-30-92	1745	32	73°18.4´N	148°39.5´W	
03-31-92	0655	33	73°19.4´N	148°44.6´W	
03-31-92	1950	34	73°19.8´N	148°50.5´W	
04-01-92	0732	35	73°19.6´N	148°51.9´W	
04-01-92	1452	36	73°19.2´N	148°53.4´W	
04-01-92	1849	37	73°19.0´N	148°54.0´W	
04-02-92	1401	38	73°18.9´N	148°55.1´W	
04-02-92	2245	39	73°19.0´N	148°56.1´W	
04-03-92	0700	40	73°19.1´N	148°57.3´W	
04-03-92	2043	41	73°19.2´N	149°01.2´W	

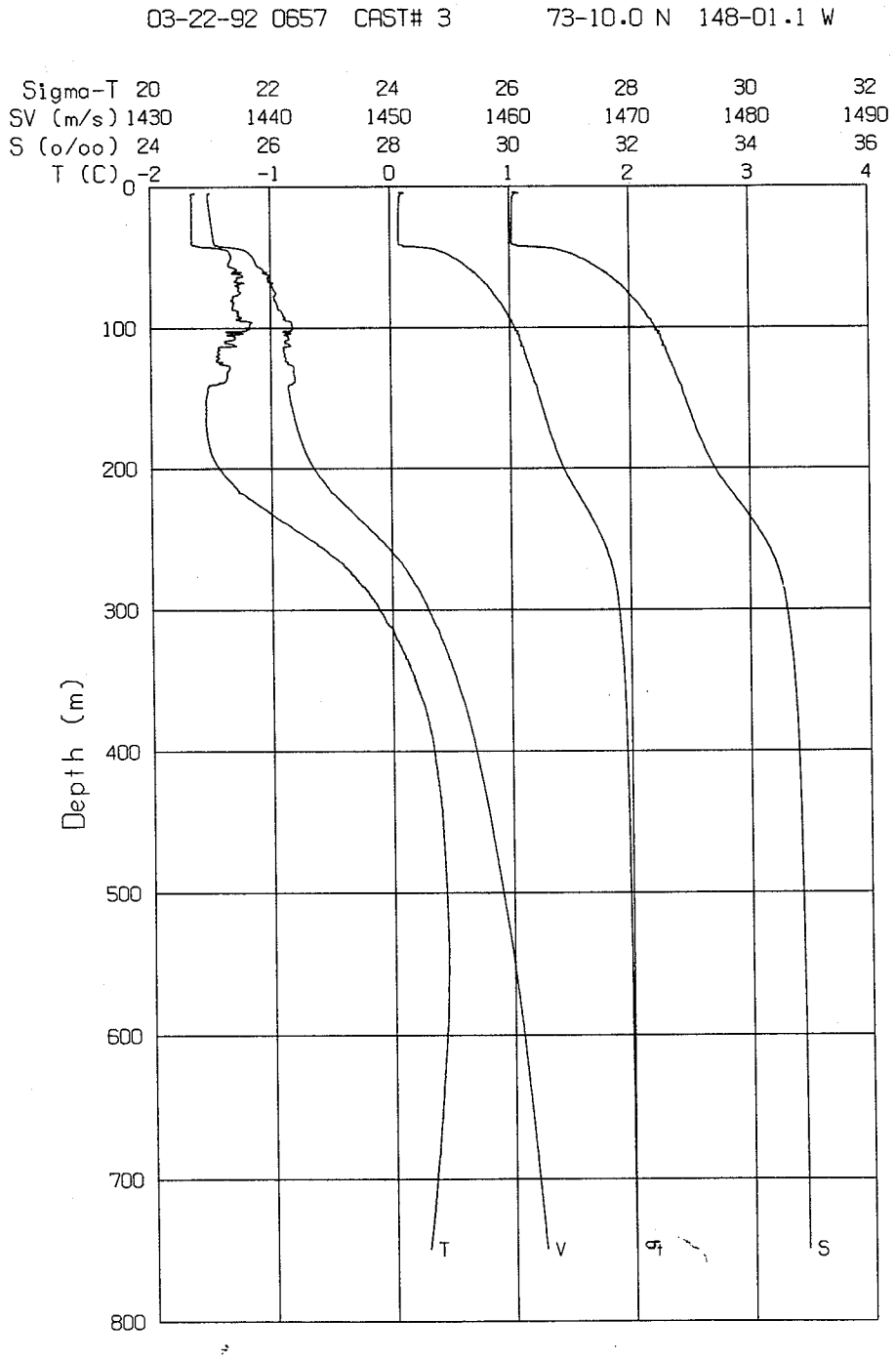

Figure 11. Sample STD profiles from cast 3.

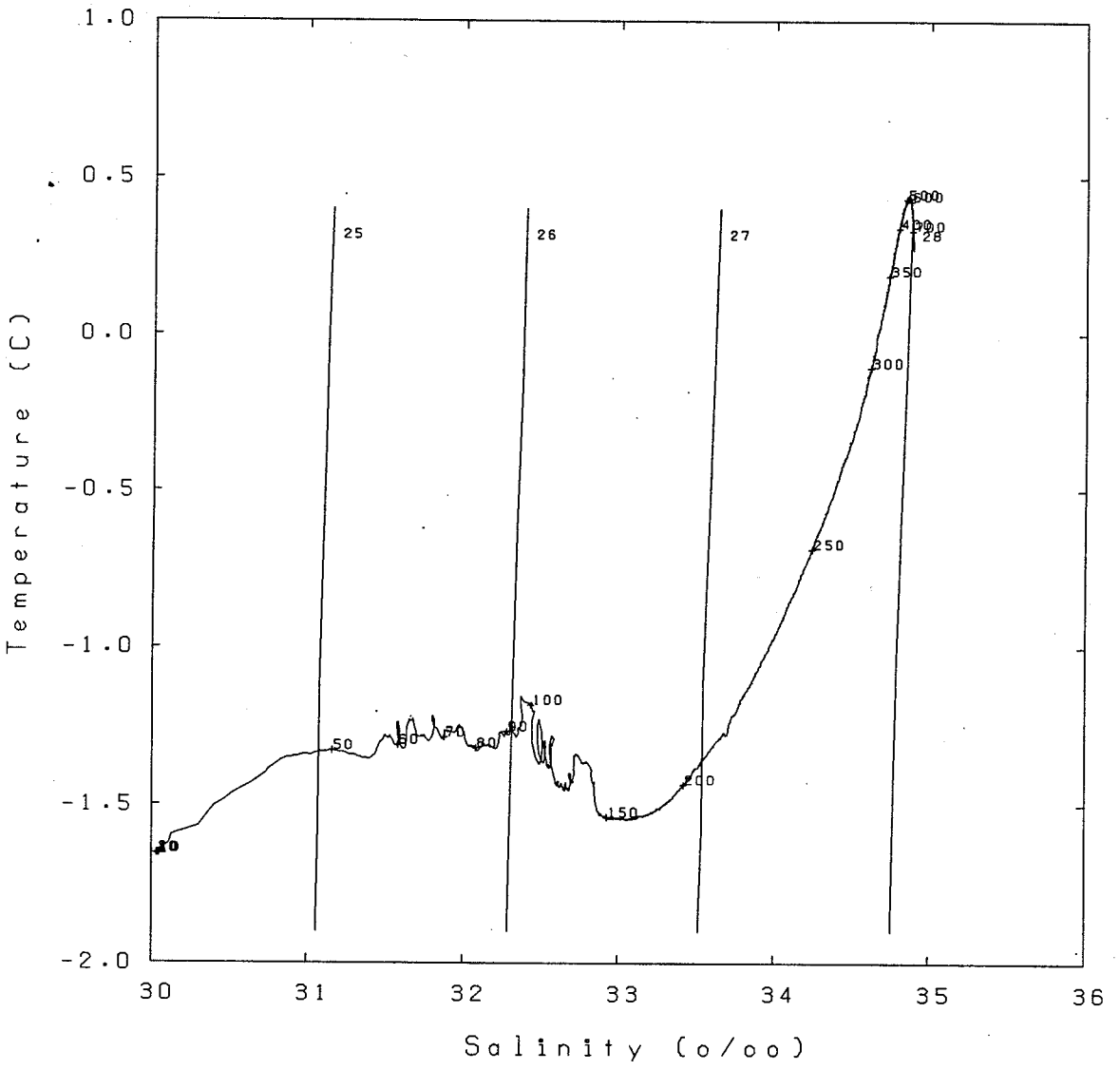

Figure 12. Temperature–salinity diagram of cast 3. Numbers along curve are depth in meters.

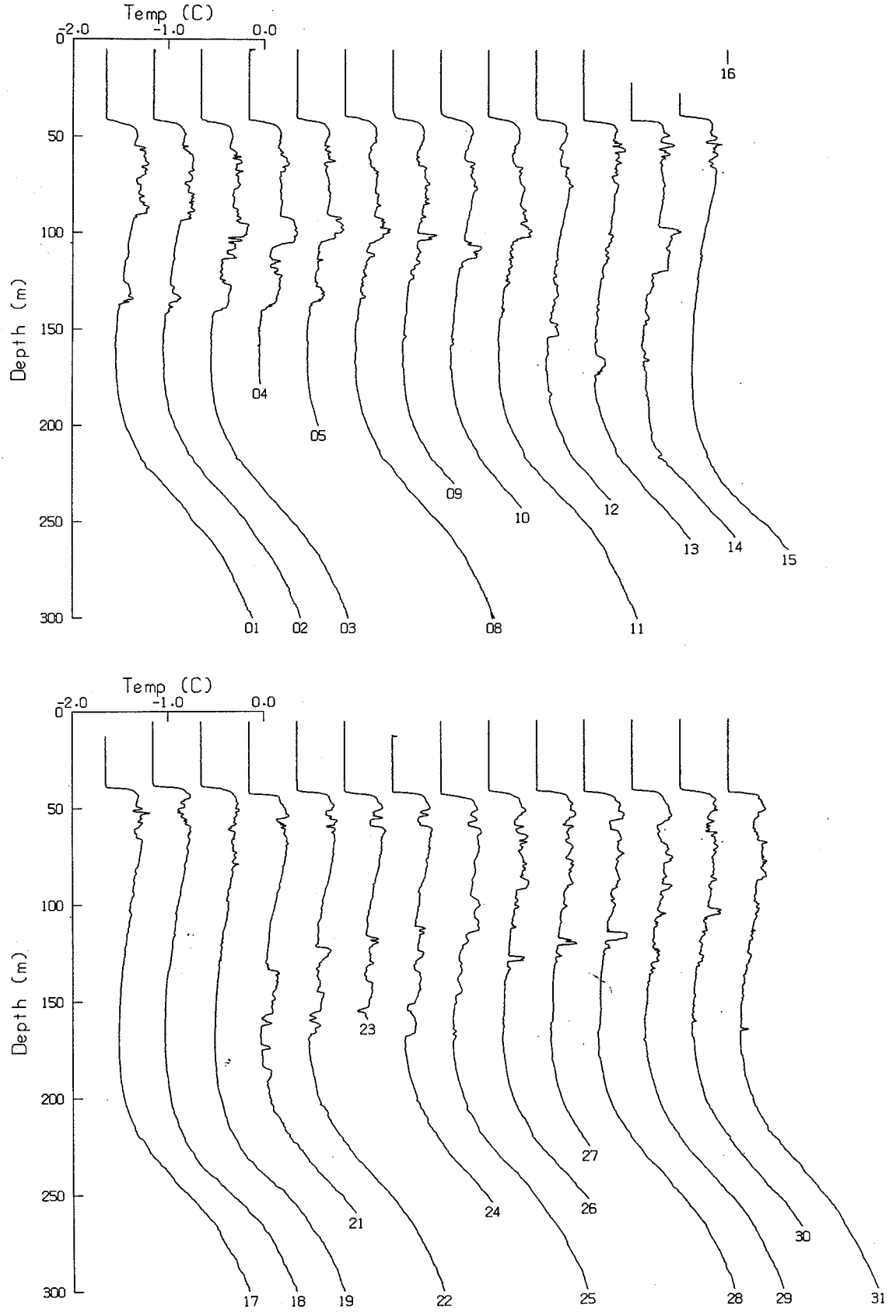

Figure 13. Temperature profile plotted in series showing warm intrusions.

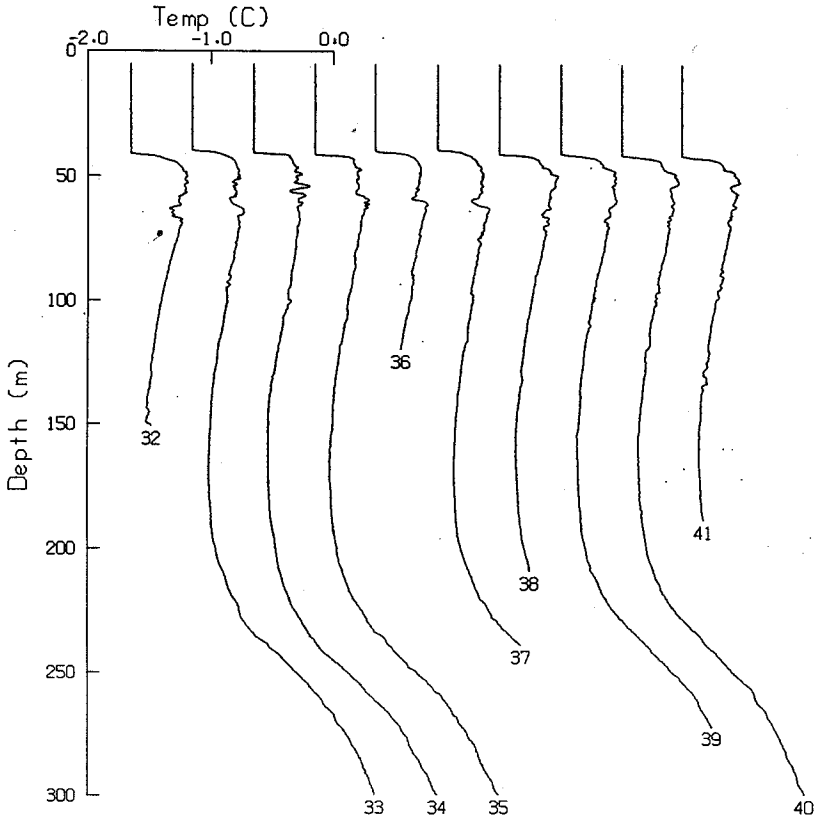

Figure 13, cont.

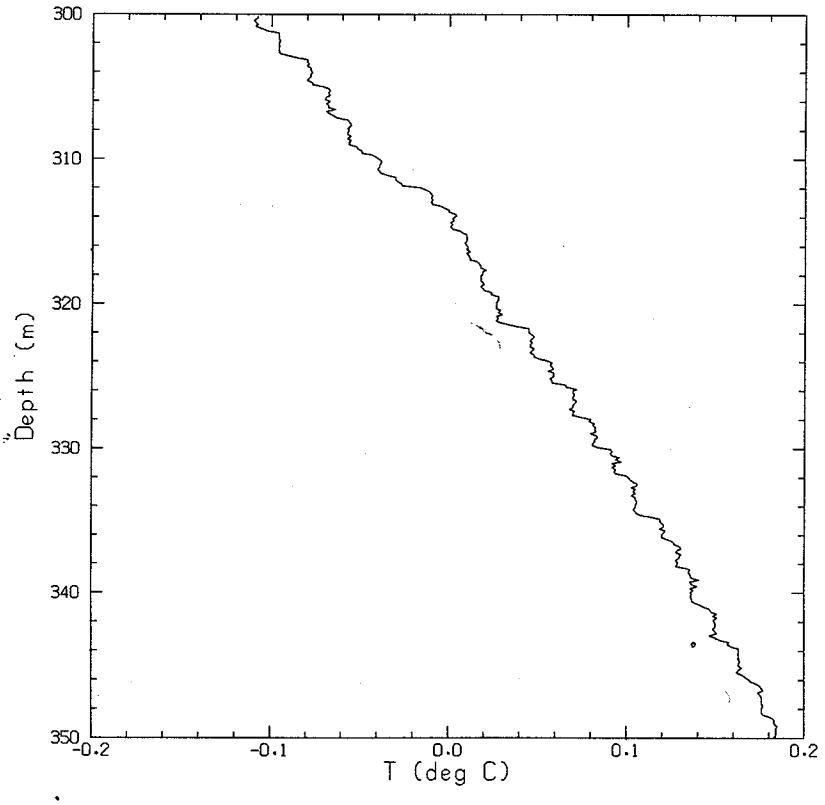

Figure 14.

Blowup of temperature profile in Figure 11 showing temperature staircase. Step changes are about 2 m and 0.007°C.

A 4-hour temperature/time series was made at 350 m depth to study the behavior of the temperature staircase. For this measurement, the conductivity cell was replaced by another thermistor. These sensors were deployed at depths of 357 m and 358 m, respectively. A 1-second average of the temperature was taken every minute. Figure 15 shows the averaged temperatures, with the readings at 358 m offset by –0.01°C. The variation in temperature may have been caused by the vertical fluctuation of up to 6 m in the water column or by different water patches of limited horizontal scale.[6]

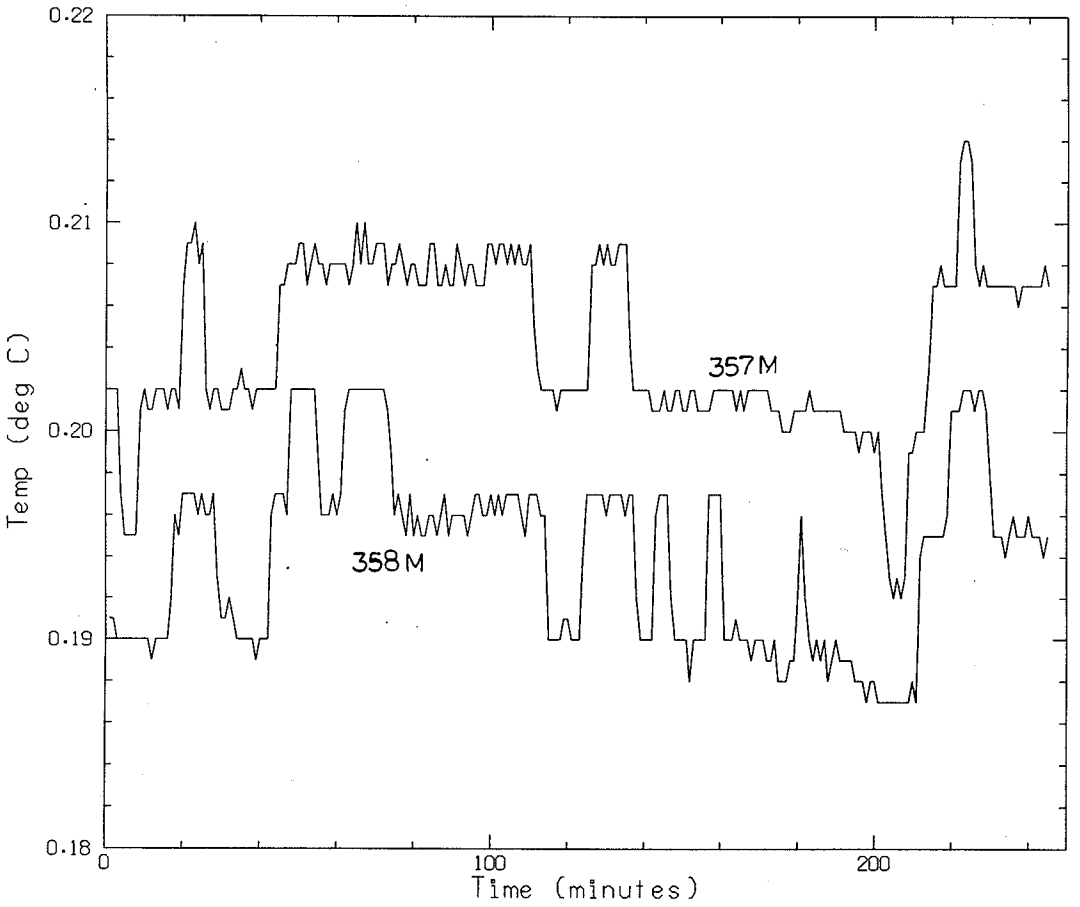

Figure 15. Two temperature/time series taken at 357 m and 358 m within a temperature staircase. Record at 358 m is offset by –0.01°.

Mesoscale eddies are fairly common in the Arctic.[7,8] In examining our STD data, we found what appeared to be telltale signs of eddies.[7] Figure 16 is a plot of successive salinity profiles for all the casts, offset by 0.5 ppt. Each dot represents a salinity increment of 0.2 ppt. The dots have been connected to show the contours. Around casts 18 and 32, the isohalines are displaced from the one at 150 m depth, a condition indicating a mesoscale eddy. A current cast (see next section) taken close to cast 18 indicated a current with an absolute speed >25 cm/s from 100 m depth downward, reinforcing the notion of an eddy. Figure 17 shows the locations of the casts. It is conceivable that the floe drifted into and then out of the fringe of an eddy during the period casts 16–19 were made and then back into the same eddy again starting with cast 31.

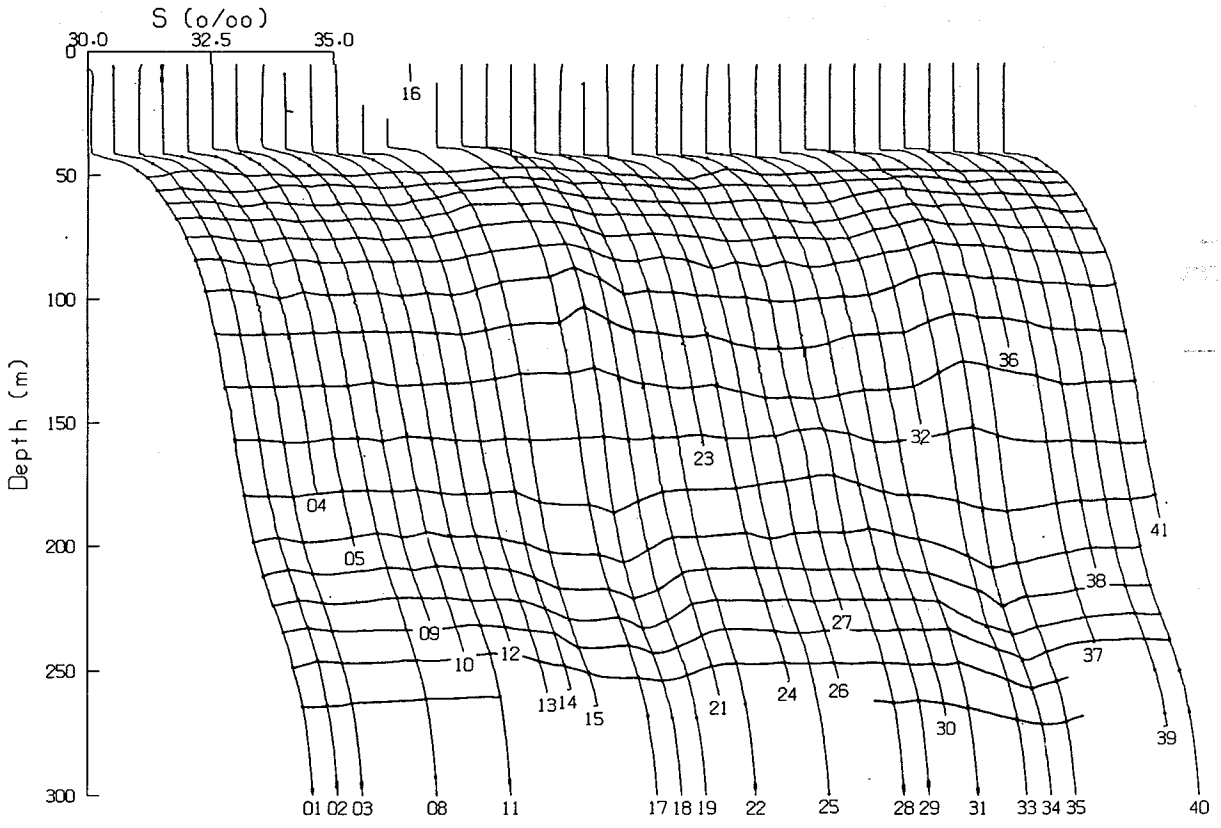

Figure 16. Salinity profile series showing salinity contours at 0.2 ppt intervals.

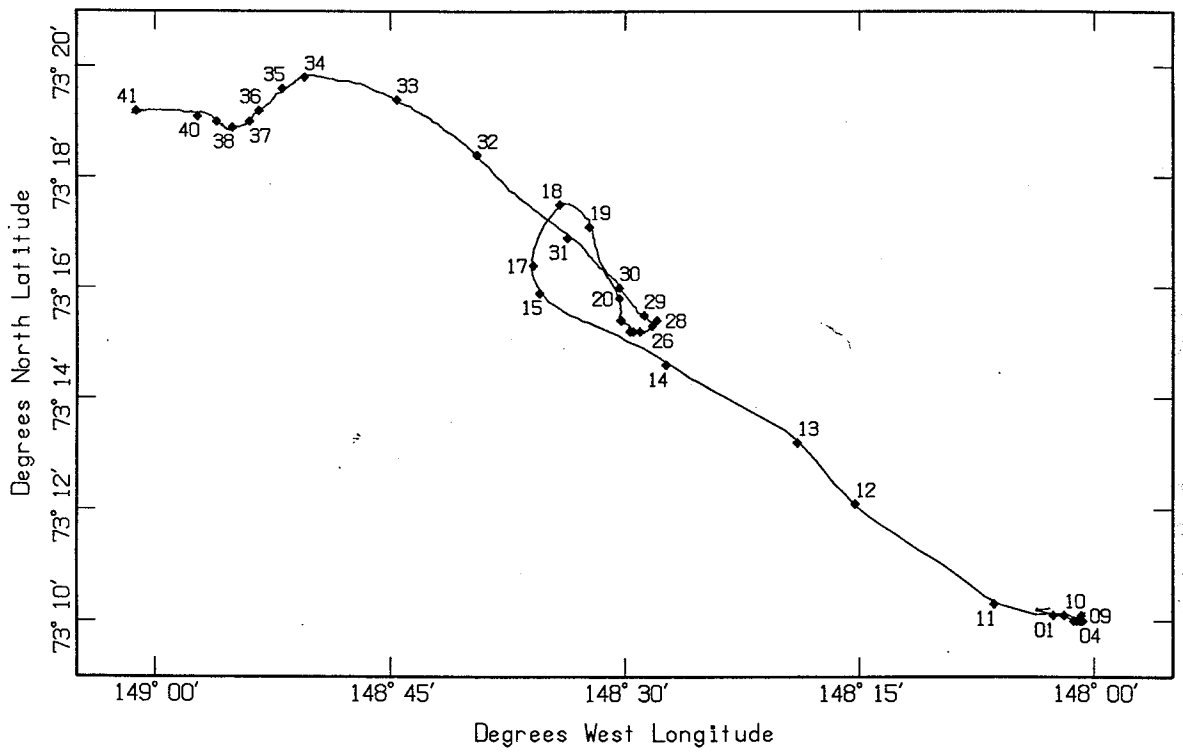

Figure 17. Location of CTD casts.

VI. CURRENTS

To measure current, the CTD profiler was replaced with an InterOcean S4 current meter. A 4.5-kg lead weight was hung 1 m below the instrument to reduce streaming. Sometimes a string of two S4 meters, separated vertically by 2.1 m, was used to compare the measurements. The default sampling rate of the current meter was 2 Hz, but generally we recorded the average of two samples. In addition to recording the magnetic north and east components of the current, the S4 also recorded depth. To obtain stable current measurements, we lowered the meter at depth increments of ~5–10 m, stopping for approximately 1 minute at each depth. When the current meter was brought back to the surface, the data were downloaded to a computer for processing. The mean and standard deviations were computed for the data at each depth. Table 3 lists the current meter casts. Vertical current profiles are shown in Appendix C. Both relative and absolute currents are shown, with the former plotted as a solid line and the latter dashed. Bars plotted at each depth represent plus or minus one standard deviation about the averages.

In general, the currents were weak, with the exception of casts 3a and 3b. On cast 3a, shown in Figure 18, current increased with depth from 100 m down. We believe this current indicated the presence of an eddy, although the cast did not go deep enough to prove it.

Table 3. Current meter casts taken at APLIS 92. The letter after the cast number refers to the current meter.

Date	Local Time	Cast No.	Comments
3-21-92	1750	01a	
3-21-92	1750	01b	
3-23-92	1825	02a	
3-23-92	1810	02b	
3-25-92	1329	03b	
3-25-92	1330	03a	
3-25-92	1532	04b	Time series at 200 m
3-26-92	1344	05a	Time series at 350 m, concurrent with CTD cast #20
3-29-92	0803	07a	
3-30-92	0651	08a	
3-30-92	1329	09a	
3-30-92	1330	09b	
3-30-92	2226	10a	Time series at 46 m
3-30-92	2223	10b	Time series at 44 m

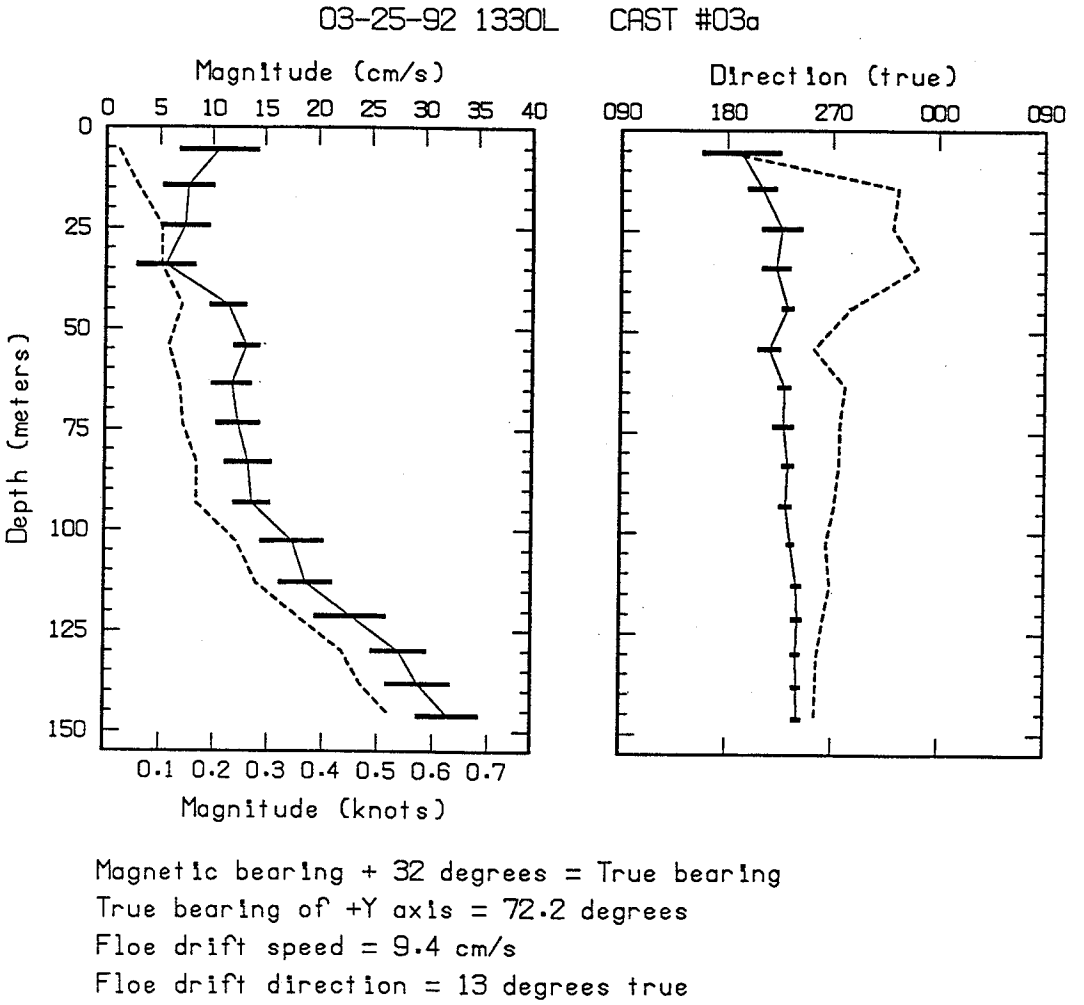

Figure 18. Sample current meter cast on 25 March 1992. Solid line is current relative to floe. Dashed line is absolute current relative to earth. Bars plotted at each depth represent plus or minus one standard deviation about the averages.

Cast 10 was a time series taken with two S4 meters at depths of 44 m and 46 m, the location of the pycnocline. The absolute current speed and direction are shown in Figures 19a and 19b. The time series at 46 m showed a periodic feature with frequencies of 0.56, 1.12, and 1.68 cycles/hour, whereas the data taken only 2 m shallower did not exhibit pronounced periodic behavior. For reference, the Brunt-Väisälä frequency at these depths was ~13 cycles/hour. Note that the direction of the current at 46 m was varying by 90°, a phenomenon for which we have no explanation.

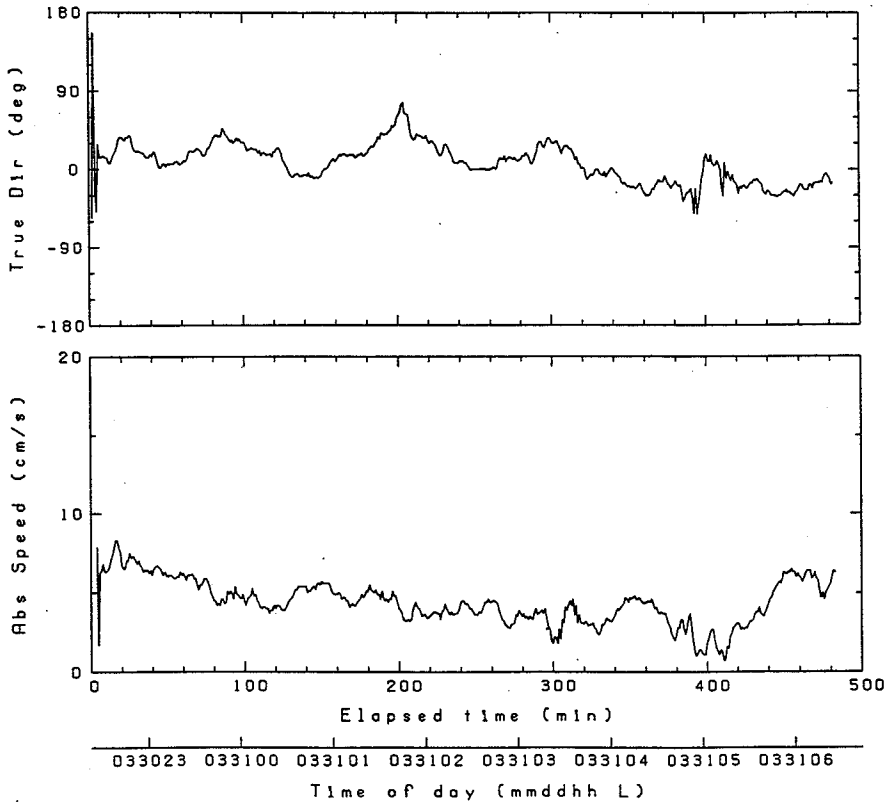

Figure 19a.

Current time series at depth of 44 m. Time is local.

Figure 19b.

Current time series at depth of 46 m. Time is local.

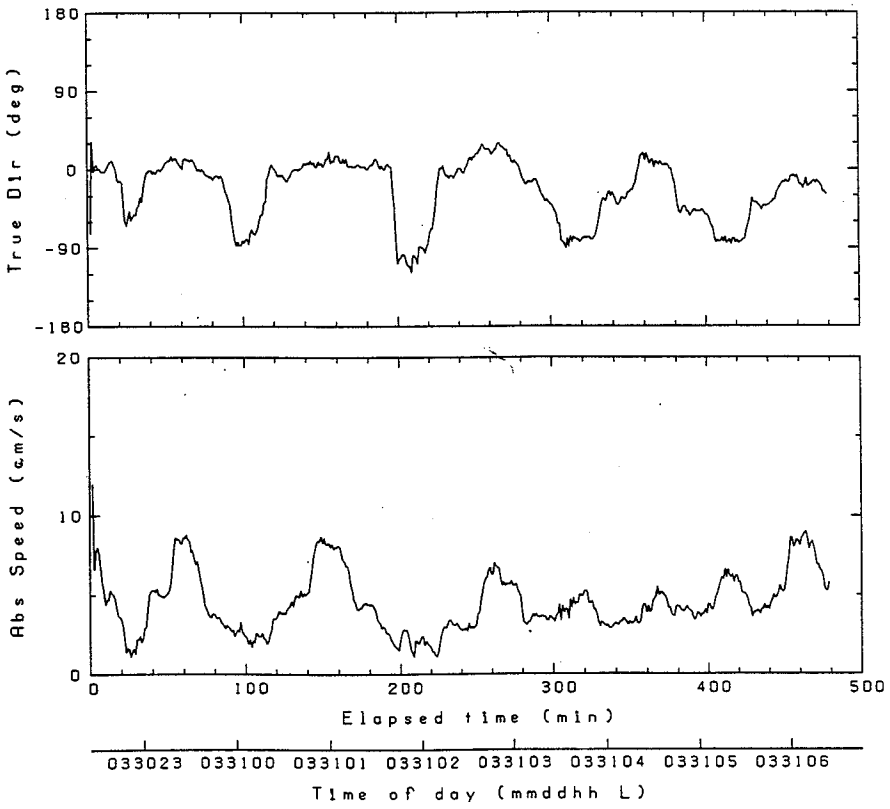

VII. ICE CORE SAMPLES

An ice core was taken in the vicinity of the NRL test hut on 1 April to determine the electrical conductivity of the sea ice. The core was removed from undisturbed, 190-cm-thick first-year ice with 5 cm of snow cover.

A 7.6-cm (inside diameter) SIPRE corer was used to remove short segments about 0.5 m in length. (Short segments were cored to reduce the time of exposure to the colder ambient air during handling and therefore limit temperature changes.) Each segment was placed in a miter box designed for cutting sections 7.5 cm and 10 cm long. For each sawed-off section, a 0.32-cm diameter hole was drilled to a depth of 3.8 cm at the midpoint. A digital thermometer was inserted to measure the temperature of the ice. The section was then sealed in a Ziploc bag and tagged. The depth of the section and the corresponding temperature were recorded. This procedure was repeated until the whole segment, and then the whole ice column, was sampled.

The air temperature at the time of core sampling was −23.1°C. The seawater temperature was −1.65°C, the salinity 30.2 ppt, and the electrical conductivity 24 mS/cm.

The samples were taken back to camp and allowed to melt at room temperature. We set up a "salinometer" with the thermistor and conductivity cell of APL's CTD profiler; this configuration allowed us to use the standard data-acquisition and reduction system. The sensors were mounted in a jig with the cell tilted to avoid trapping air bubbles. Tygon tubing was attached to both ends of the 1 cm × 18 cm cylindrical conductivity cell, and the thermistor was inserted into the tubing close to the cell. When the melted sample was shaken and poured into the tubings and the cell, both the conductivity and the temperature were measured simultaneously, and the salinity was computed. Prior to analysis, the samples and the sensors were placed on a bench top for several hours to bring them to the same temperature. This was necessary because any large temperature differential would have affected the conductivity results. To reduce the temperature differential further, the water sample was mixed within the cell by raising and lowering the pinched-off Tygon tubing at one end to pass the water sample back and forth.

Figure 20 shows the measured and computed properties of the ice cores. To obtain the electrical conductivity, the brine volume was required.[9] To compute the brine volume, density was required. Because of the irregular diameters of the cores and brine drainage, it was not appropriate to measure the ice density by dividing the core weight by its volume. To obtain more precise results, density and brine volume were calculated using relationships derived by Cox and Weeks[10] from measured temperature and salinity.

In general, the temperature profiles were fairly linear. Because the temperature profile of the ice column in spring is practically linear, we believe that any deviation from linearity was caused by measurement errors and by the exposure of core sections to colder ambient air.

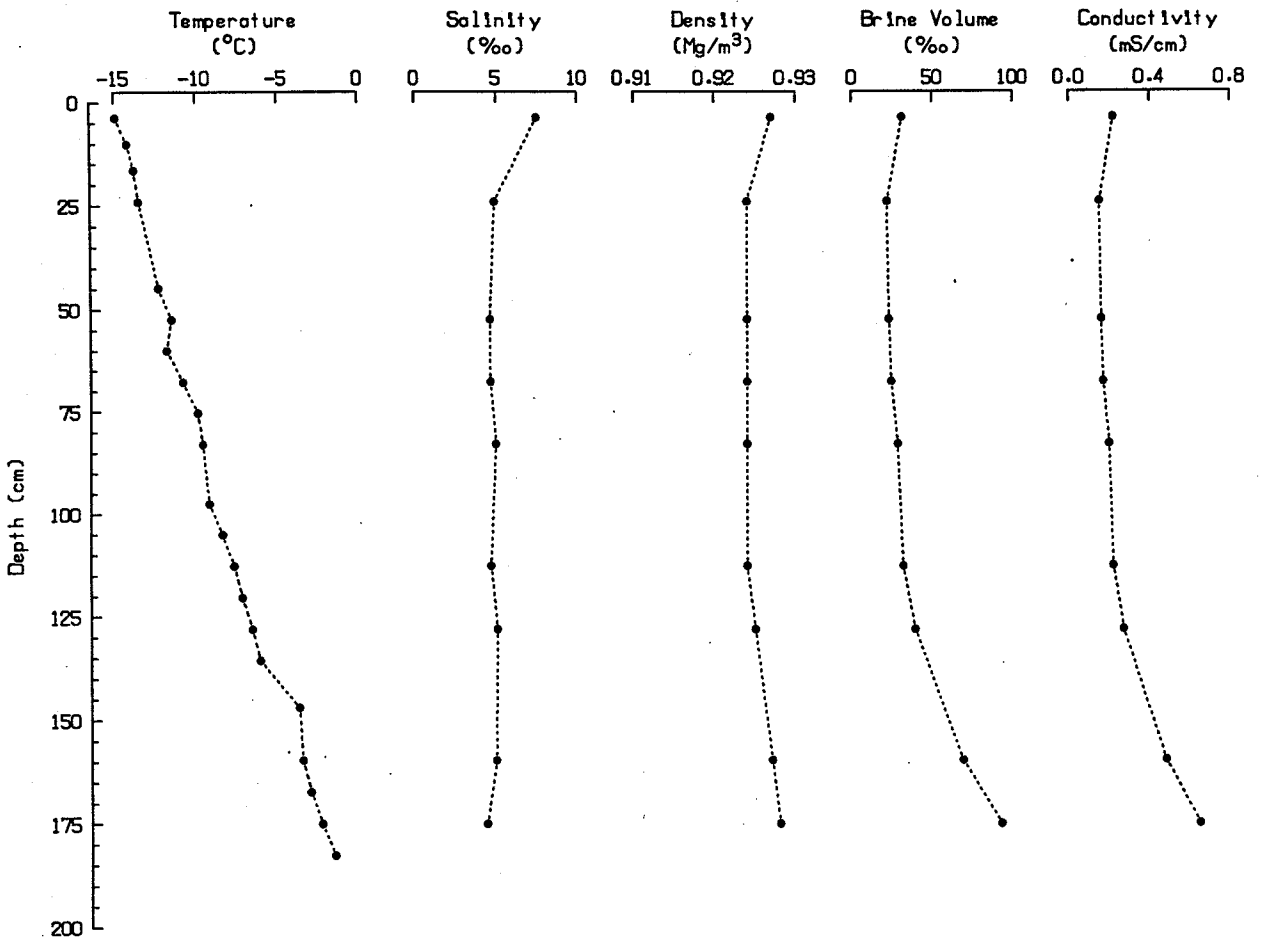

Figure 20. Measured and computed properties of first-year ice.

The salinity profile of the core is typical of first-year ice. The salinity is high near the surface owing to a faster freezing rate and decreases as the ice grows thicker and more slowly, allowing a longer time for brine expulsion. Although the salinity should increase again near the bottom because the brine has not had enough time to drain out, the measurements show relatively low salinities there. This could be explained by brine drainage during core retrieval and seawater dilution or displacement of brine, which has a higher salinity (for example, 37.6 ppt at −2°C and 70.6 ppt at −4°C) than that of seawater (~30 ppt).

Figure 21 shows salinity profiles of new ice (<1 month old) and multiyear ice, respectively, from cores obtained by ASL/NUWC. The salinity of the multiyear ice is very low near the surface because of brine drainage through the seasons, especially during the summer. This drainage mechanism produces nearly salt-free ice on multiyear ridges.

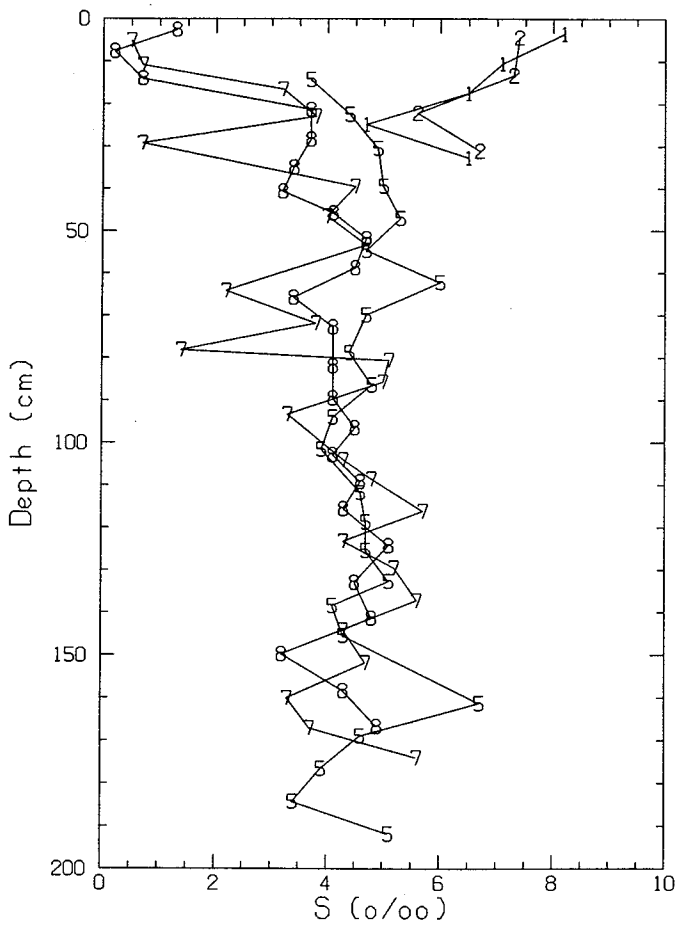

Figure 21. Salinity profiles of young ice (1,2) and multiyear ice (5,7,8).

VIII. UNDER-ICE AMBIENT NOISE

An omnidirectional hydrophone (ITC 6050C) was deployed at 30.5 m depth about 290 m from camp to minimize interference from noise generated by camp activities. The ambient noise signals were cabled back to camp, amplified by 40 dB, and recorded on a VCR system with a dynamic range of 88 dB and a bandwidth of 20 kHz. Because of the presence of a submarine, contamination of the ambient noise was a potential problem. To avoid such contamination, we recorded data only when the submarine was 25 km or more away from the camp. The recordings were therefore measurements of opportunity and few in number.

During the camp period, the floe experienced no apparent deformation, although leads constantly opened and closed to the north and south. There were continuously open leads in the other two directions, which could have been sources of strong noise during high winds as wind-generated waves interacted with the ice.

Data recording periods are listed in Table 4. The data tapes were played back at APL-UW, and the signal from the hydrophone was recorded at 50 kHz on a digital oscilloscope. For each recording period, 20 nearly consecutive traces 317.4 ms in length were digitized. The data were then downloaded to a computer, and a spectral analysis was performed on each trace. The length of the time series resulted in a bandwidth of 3.15 Hz. Finally, an average spectrum was obtained by power-summing the 20 spectra and averaging the sum. Ambient noise level plots are given in Appendix D. The noise signal was also monitored audibly during playback. We heard few loud pops and crackles, but there was a lot of low rumbling in the background.

Table 4. Ambient noise measurements taken at APLIS 92.

Date	Local Time
03-25	2330
03-26	0705
03-26	1150
03-26	1640
03-26	2004
03-28	1448

Figure 22 shows an average ambient noise spectrum, taken at 2330 local time on 25 March. The ambient noise level is quite high across the frequency spectrum, except at higher frequencies where it falls to or below the system noise level indicated by the dashed line. For comparison, the 50th percentile level measured in the spring of 1988[11] is shown as a dotted line. For a period of light wind (<5 m/s) and no floe deformation and ridging, we would expect the noise level to be about 20 dB lower than the measured values and below the 50th percentile level. During this recording period, tones of 1.3–1.7 kHz were also heard in the background, quite possibly generated by whales at a long distance.

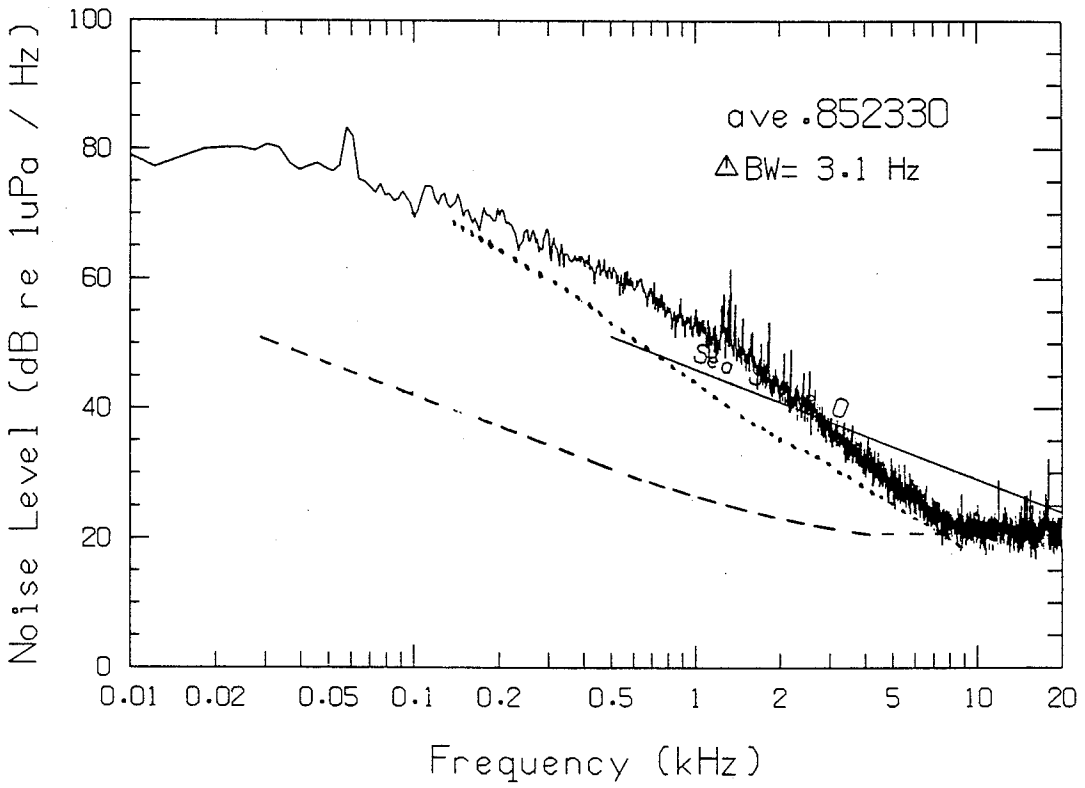

Figure 22. Sample ambient noise spectrum. Dashed line shows system noise. Dotted line is the 50th percentile level measured in the spring of 1988.

IX. REFERENCES

1. T. Wen, W.J. Felton, J.C. Luby, W.L.J. Fox, and K.L. Kientz, Environmental Measurements in the Beaufort Sea, Spring 1988, APL-UW TR 8822, Applied Physics Laboratory, University of Washington, Seattle, Washington, March 1989.

2. G.R. Garrison, T. Wen, R.E. Francois, W.J. Felton, and M.L. Welch, Environmental Measurements in the Beaufort Sea, Spring 1986, APL-UW 4-86, Applied Physics Laboratory, University of Washington, Seattle, Washington, January 1987.

3. T. Wen, F.W. Karig, W.J. Felton, J.C. Luby, and K.L. Williams, Environmental Measurements in the Beaufort Sea, Spring 1990, APL-UW TR 9105, Applied Physics Laboratory, University of Washington, Seattle, Washington, December 1990.

4. T. Wen, F.W. Karig, W.J. Felton, P. Keller, Environmental Measurements in the Beaufort Sea, Spring 1991, APL-UW TR 9204, Applied Physics Laboratory, University of Washington, Seattle, Washington, January 1992.

5. N.P. Fofonoff and R.C. Millard, Jr., "Algorithms for computation of fundamental properties of seawater," UNESCO Technical Papers in Marine Science, #44, Paris, 1983.

6. L. Padman and T.M. Dillon, "On the horizontal extent of the Canada Basin thermohaline steps," *J. Phys. Oceanog., 18,* 1458–1462 (1988).

7. J.L. Newton, K. Aagaard, and L.K. Coachman, "Baroclinic eddies in the Arctic Ocean," *Deep-Sea Res., 21,* 707–719 (1974).

8. T.O. Manley and K. Hunkins, "Mesoscale eddies of the Arctic Ocean," *J. Geophys. Res., 90,* 4911–4930 (1985).

9. R.M. Morey, A. Kovacs, and G.F.N. Cox, Electromagnetic Properties of Sea Ice, CRREL Report 84-2, Cold Regions Research and Engineering Laboratory, Hanover, New Hampshire, 1984.

10. G.F.N. Cox and W.F. Weeks, "Equations for determining the gas and brine volumes in sea-ice samples," *J. Glaciol., 29,* 306–316 (1983).

11. T. Wen, Ambient Noise in the Beaufort Sea, Spring 1988, APL-UW TM 2-90, Applied Physics Laboratory, University of Washington, Seattle, Washington, February 1990.

APPENDIX A

Floe Position and Drift Data

(time is UTC)

Date mm dd	Time hhmm	Latitude dd mm.mm	Longitude ddd mm.mm	Speed km/hr	Dir
03 21	0159	73 10.21	148 3.32		
03 21	1059	73 10.20	148 3.62	0.00	
03 21	1659	73 10.16	148 3.23	0.04	108
03 21	1959	73 10.13	148 2.84	0.07	103
03 21	2300	73 10.10	148 2.37	0.09	104
03 22	0159	73 10.08	148 1.98	0.07	100
03 22	0459	73 10.05	148 1.60	0.07	106
03 22	0835	73 10.01	148 1.23	0.06	109
03 22	1659	73 9.98	148 1.06	0.00	
03 23	0100	73 10.02	148 0.84	0.00	
03 23	0947	73 10.12	148 0.62	0.02	034
03 23	1800	73 10.09	148 0.83	0.00	
03 23	2200	73 10.07	148 1.24	0.05	263
03 24	0000	73 10.10	148 1.79	0.15	279
03 24	0100	73 10.11	148 2.28	0.27	273
03 24	0159	73 10.14	148 2.96	0.37	277
03 24	0300	73 10.17	148 3.85	0.48	278
03 24	0400	73 10.24	148 4.85	0.55	281
03 24	0459	73 10.33	148 5.88	0.58	287
03 24	0611	73 10.51	148 7.05	0.59	297
03 24	0724	73 10.69	148 8.16	0.57	300
03 24	0835	73 10.89	148 9.20	0.55	303
03 24	0947	73 11.08	148 10.18	0.53	304
03 24	1100	73 11.28	148 11.17	0.53	304
03 24	1200	73 11.42	148 11.98	0.51	302
03 24	1300	73 11.57	148 12.78	0.51	302
03 24	1359	73 11.74	148 13.60	0.53	304
03 24	1500	73 11.91	148 14.40	0.53	307
03 24	1600	73 12.09	148 15.18	0.53	308
03 24	1659	73 12.28	148 15.91	0.53	312
03 24	1800	73 12.48	148 16.59	0.52	315
03 24	1900	73 12.68	148 17.23	0.50	317
03 24	1959	73 12.87	148 17.87	0.50	316
03 24	2100	73 13.07	148 18.49	0.49	316
03 24	2248	73 13.35	148 19.91	0.52	305
03 25	0029	73 13.62	148 21.33	0.53	303
03 25	0205	73 13.87	148 22.72	0.54	301
03 25	0336	73 14.09	148 24.06	0.55	299
03 25	0459	73 14.30	148 25.39	0.58	298
03 25	0530	73 14.39	148 25.92	0.65	300
03 25	0600	73 14.48	148 26.43	0.64	300
03 25	0629	73 14.56	148 26.95	0.64	301
03 25	0705	73 14.68	148 27.56	0.64	302
03 25	0741	73 14.78	148 28.18	0.64	299
03 25	0817	73 14.87	148 28.78	0.61	297
03 25	0854	73 14.97	148 29.37	0.60	298
03 25	0930	73 15.05	148 29.98	0.61	297
03 25	0959	73 15.12	148 30.50	0.60	294
03 25	1030	73 15.19	148 30.98	0.57	294
03 25	1059	73 15.25	148 31.45	0.55	295
03 25	1130	73 15.31	148 31.91	0.54	292
03 25	1159	73 15.36	148 32.33	0.49	292
03 25	1229	73 15.41	148 32.75	0.48	292
03 25	1300	73 15.45	148 33.12	0.43	293
03 25	1359	73 15.54	148 33.77	0.39	296
03 25	1500	73 15.64	148 34.35	0.36	300
03 25	1600	73 15.76	148 34.87	0.35	307
03 25	1700	73 15.88	148 35.30	0.32	315
03 25	1800	73 16.02	148 35.62	0.32	327
03 25	1900	73 16.18	148 35.86	0.31	335
03 25	1959	73 16.35	148 35.97	0.33	349
03 25	2100	73 16.52	148 35.96	0.32	001
03 25	2200	73 16.69	148 35.85	0.32	010
03 25	2259	73 16.88	148 35.63	0.36	018
03 26	0000	73 17.05	148 35.35	0.35	025
03 26	0059	73 17.20	148 35.02	0.33	032
03 26	0159	73 17.32	148 34.70	0.29	037
03 26	0259	73 17.42	148 34.42	0.23	041
03 26	0430	73 17.50	148 34.16	0.14	041
03 26	0854	73 17.52	148 33.78	0.05	076
03 26	1130	73 17.48	148 33.34	0.10	110
03 26	1300	73 17.41	148 33.00	0.14	124
03 26	1430	73 17.31	148 32.66	0.17	133
03 26	1530	73 17.22	148 32.45	0.21	147
03 26	1630	73 17.12	148 32.25	0.21	150
03 26	1730	73 16.99	148 32.13	0.24	165
03 26	1829	73 16.86	148 32.02	0.25	165
03 26	1930	73 16.74	148 31.90	0.24	164
03 26	2030	73 16.61	148 31.78	0.24	165
03 26	2129	73 16.49	148 31.63	0.24	160
03 26	2230	73 16.37	148 31.46	0.24	158
03 26	2329	73 16.26	148 31.27	0.23	152
03 27	0029	73 16.15	148 31.06	0.22	150
03 27	0129	73 16.04	148 30.82	0.24	147
03 27	0230	73 15.92	148 30.63	0.25	154
03 27	0329	73 15.81	148 30.47	0.22	157
03 27	0459	73 15.66	148 30.34	0.18	166
03 27	0630	73 15.54	148 30.36	0.15	182
03 27	0853	73 15.42	148 30.34	0.09	177
03 27	1300	73 15.35	148 30.00	0.05	124
03 27	1659	73 15.28	148 29.70	0.05	132
03 28	0100	73 15.23	148 29.47	0.00	
03 28	0500	73 15.18	148 29.11	0.05	116
03 28	1200	73 15.21	148 28.72	0.03	072
03 28	1829	73 15.27	148 28.37	0.03	059
03 29	0130	73 15.34	148 28.08	0.03	050
03 29	1000	73 15.38	148 28.27	0.00	
03 29	1359	73 15.43	148 28.60	0.05	300
03 29	1800	73 15.50	148 28.90	0.05	309
03 29	2059	73 15.58	148 29.25	0.08	307
03 29	2329	73 15.73	148 29.65	0.14	322
03 30	0130	73 15.86	148 30.00	0.16	322
03 30	0329	73 16.00	148 30.35	0.16	324
03 30	0459	73 16.10	148 30.59	0.15	325
03 30	0629	73 16.19	148 30.89	0.15	314
03 30	0741	73 16.26	148 31.18	0.17	311
03 30	0854	73 16.34	148 31.51	0.19	308
03 30	0959	73 16.41	148 31.81	0.19	311
03 30	1059	73 16.50	148 32.07	0.21	318
03 30	1159	73 16.58	148 32.33	0.21	319
03 30	1300	73 16.68	148 32.59	0.22	320
03 30	1359	73 16.78	148 32.90	0.25	318
03 30	1500	73 16.87	148 33.28	0.26	310
03 30	1600	73 16.97	148 33.74	0.31	306
03 30	1700	73 17.08	148 34.23	0.33	307
03 30	1800	73 17.19	148 34.79	0.36	305
03 30	1900	73 17.31	148 35.33	0.36	306
03 30	1959	73 17.43	148 35.90	0.38	307
03 30	2030	73 17.50	148 36.20	0.40	307
03 30	2100	73 17.57	148 36.51	0.42	308
03 30	2129	73 17.64	148 36.82	0.42	306
03 30	2200	73 17.71	148 37.12	0.42	309
03 30	2230	73 17.78	148 37.41	0.41	312
03 30	2259	73 17.86	148 37.69	0.41	312
03 30	2330	73 17.94	148 37.99	0.43	312
03 31	0000	73 18.02	148 38.24	0.41	318
03 31	0059	73 18.17	148 38.76	0.39	315
03 31	0159	73 18.31	148 39.23	0.36	315
03 31	0259	73 18.43	148 39.66	0.32	314
03 31	0400	73 18.54	148 40.06	0.29	313
03 31	0459	73 18.64	148 40.49	0.30	310
03 31	0600	73 18.74	148 40.93	0.29	306
03 31	0706	73 18.84	148 41.42	0.29	305
03 31	0817	73 18.94	148 41.96	0.29	304
03 31	0929	73 19.05	148 42.51	0.30	305
03 31	1029	73 19.13	148 42.96	0.28	300
03 31	1130	73 19.20	148 43.38	0.26	299
03 31	1229	73 19.27	148 43.81	0.26	298
03 31	1330	73 19.33	148 44.20	0.24	298
03 31	1430	73 19.38	148 44.61	0.24	295
03 31	1530	73 19.44	148 45.01	0.25	298
03 31	1630	73 19.50	148 45.45	0.25	293
03 31	1754	73 19.57	148 46.06	0.25	293
03 31	1918	73 19.64	148 46.67	0.25	291
03 31	2030	73 19.70	148 47.23	0.26	288
03 31	2129	73 19.72	148 47.72	0.26	278
03 31	2230	73 19.74	148 48.21	0.26	278
03 31	2329	73 19.76	148 48.69	0.26	278
04 01	0029	73 19.79	148 49.13	0.24	282
04 01	0129	73 19.81	148 49.52	0.21	279
04 01	0300	73 19.83	148 50.00	0.17	277
04 01	0459	73 19.82	148 50.48	0.13	268
04 01	0741	73 19.77	148 50.87	0.09	243
04 01	1030	73 19.70	148 51.18	0.07	231
04 01	1229	73 19.63	148 51.53	0.11	236
04 01	1500	73 19.57	148 51.91	0.09	239
04 01	1730	73 19.49	148 52.27	0.09	233
04 01	1930	73 19.40	148 52.52	0.11	218
04 01	2112	73 19.32	148 52.79	0.12	225
04 01	2235	73 19.26	148 53.09	0.15	232
04 01	2359	73 19.19	148 53.40	0.14	235
04 02	0130	73 19.12	148 53.71	0.15	229
04 02	0329	73 19.03	148 53.98	0.11	218
04 02	0929	73 18.95	148 54.25	0.03	226
04 02	1330	73 18.91	148 54.62	0.05	250
04 02	2200	73 18.86	148 54.96	0.02	244
04 03	0159	73 18.85	148 55.35	0.05	263
04 03	0530	73 18.93	148 55.71	0.07	306
04 03	0741	73 19.00	148 56.01	0.09	309
04 03	1000	73 19.07	148 56.28	0.09	315
04 03	1200	73 19.13	148 56.64	0.11	298
04 03	1430	73 19.16	148 57.07	0.10	284
04 03	1659	73 19.17	148 57.52	0.10	272
04 03	1859	73 19.17	148 57.92	0.11	272
04 03	2142	73 19.19	148 58.69	0.15	273
04 03	2323	73 19.19	148 59.22	0.16	271
04 04	0105	73 19.20	148 59.76	0.17	271
04 04	0248	73 19.19	149 0.28	0.16	267
04 04	0429	73 19.18	149 0.81	0.17	266
04 04	0600	73 19.16	149 1.19	0.14	257

APPENDIX B

STD Plots

Date	Time (UTC)	Cast No.	Latitude	Longitude	Comments
3-21-92	1236	01	73°10.1´N	148°02.6´W	
3-21-92	2102	02	73°10.0´N	148°01.3´W	
3-22-92	0657	03	73°10.0´N	148°01.1´W	Deep cast to 750 m
3-22-92	1232	04	73°10.0´N	148°00.9´W	
3-22-92	1410	05	73°10.0´N	148°00.8´W	
		06			Thermistor comparison test
3-22-92	2052	07			Aborted
3-22-92	2134	08	73°10.0´N	148°00.7´W	
3-23-92	0645	09	73°10.1´N	148°00.8´W	
3-23-92	1537	10	73°10.1´N	148°01.9´W	
3-23-92	2011	11	73°10.3´N	148°06.4´W	
3-24-92	0651	12	73°12.1´N	148°15.3´W	
3-24-92	1240	13	73°13.2´N	148°19.0´W	
3-24-92	2146	14	73°14.6´N	148°27.4´W	
3-25-92	0808	15	73°15.9´N	148°35.5´W	
3-25-92	1008	16	73°16.2´N	148°36.0´W	
3-25-92	1101	17	73°16.4´N	148°35.9´W	Deep cast to 610 m
3-25-92	1825	18	73°17.5´N	148°34.2´W	Deep cast to 600 m
3-26-92	0633	19	73°17.1´N	148°32.3´W	
3-26-99	1349	20	73°15.8´N	148°30.4´W	Temperature time series (not shown)
3-26-92	2254	21	73°15.4´N	148°30.3´W	
3-27-92	0701	22	73°15.2´N	148°29.7´W	
3-27-92	1354	23	73°15.2´N	148°29.5´W	
3-27-92	1623	24	73°15.2´N	148°29.5´W	
3-27-92	2007	25	73°15.2´N	148°29.1´W	1-second averages
3-28-92	1218	26	73°15.3´N	148°28.3´W	
3-28-92	1754	27	73°15.4´N	148°28.0´W	
3-28-92	2049	28	73°15.4´N	148°28.0´W	
3-29-92	0740	29	73°15.5´N	148°28.8´W	
3-29-92	1824	30	73°16.0´N	148°30.4´W	
3-30-92	0627	31	73°16.9´N	148°33.7´W	
3-30-92	1745	32	73°18.4´N	148°39.5´W	
3-31-92	0655	33	73°19.4´N	148°44.6´W	
3-31-92	1950	34	73°19.8´N	148°50.5´W	
4-01-92	0732	35	73°19.6´N	148°51.9´W	
4-01-92	1452	36	73°19.2´N	148°53.4´W	
4-01-92	1849	37	73°19.0´N	148°54.0´W	
4-02-92	1401	38	73°18.9´N	148°55.1´W	
4-02-92	2245	39	73°19.0´N	148°56.1´W	
4-03-92	0700	40	73°19.1´N	148°57.3´W	
4-03-92	2043	41	73°19.2´N	149°01.2´W	

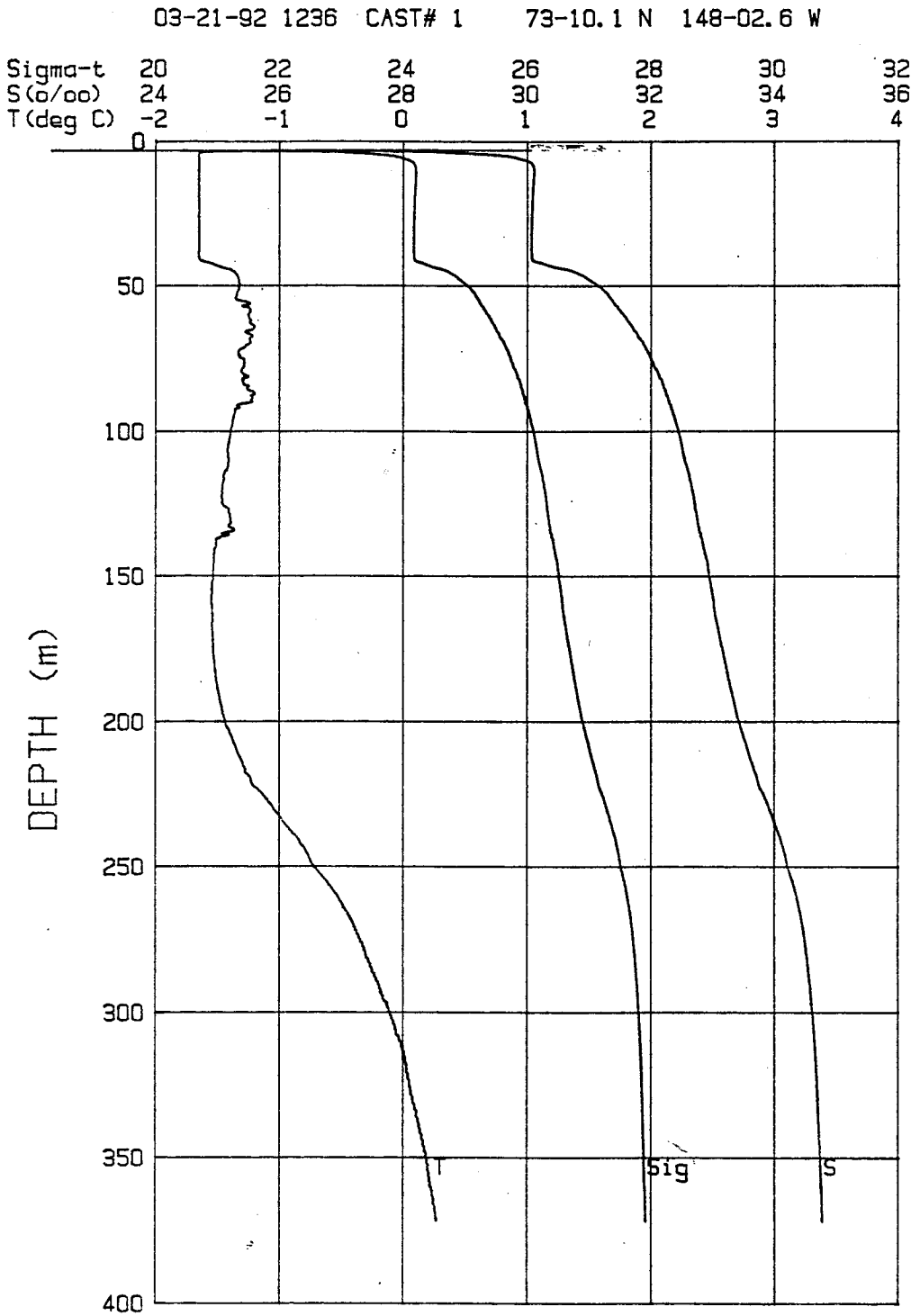
03-21-92 1236 CAST# 1 73-10.1 N 148-02.6 W
Sigma-t 20 22 24 26 28 30 32
S(o/oo) 24 26 28 30 32 34 36
T(deg C) -2 -1 0 1 2 3 4
0
50
100
150
200
250
300
350
400
DEPTH (m)
T
Sig
S

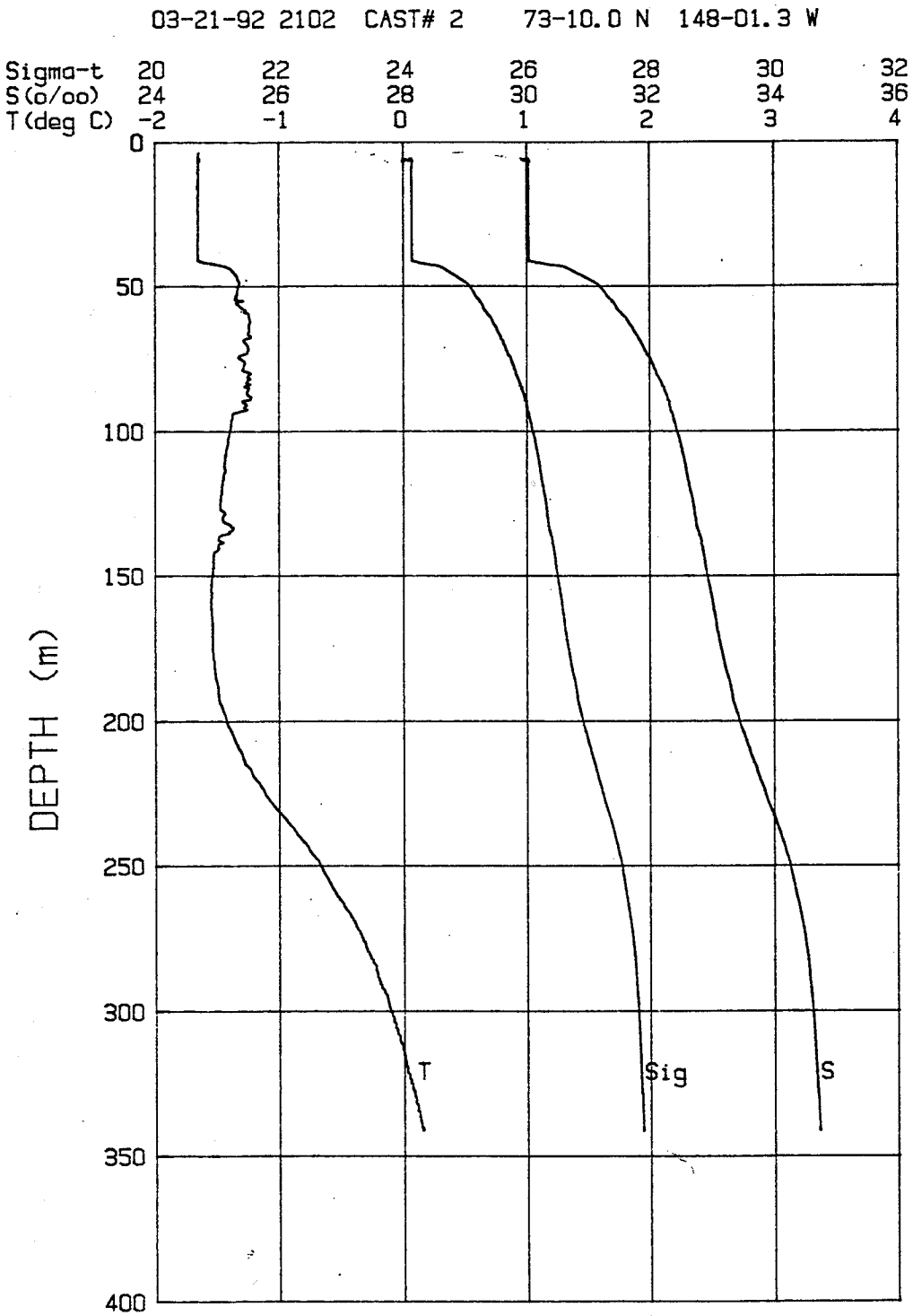
03-21-92 2102 CAST# 2 73-10.0 N 148-01.3 W
Sigma-t 20 22 24 26 28 30 32
S(o/oo) 24 26 28 30 32 34 36
T(deg C) -2 -1 0 1 2 3 4
DEPTH (m)
0
50
100
150
200
250
300
350
400
T
Sig
S

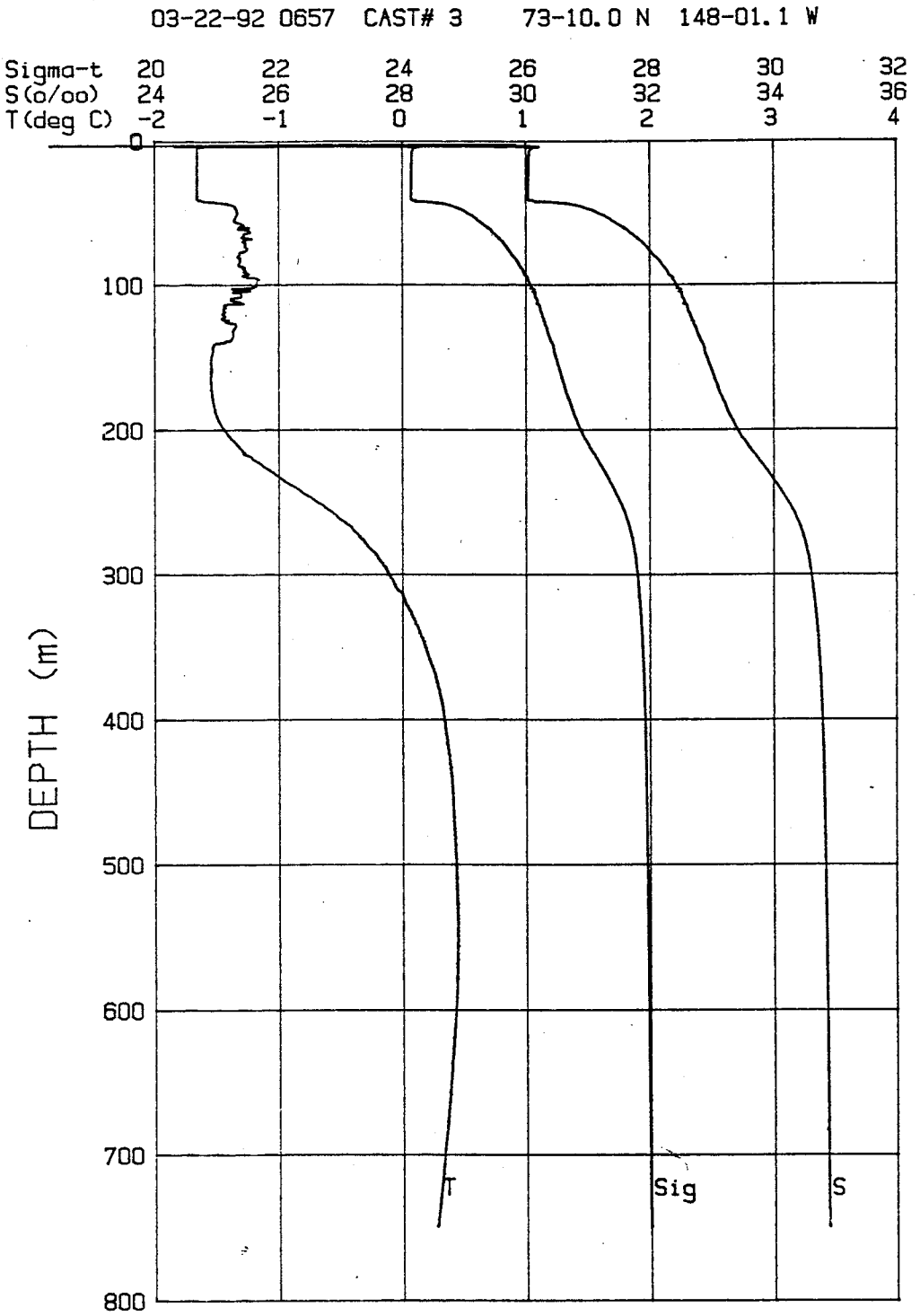
03-22-92 0657 CAST# 3 73-10.0 N 148-01.1 W
Sigma-t 20 22 24 26 28 30 32
S(o/oo) 24 26 28 30 32 34 36
T(deg C) -2 -1 0 1 2 3 4
0
100
200
300
400
500
600
700
800
DEPTH (m)
T
Sig
S

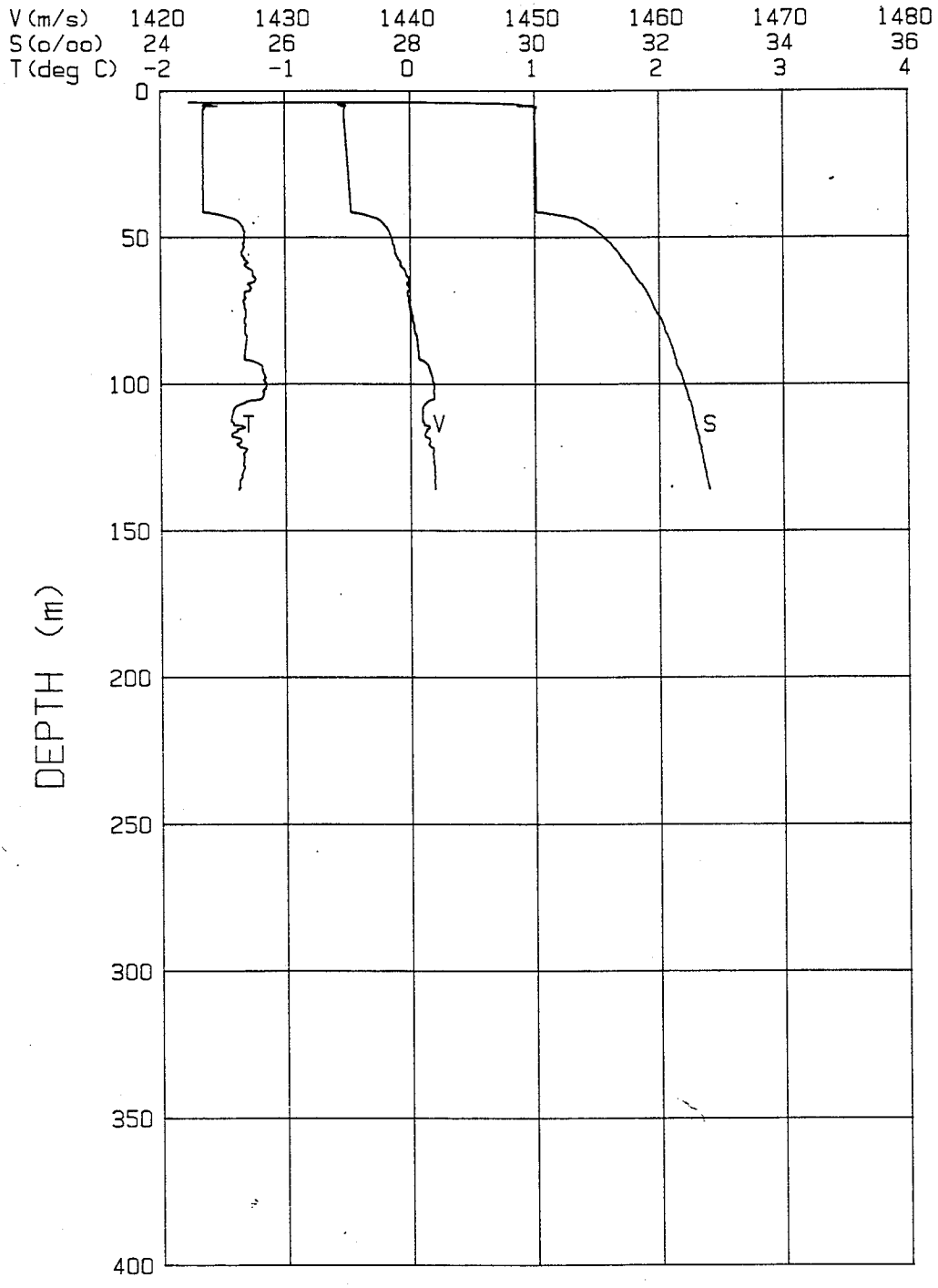
03-22-92 1232 CAST# 4 73-10.0 N 148-00.9 W
V(m/s) 1420 1430 1440 1450 1460 1470 1480
S(o/oo) 24 26 28 30 32 34 36
T(deg C) -2 -1 0 1 2 3 4
0
50
100
150
200
250
300
350
400
DEPTH (m)
T
V
S

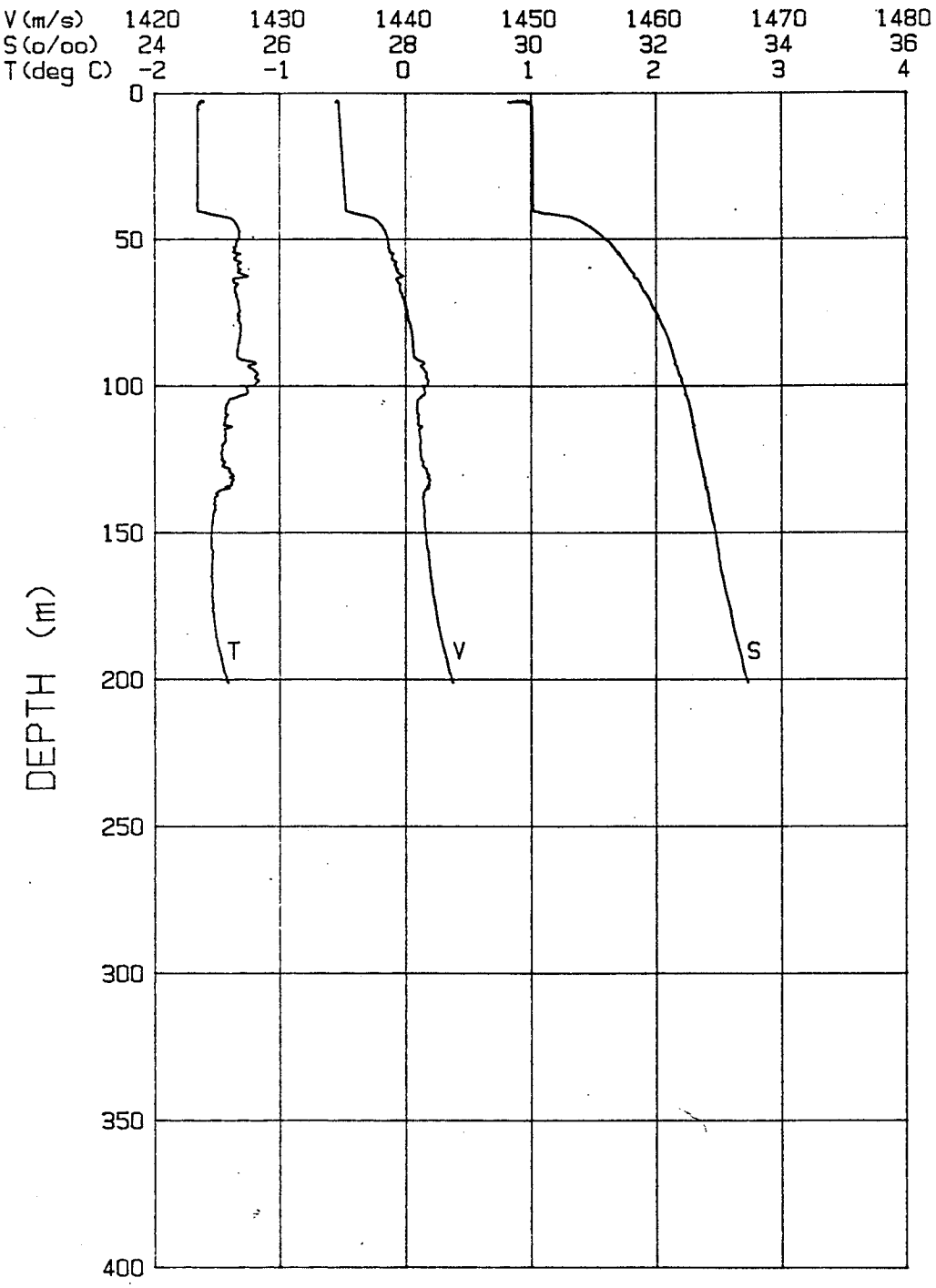
03-22-92 1410 CAST# 5 73-10.0 N 148-00.8 W
V(m/s) 1420 1430 1440 1450 1460 1470 1480
S(o/oo) 24 26 28 30 32 34 36
T(deg C) -2 -1 0 1 2 3 4
0
50
100
150
200
250
300
350
400
DEPTH (m)
T
V
S

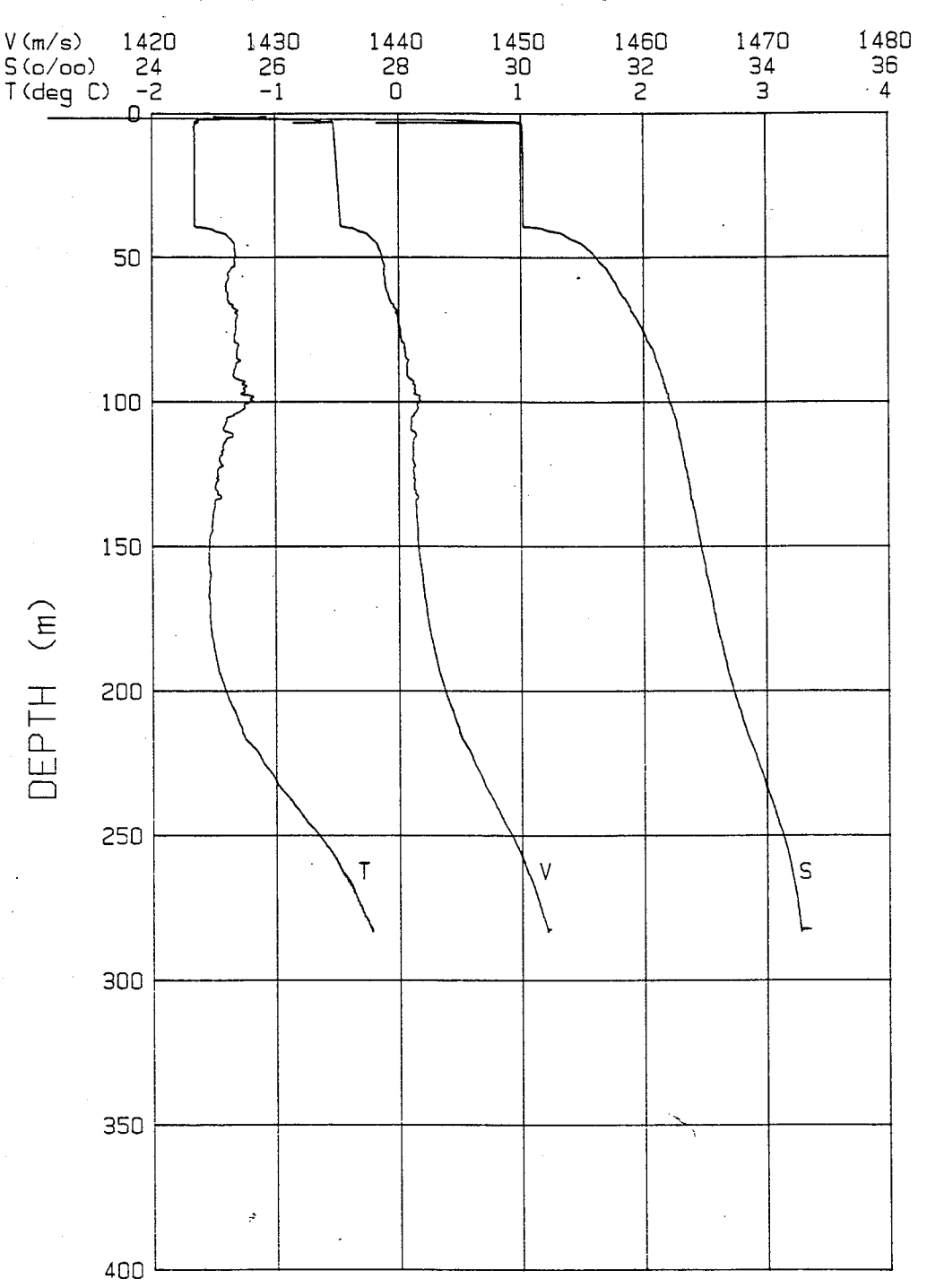
03-22-92 2134 CAST# 8
73-10.0 N 148-00.7 W
V(m/s) 1420 1430 1440 1450 1460 1470 1480
S(o/oo) 24 26 28 30 32 34 36
T(deg C) -2 -1 0 1 2 3 4
0
50
100
150
200
250
300
350
400
DEPTH (m)
T
V
S

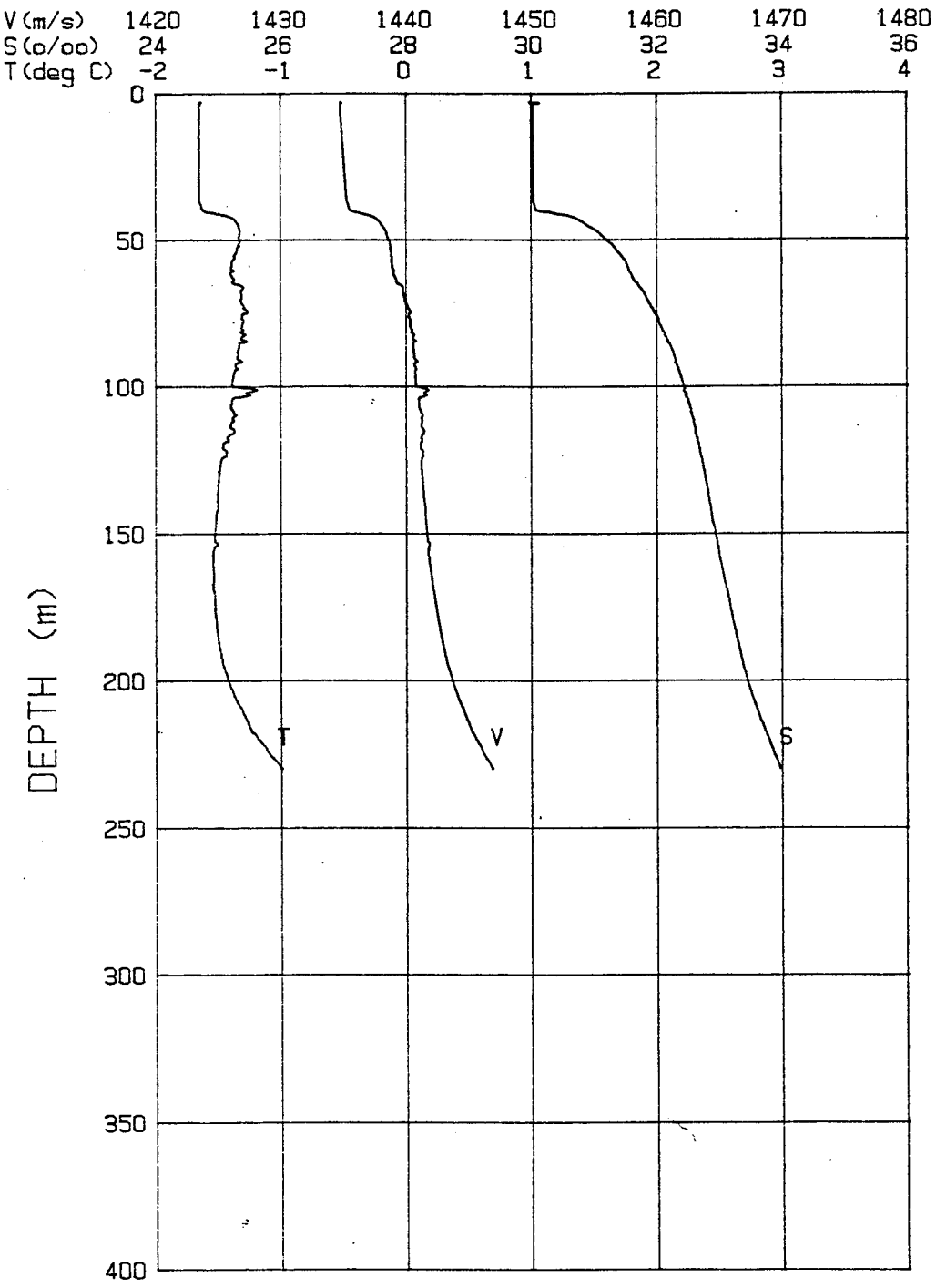
03-23-92 0645 CAST# 9 73-10.1 N 148-00.8 W
V(m/s) 1420 1430 1440 1450 1460 1470 1480
S(o/oo) 24 26 28 30 32 34 36
T(deg C) -2 -1 0 1 2 3 4
0
50
100
150
200
250
300
350
400
DEPTH (m)
T
V
S

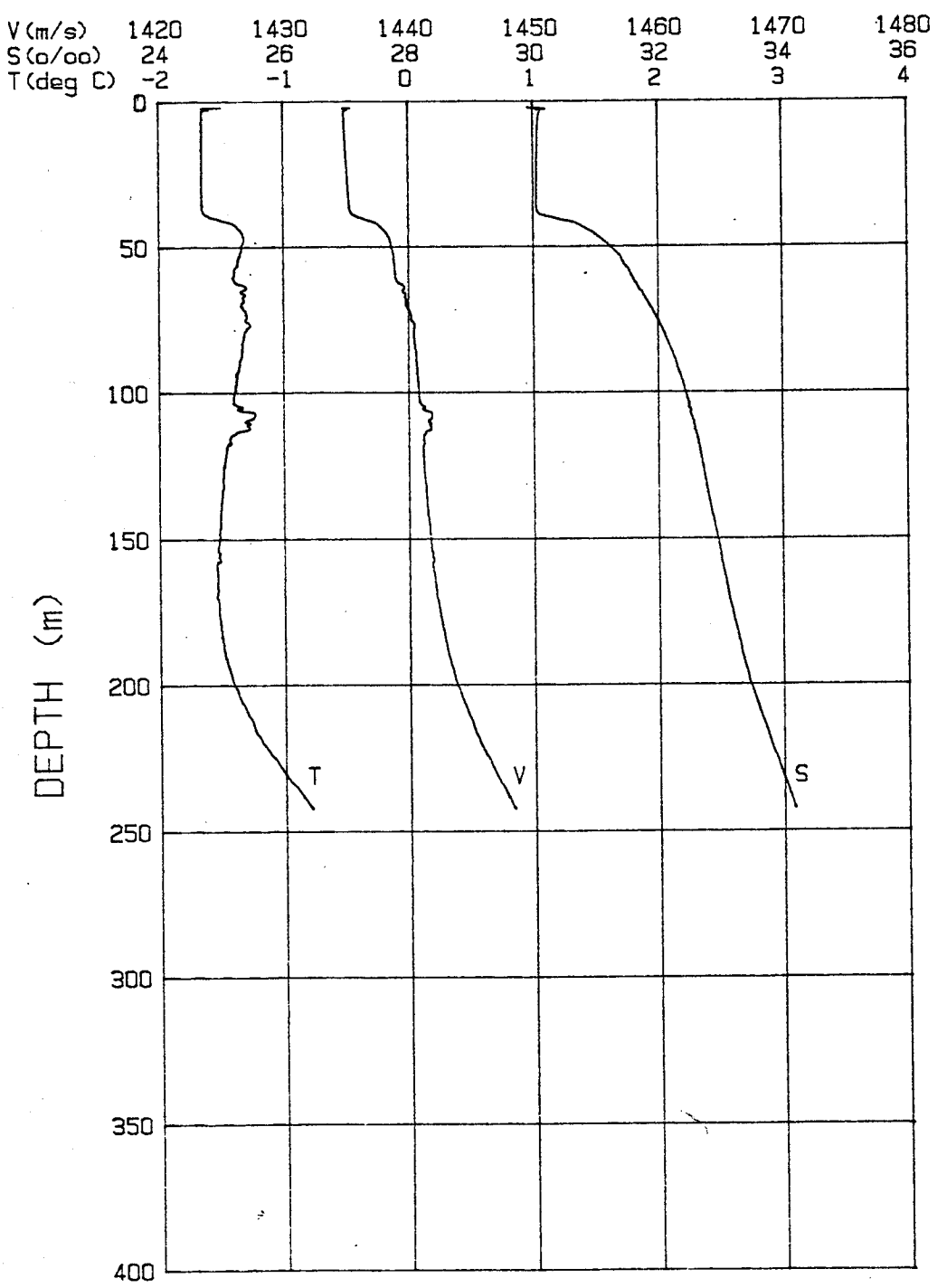
03-23-92 1537 CAST# 10 73-10.1 N 148-01.9 W
V(m/s) 1420 1430 1440 1450 1460 1470 1480
S(o/oo) 24 26 28 30 32 34 36
T(deg C) -2 -1 0 1 2 3 4
DEPTH (m)
0
50
100
150
200
250
300
350
400
T
V
S

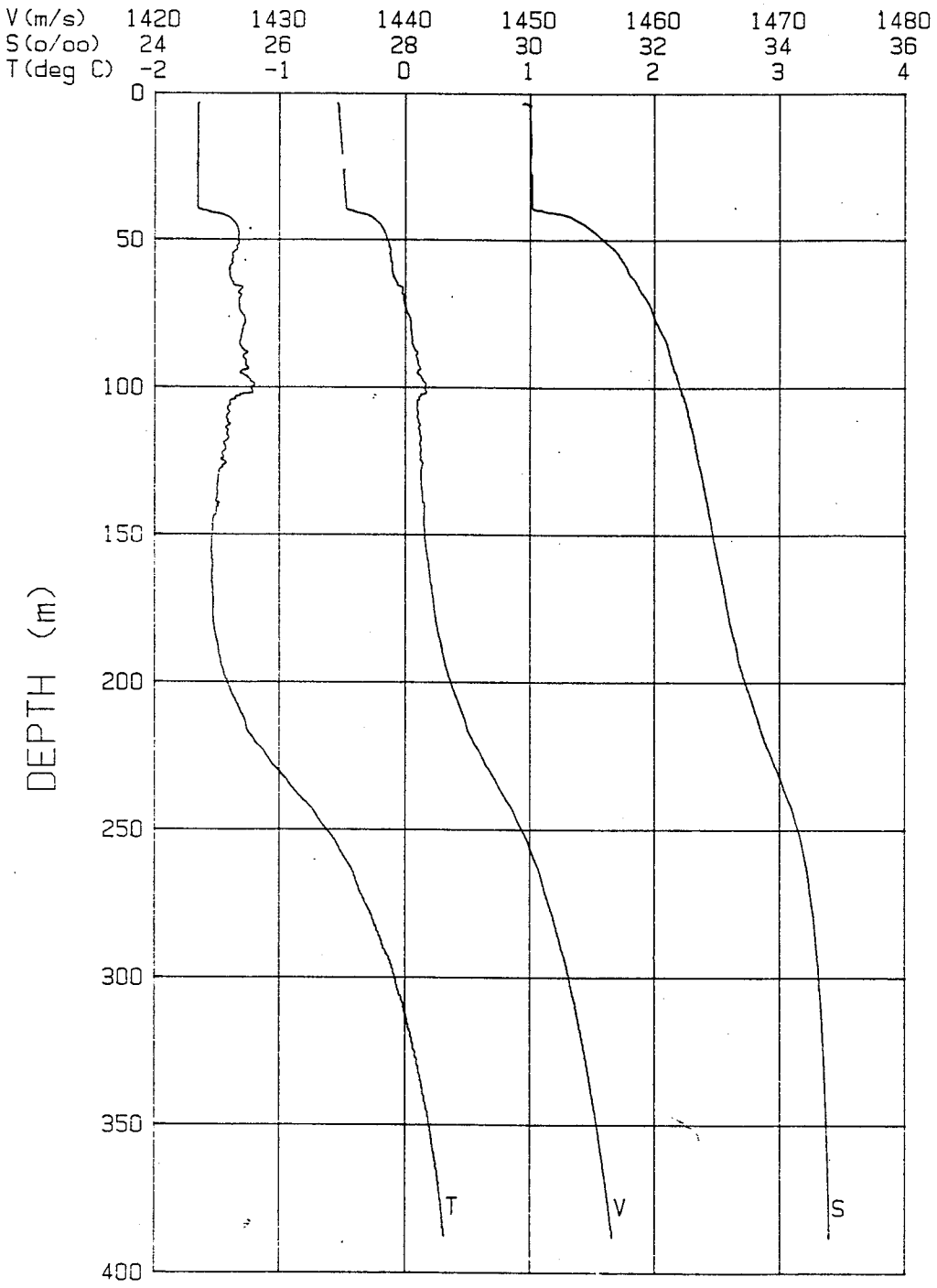
03-23-92 2011 CAST# 11 73-10.3 N 148-06.4 W
V(m/s) 1420 1430 1440 1450 1460 1470 1480
S(o/oo) 24 26 28 30 32 34 36
T(deg C) -2 -1 0 1 2 3 4
0
50
100
150
200
250
300
350
400
DEPTH (m)
T
V
S

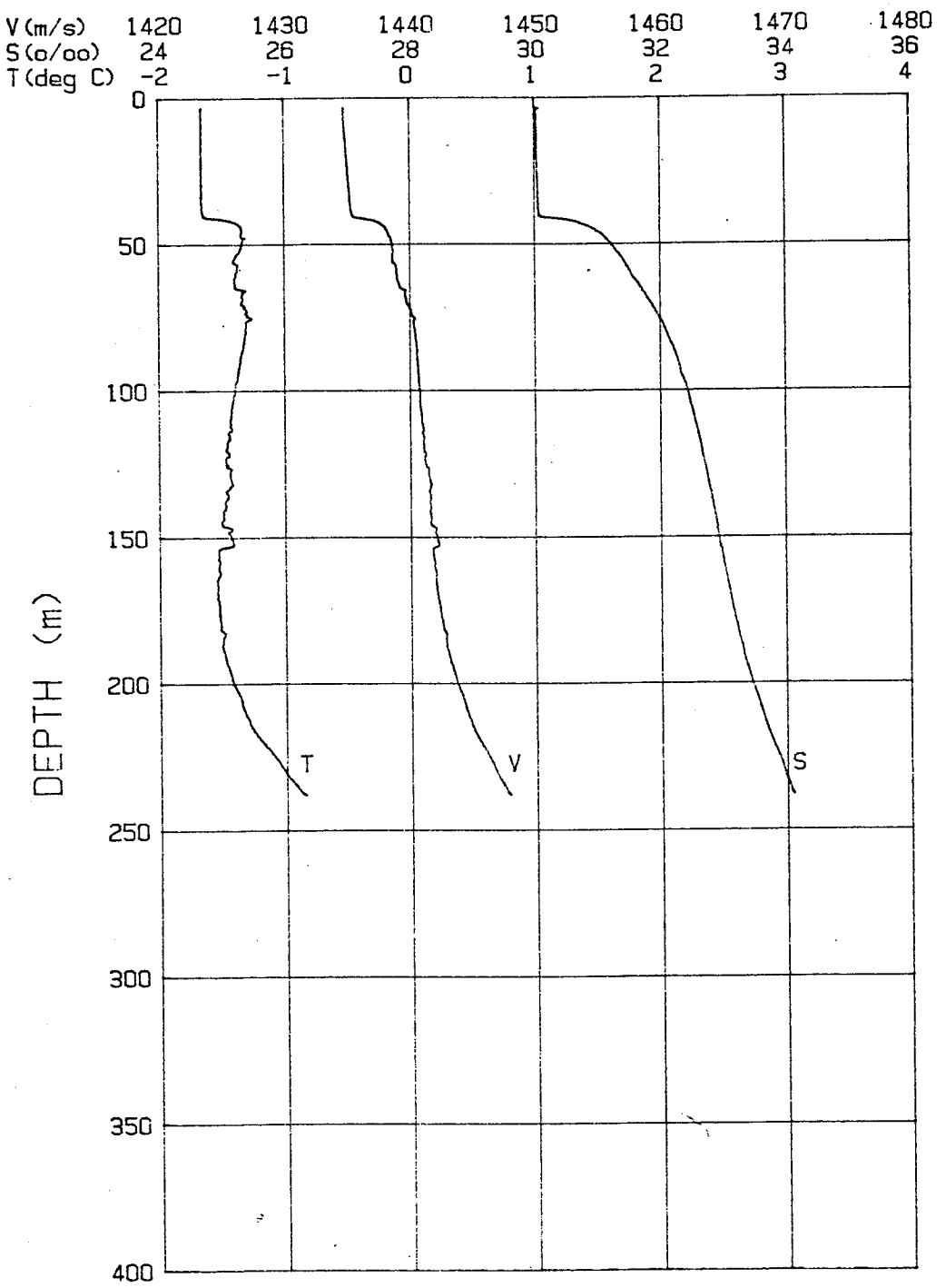
03-24-92 0651 CAST# 12 73-12.1 N 148-15.3 W
V(m/s) 1420 1430 1440 1450 1460 1470 1480
S(o/oo) 24 26 28 30 32 34 36
T(deg C) -2 -1 0 1 2 3 4
0
50
100
150
200
250
300
350
400
DEPTH (m)
T
V
S

03-24-92 1240 CAST# 13 73-13.2 N 148-19.0 W

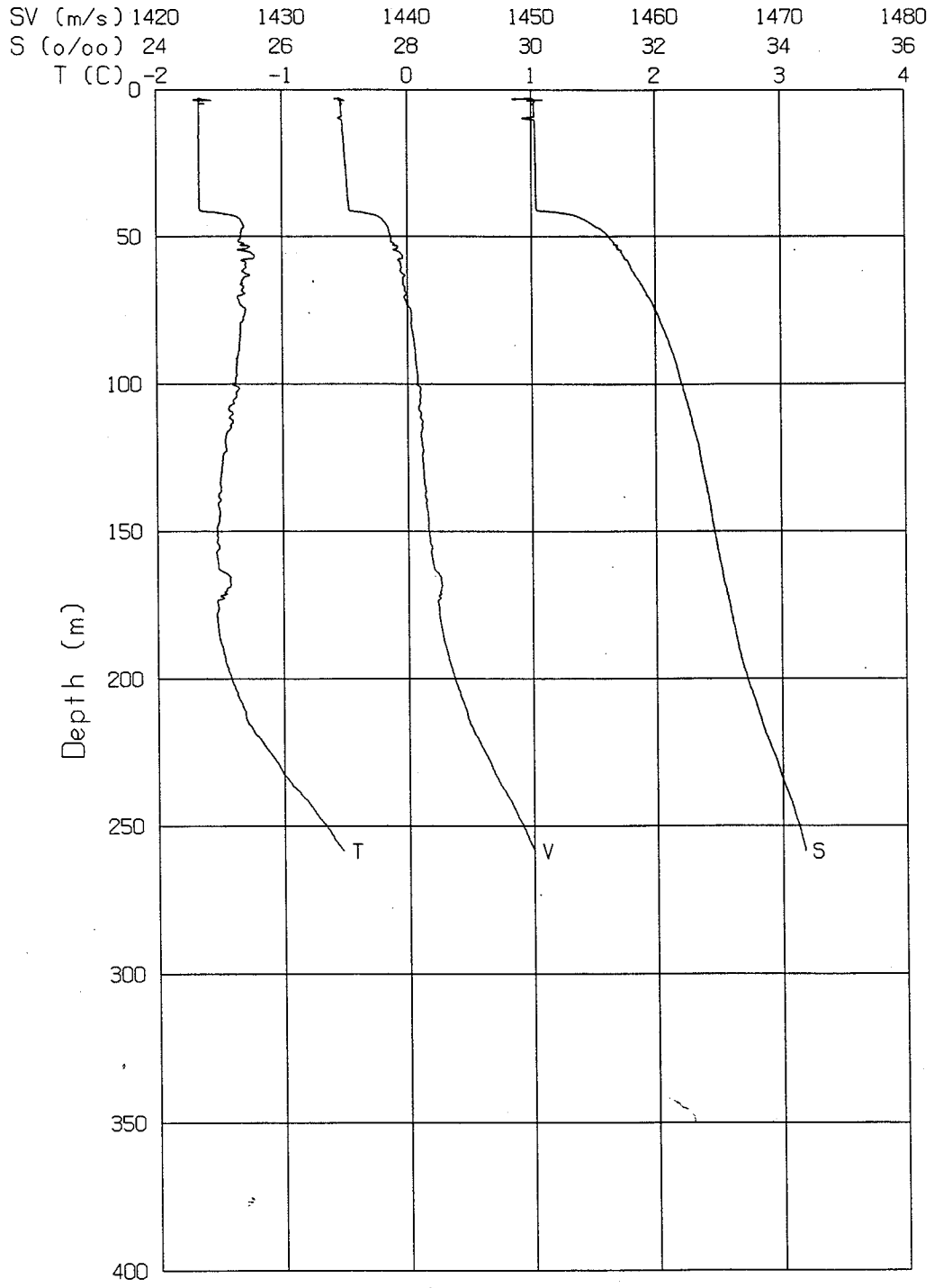

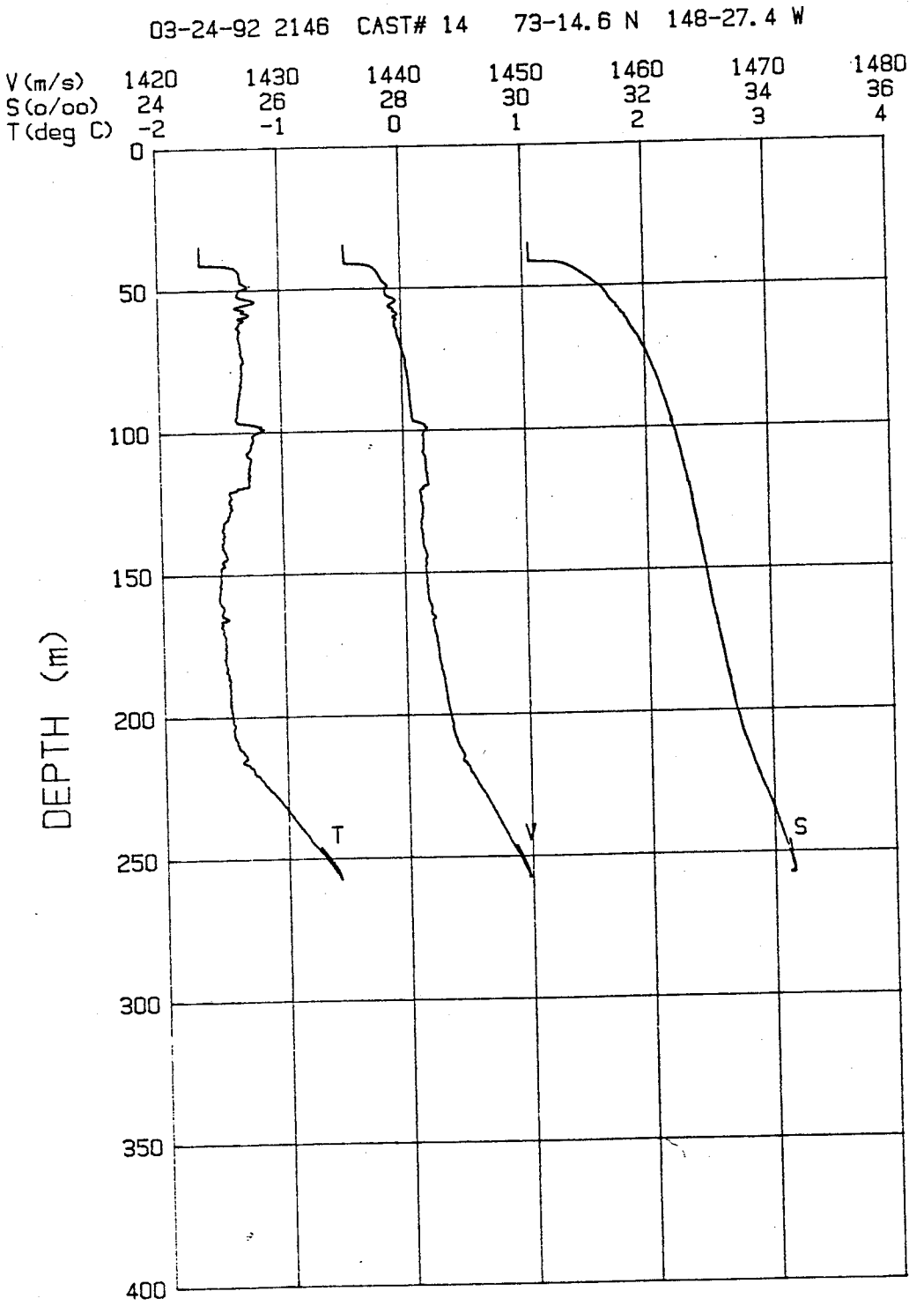
03-24-92 2146 CAST# 14 73-14.6 N 148-27.4 W
V(m/s) 1420 1430 1440 1450 1460 1470 1480
S(o/oo) 24 26 28 30 32 34 36
T(deg C) -2 -1 0 1 2 3 4
0
50
100
150
200
250
300
350
400
DEPTH (m)
T
V
S

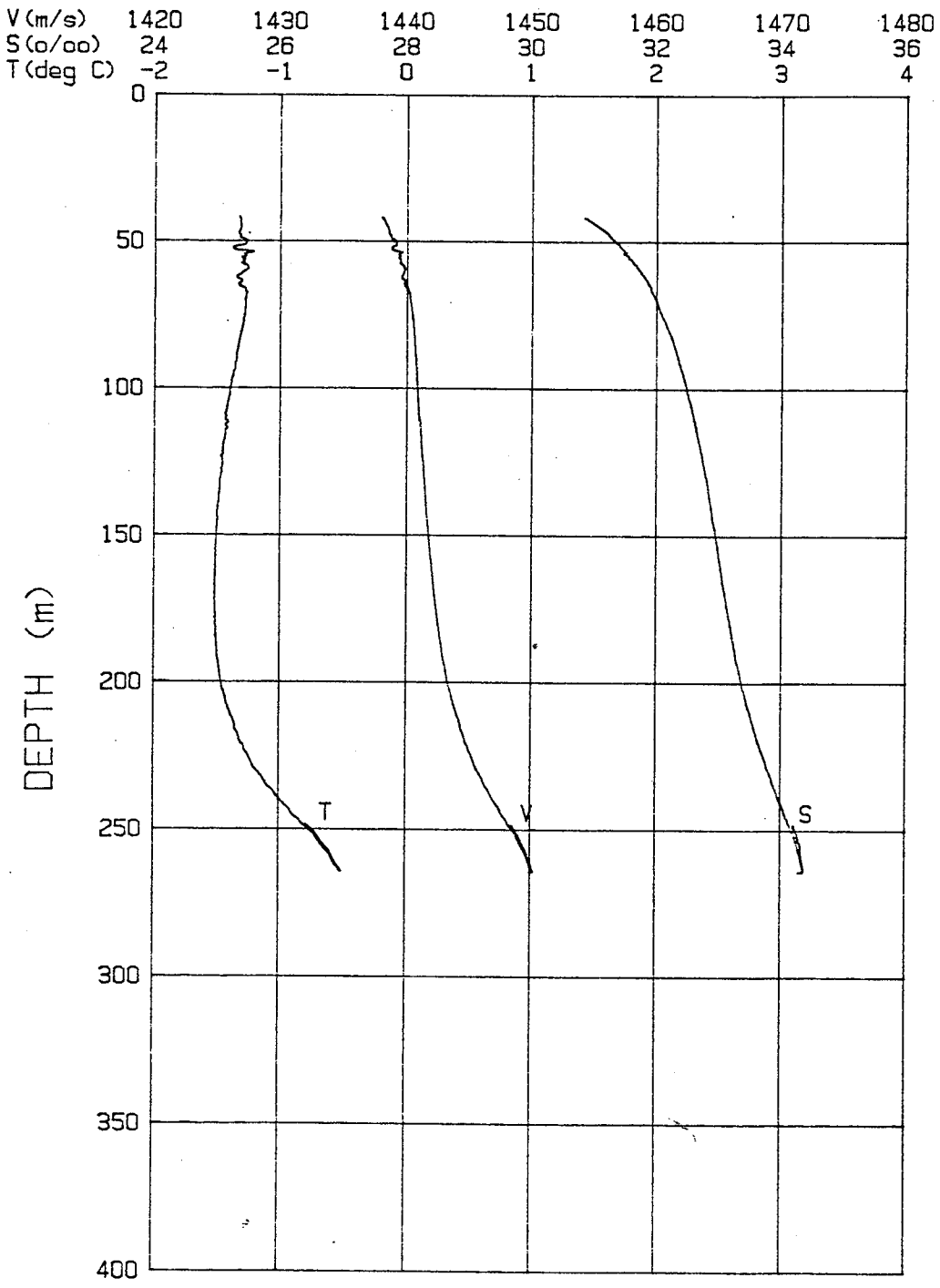
03-25-92 0808 CAST# 15 73-15.9 N 148-35.5 W
V(m/s) 1420 1430 1440 1450 1460 1470 1480
S(o/oo) 24 26 28 30 32 34 36
T(deg C) -2 -1 0 1 2 3 4
0
50
100
150
200
250
300
350
400
DEPTH (m)
T
V
S

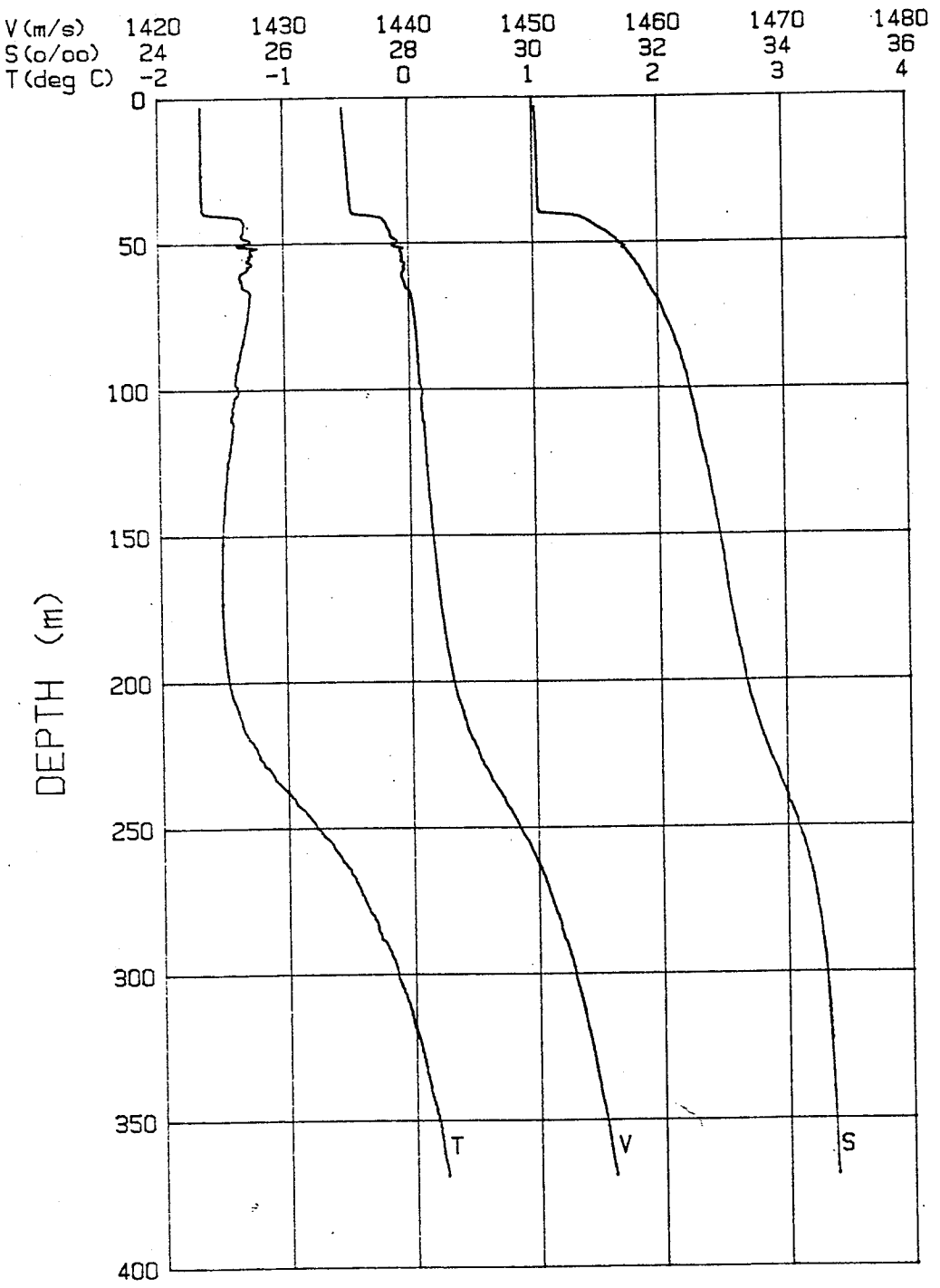
03-25-92 1008 CAST# 16 73-16.2 N 148-36.0 W
V(m/s) 1420 1430 1440 1450 1460 1470 1480
S(o/oo) 24 26 28 30 32 34 36
T(deg C) -2 -1 0 1 2 3 4
0
50
100
150
200
250
300
350
400
DEPTH (m)
T
V
S

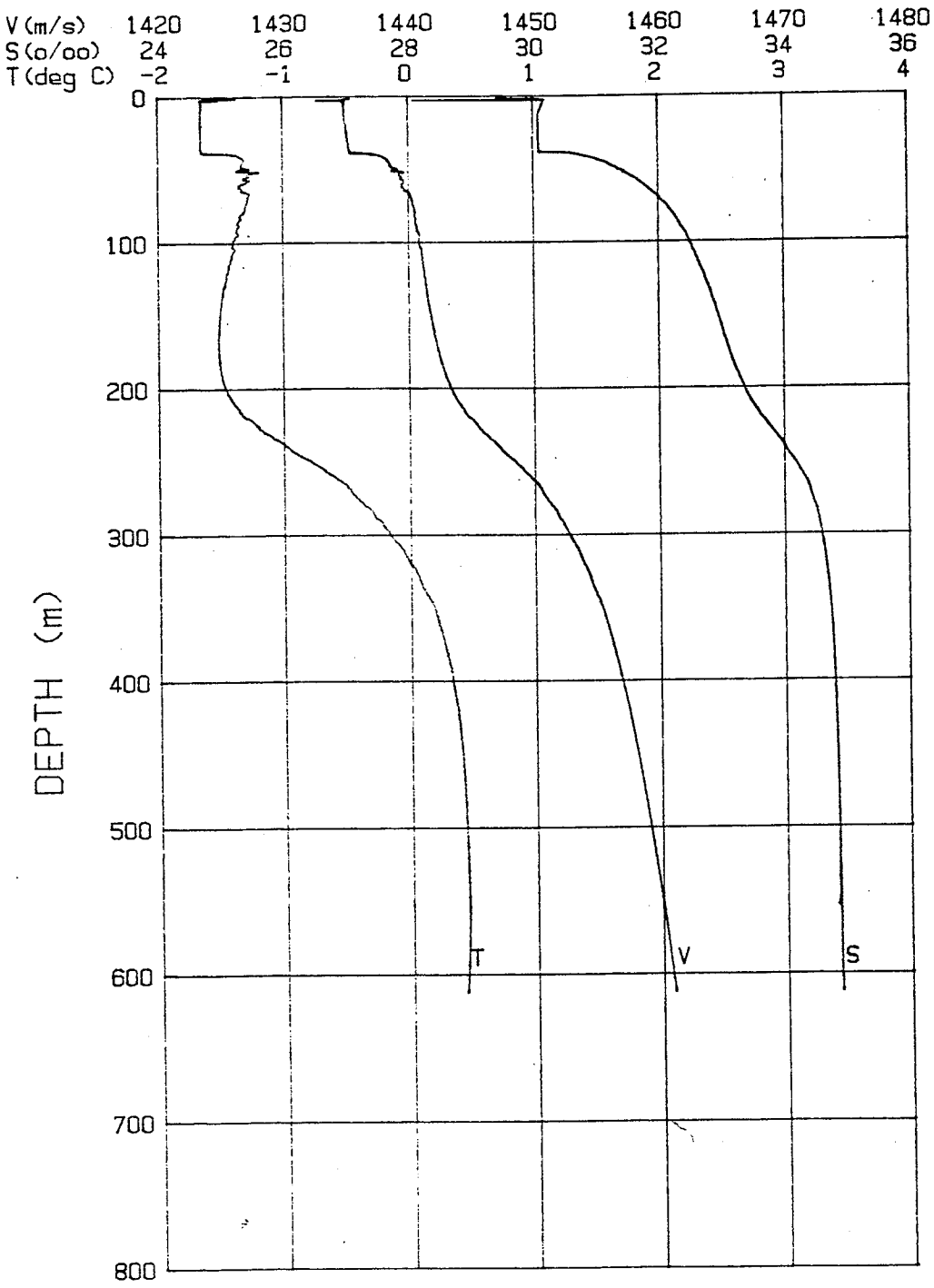
03-25-92 1101 CAST# 17 73-16.4 N 148-35.9 W
V(m/s) 1420 1430 1440 1450 1460 1470 1480
S(o/oo) 24 26 28 30 32 34 36
T(deg C) -2 -i 0 1 2 3 4
0
100
200
300
400
500
600
700
800
DEPTH (m)
T
V
S

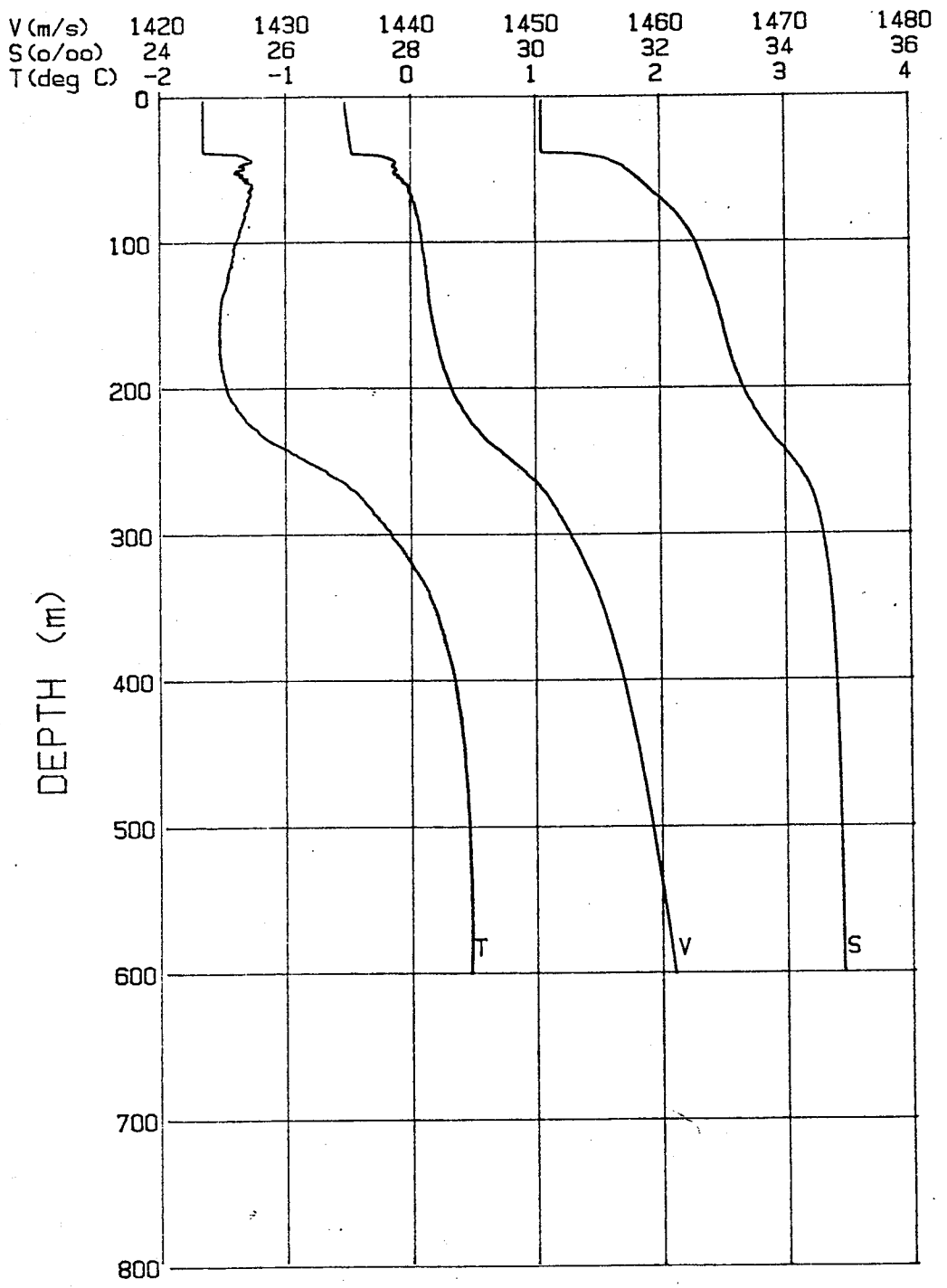
03-25-92 1825 CAST# 18 73-17.5 N 148-34.2 W
V(m/s) 1420 1430 1440 1450 1460 1470 1480
S(o/oo) 24 26 28 30 32 34 36
T(deg C) -2 -1 0 1 2 3 4
0
100
200
300
400
500
600
700
800
DEPTH (m)
T
V
S

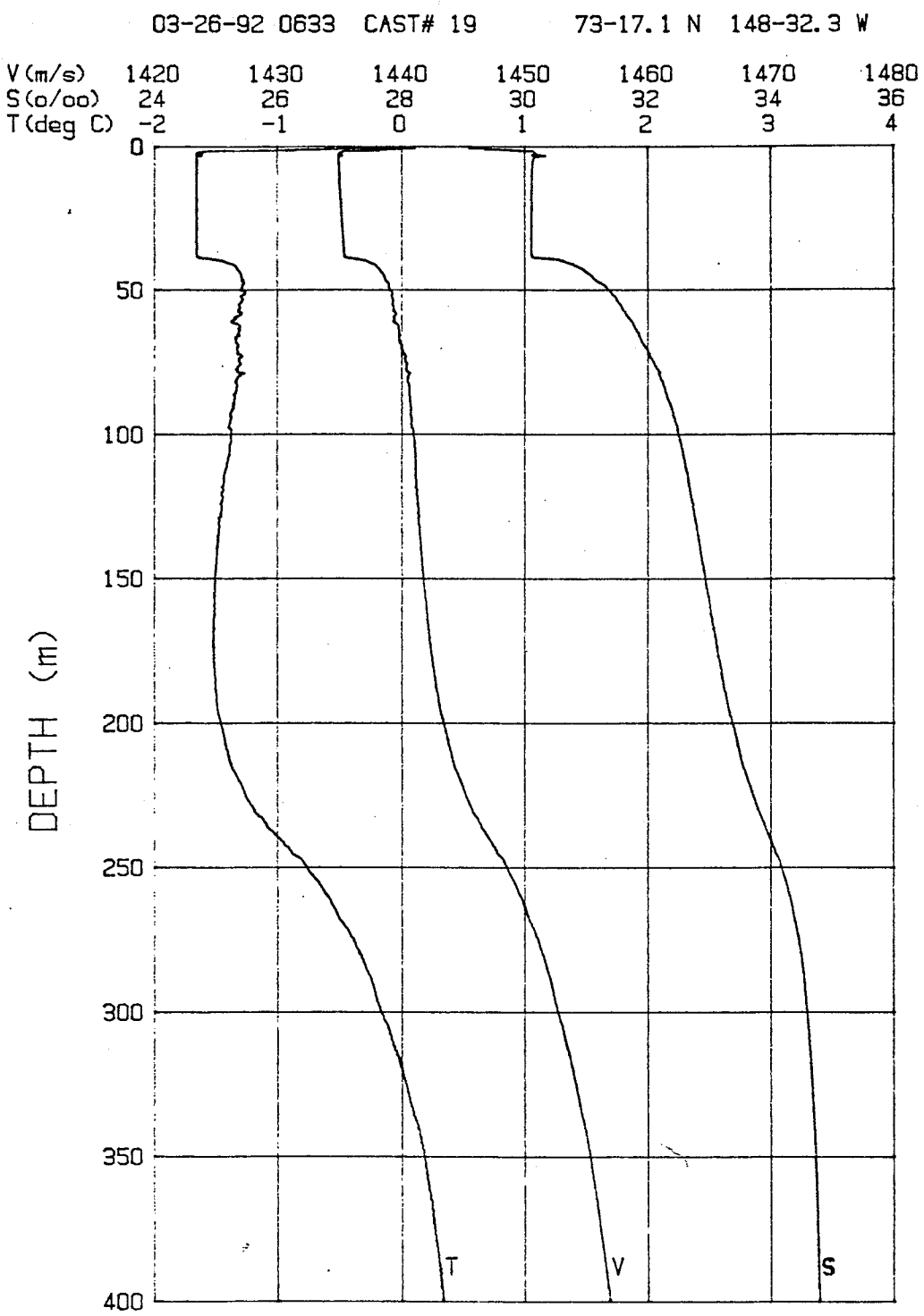
03-26-92 0633 CAST# 19
73-17.1 N 148-32.3 W
V(m/s) 1420 1430 1440 1450 1460 1470 1480
S(o/oo) 24 26 28 30 32 34 36
T(deg C) -2 -1 0 1 2 3 4
DEPTH (m)
0
50
100
150
200
250
300
350
400
T
V
S

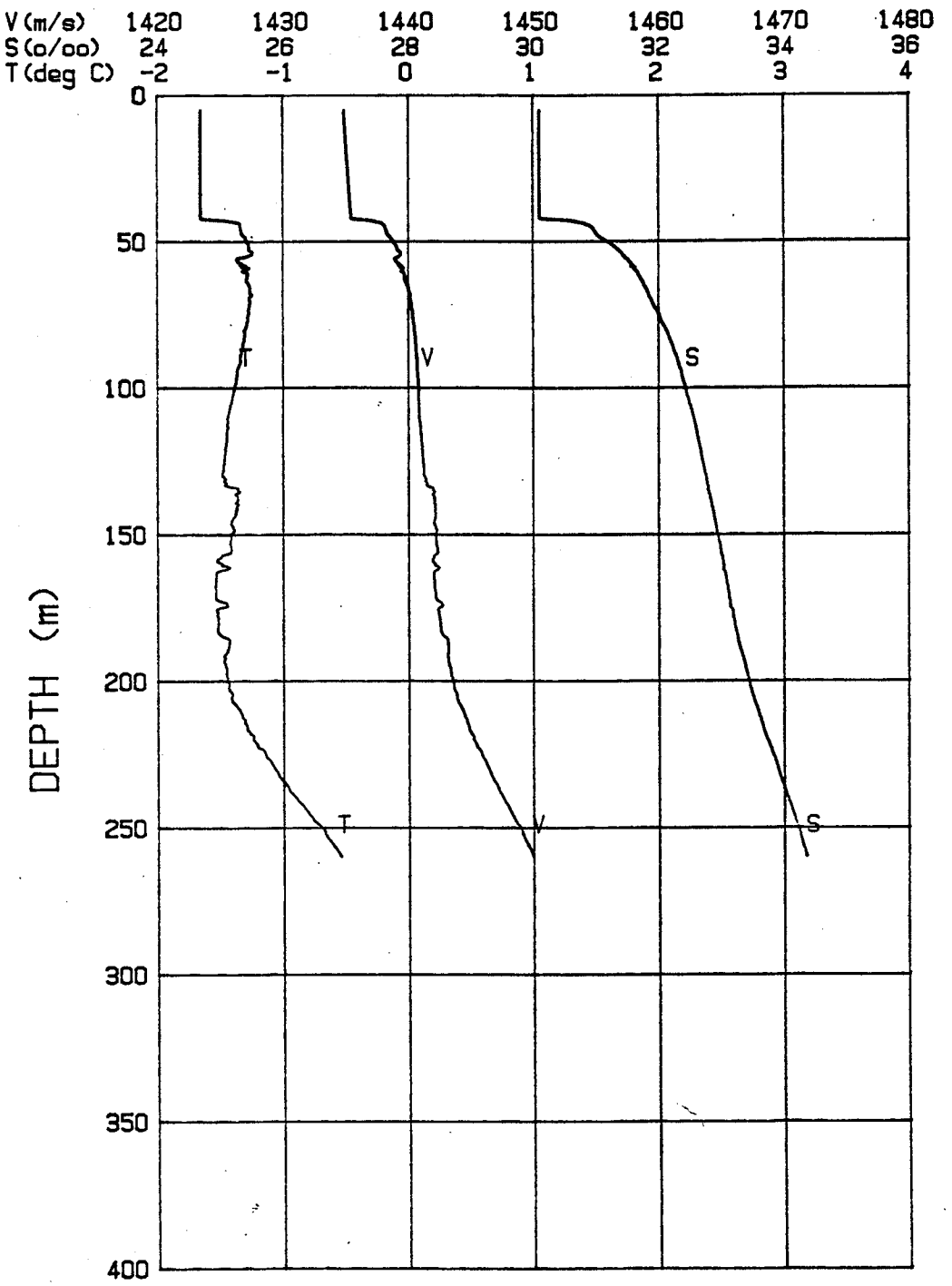
03-26-92 2254 CAST# 21 73-15.4 N 148-30.3 W
V(m/s) 1420 1430 1440 1450 1460 1470 1480
S(o/oo) 24 26 28 30 32 34 36
T(deg C) -2 -1 0 1 2 3 4
0
50
100
150
200
250
300
350
400
DEPTH (m)
T
V
S
T
V
S

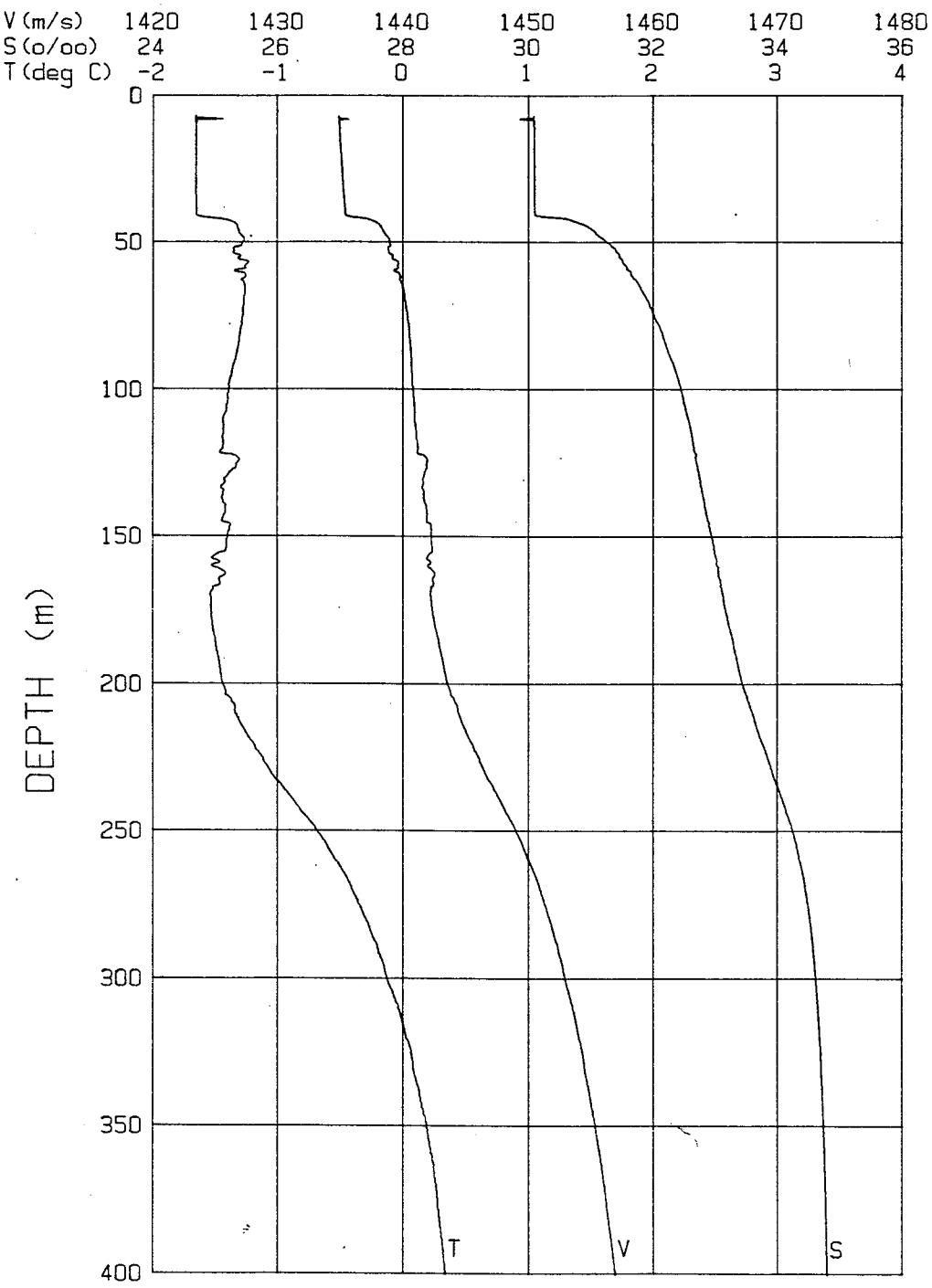
03-27-92 0701 CAST# 22 73-15.2 N 148-29.7 W
V(m/s) 1420 1430 1440 1450 1460 1470 1480
S(o/oo) 24 26 28 30 32 34 36
T(deg C) -2 -1 0 1 2 3 4
0
50
100
150
200
250
300
350
400
DEPTH (m)
T
V
S

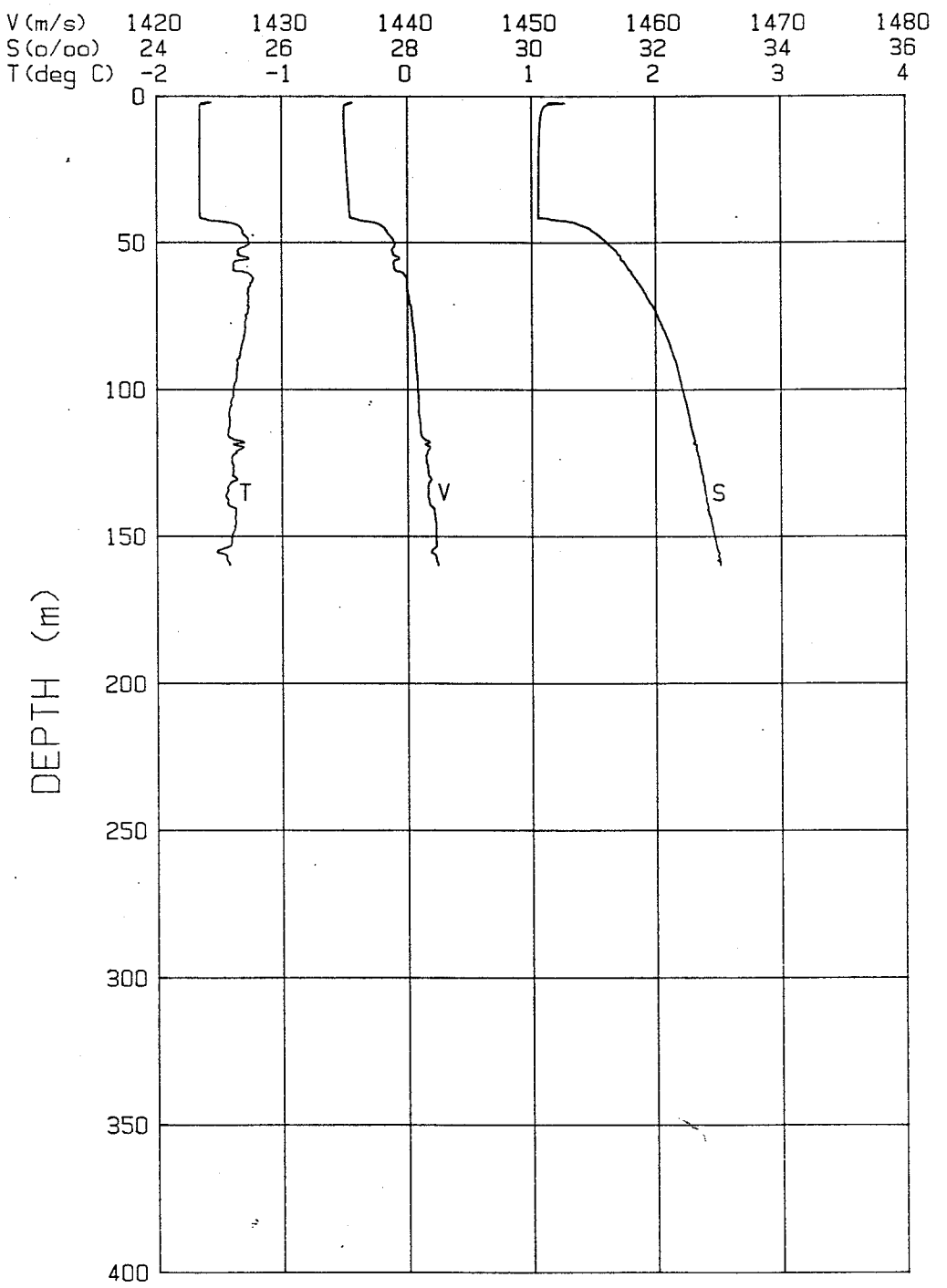
03-27-92 1354 CAST# 23 73-15.2 N 148-29.5 W
V(m/s) 1420 1430 1440 1450 1460 1470 1480
S(o/oo) 24 26 28 30 32 34 36
T(deg C) -2 -1 0 1 2 3 4
0
50
100
150
200
250
300
350
400
DEPTH (m)
T
V
S

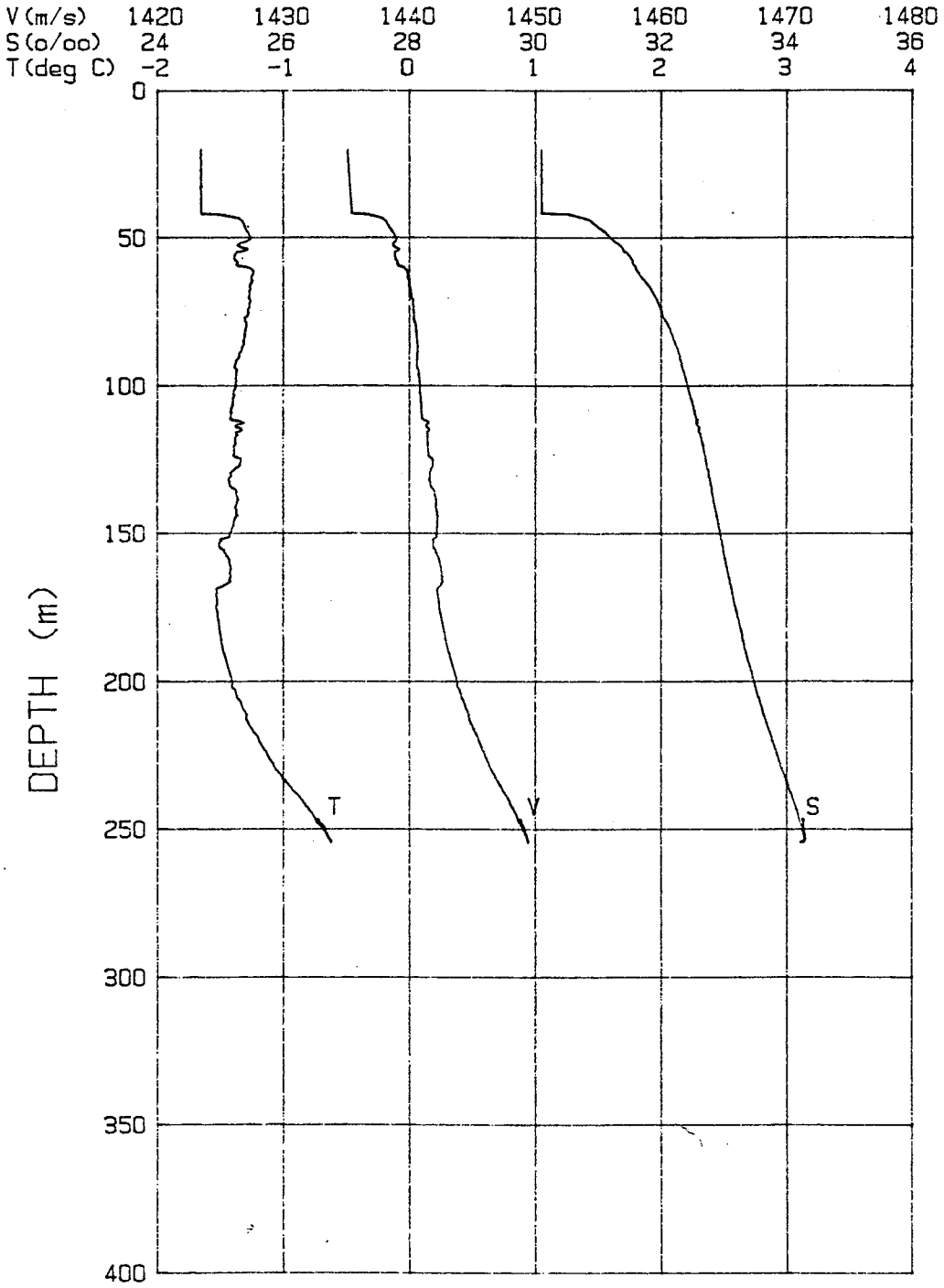
03-27-92 1623 CAST# 24 73-15.2 N 148-29.5 W
V(m/s) 1420 1430 1440 1450 1460 1470 1480
S(o/oo) 24 26 28 30 32 34 36
T(deg C) -2 -1 0 1 2 3 4
DEPTH (m)
0
50
100
150
200
250
300
350
400
T
V
S

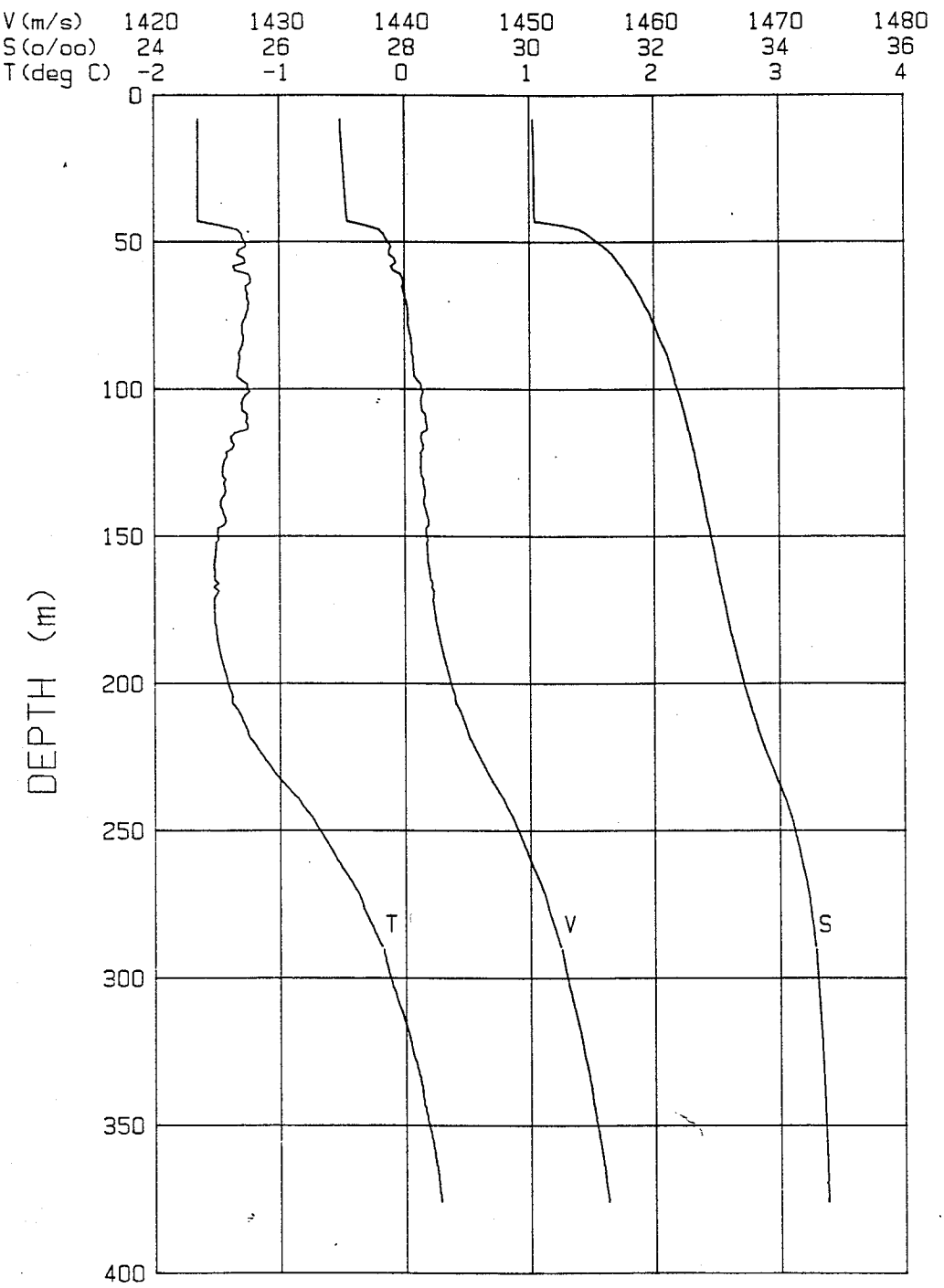
03-27-92 2007 CAST# 25 73-15.2 N 148-29.1 W
V(m/s) 1420 1430 1440 1450 1460 1470 1480
S(o/oo) 24 26 28 30 32 34 36
T(deg C) -2 -1 0 1 2 3 4
0
50
100
150
200
250
300
350
400
DEPTH (m)
T
V
S

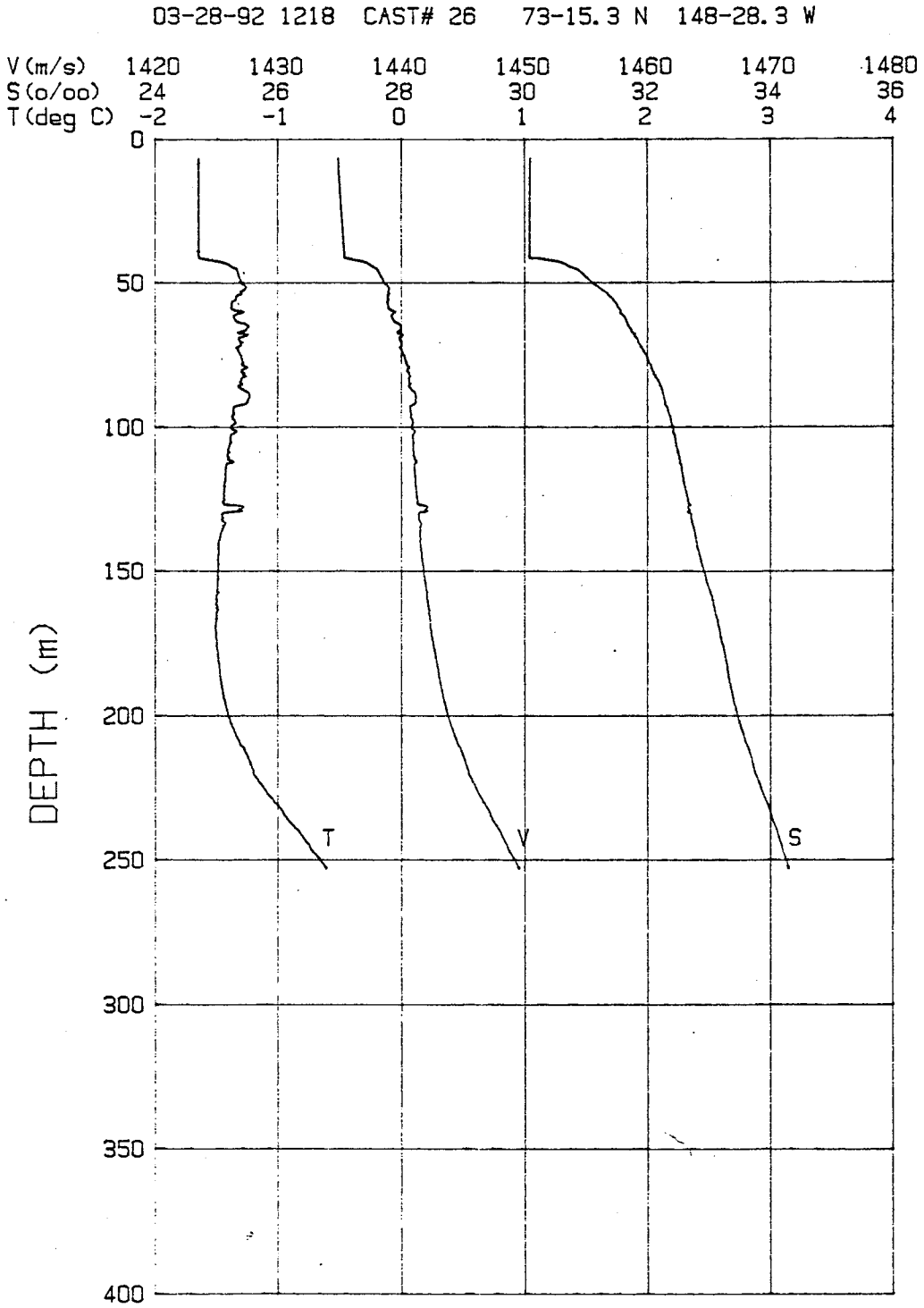
03-28-92 1218 CAST# 26 73-15.3 N 148-28.3 W
V(m/s) 1420 1430 1440 1450 1460 1470 1480
S(o/oo) 24 26 28 30 32 34 36
T(deg C) -2 -1 0 1 2 3 4
0
50
100
150
200
250
300
350
400
DEPTH (m)
T
V
S

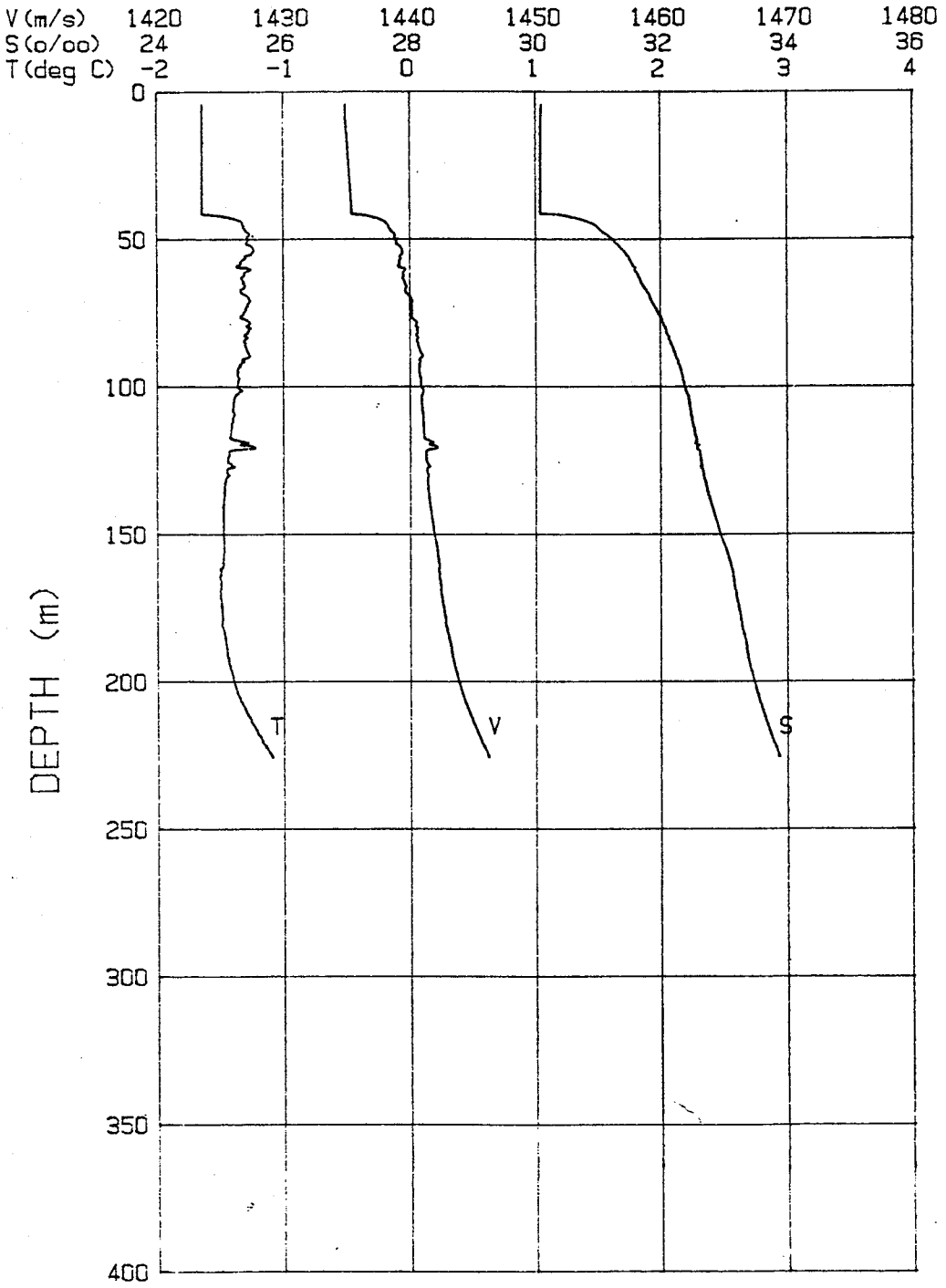
03-28-92 1754 CAST# 27 73-15.4 N 148-28.0 W
V(m/s) 1420 1430 1440 1450 1460 1470 1480
S(o/oo) 24 26 28 30 32 34 36
T(deg C) -2 -1 0 1 2 3 4
0
50
100
150
200
250
300
350
400
DEPTH (m)
T
V
S

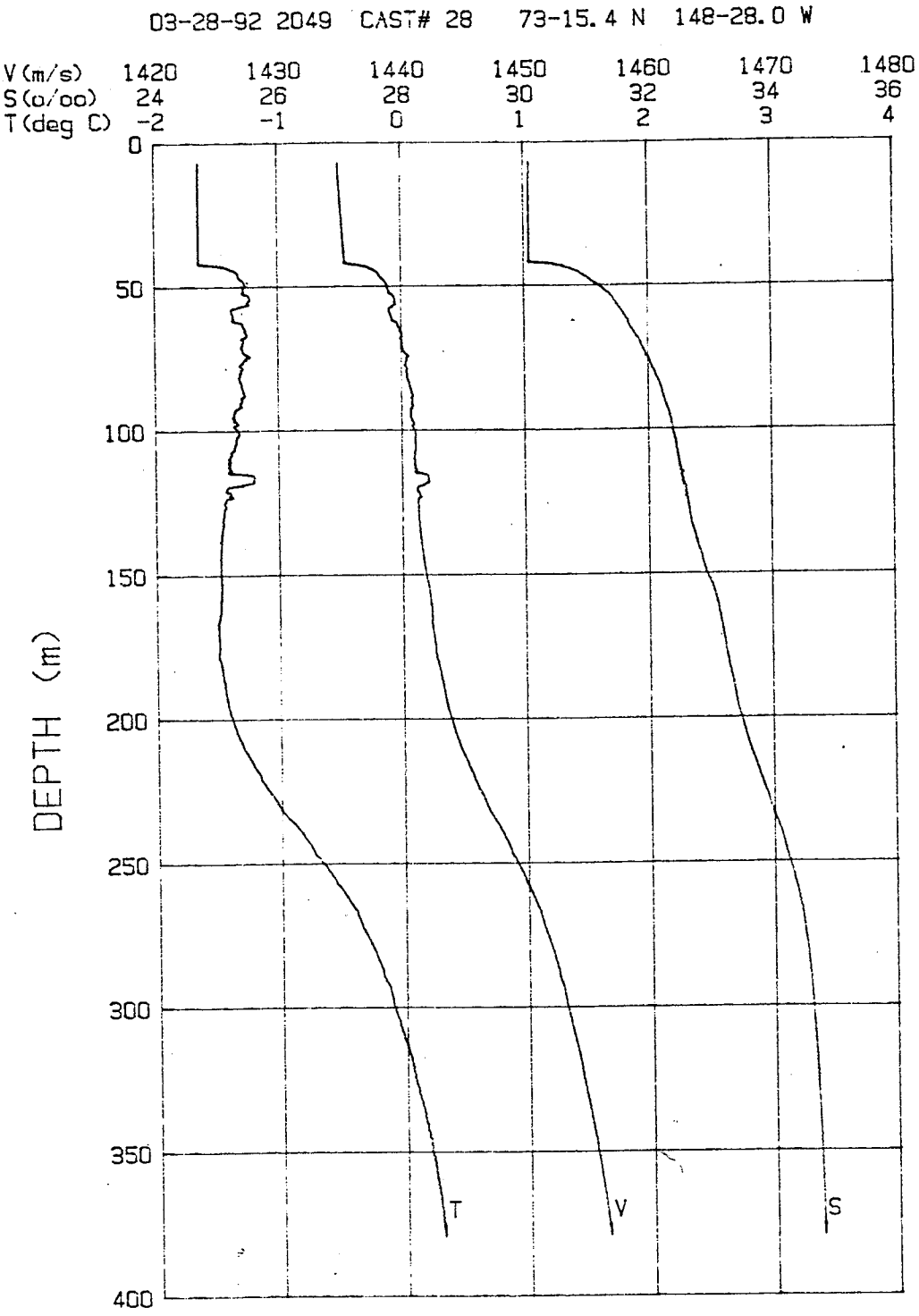
03-28-92 2049 CAST# 28 73-15.4 N 148-28.0 W
V(m/s) 1420 1430 1440 1450 1460 1470 1480
S(o/oo) 24 26 28 30 32 34 36
T(deg C) -2 -1 0 1 2 3 4
DEPTH (m)
0
50
100
150
200
250
300
350
400
T
V
S

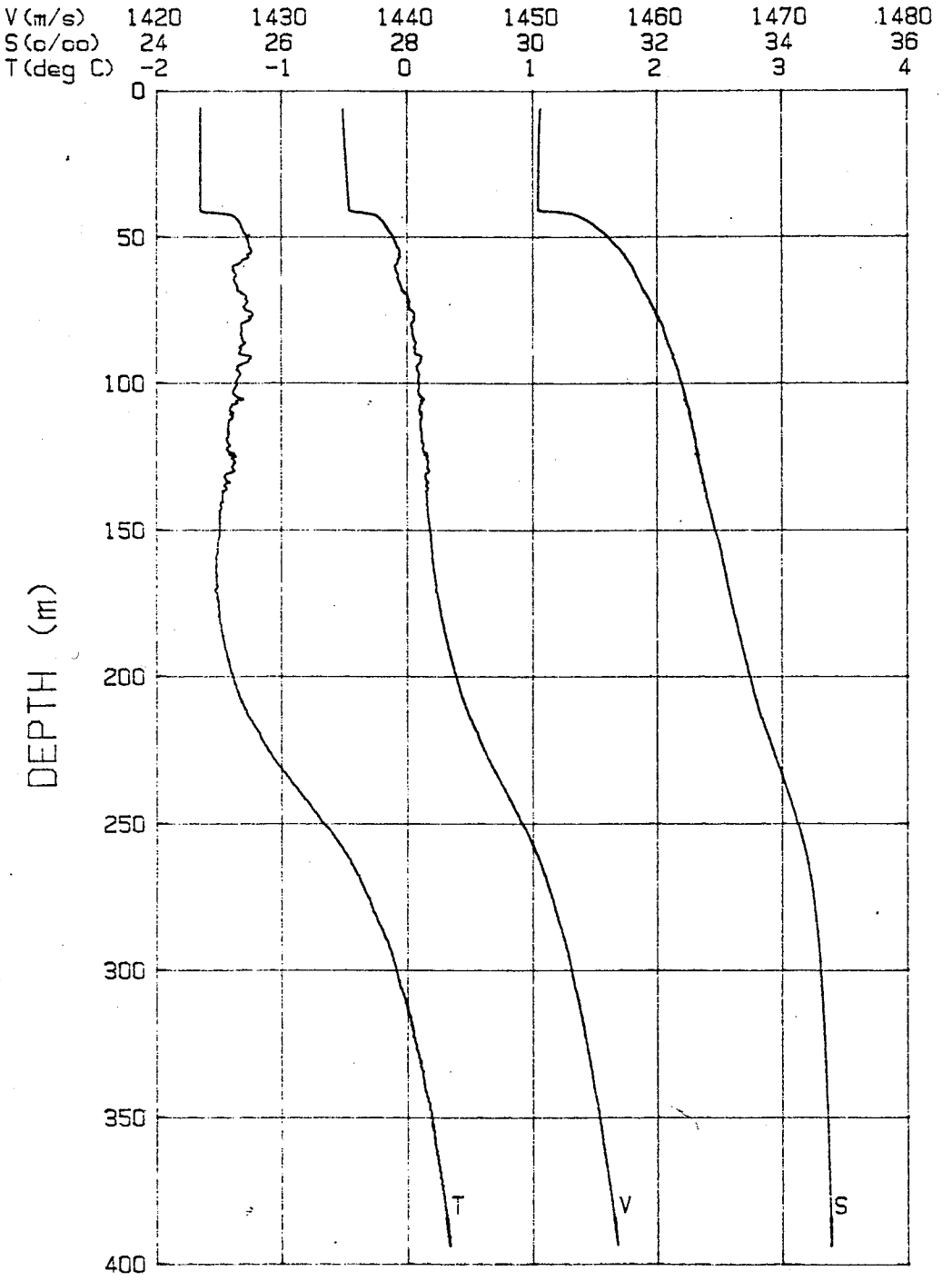
03-29-92 0740 CAST# 29 73-15.5 N 148-18.8 W
V(m/s) 1420 1430 1440 1450 1460 1470 1480
S(o/oo) 24 26 28 30 32 34 36
T(deg C) -2 -1 0 1 2 3 4
0
50
100
150
200
250
300
350
400
DEPTH (m)
T
V
S

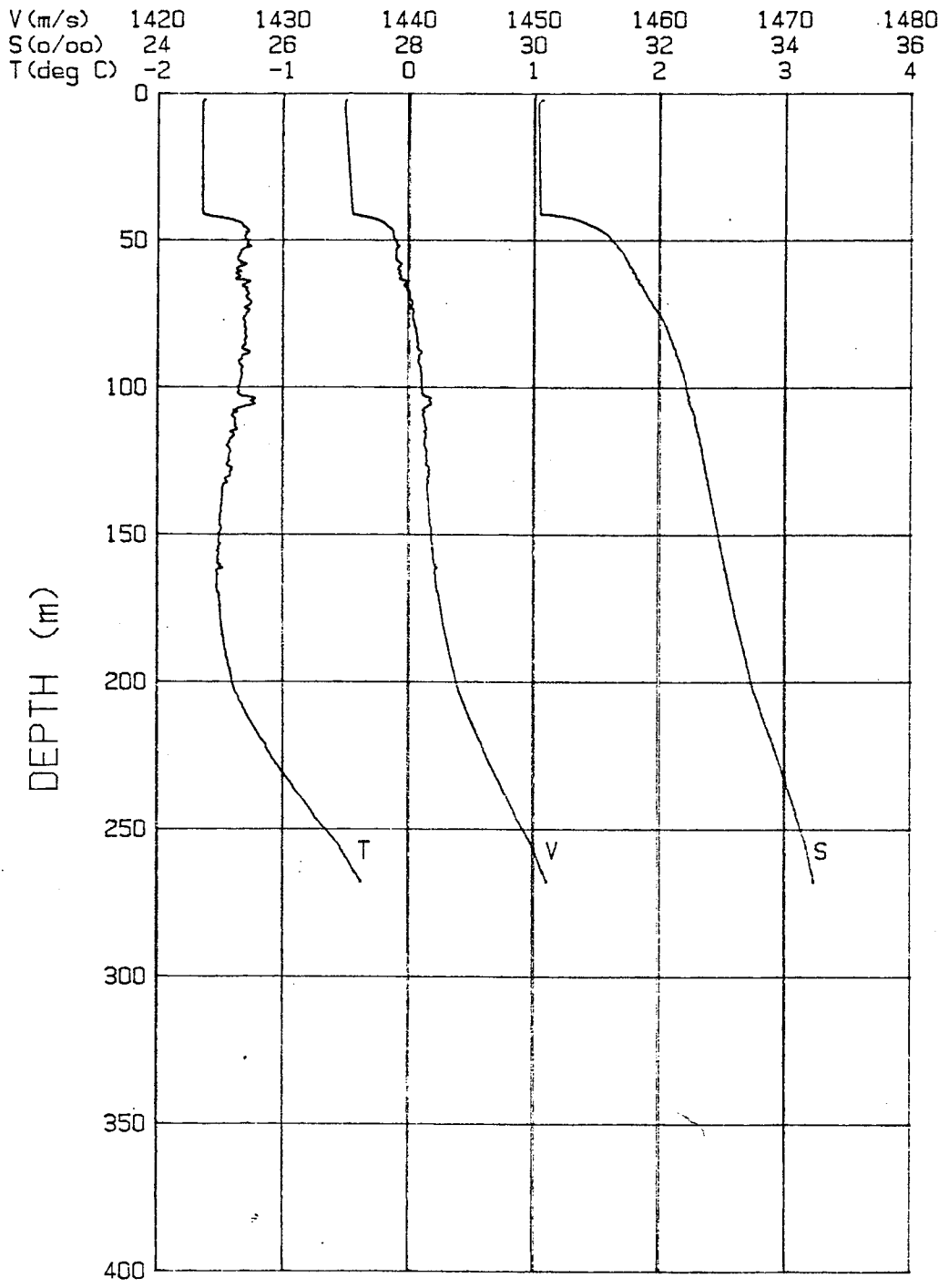
03-29-92 1824 CAST# 30 73-16.0 N 148-30.4 W
V(m/s) 1420 1430 1440 1450 1460 1470 1480
S(o/oo) 24 26 28 30 32 34 36
T(deg C) -2 -1 0 1 2 3 4
DEPTH (m)
0
50
100
150
200
250
300
350
400
T
V
S

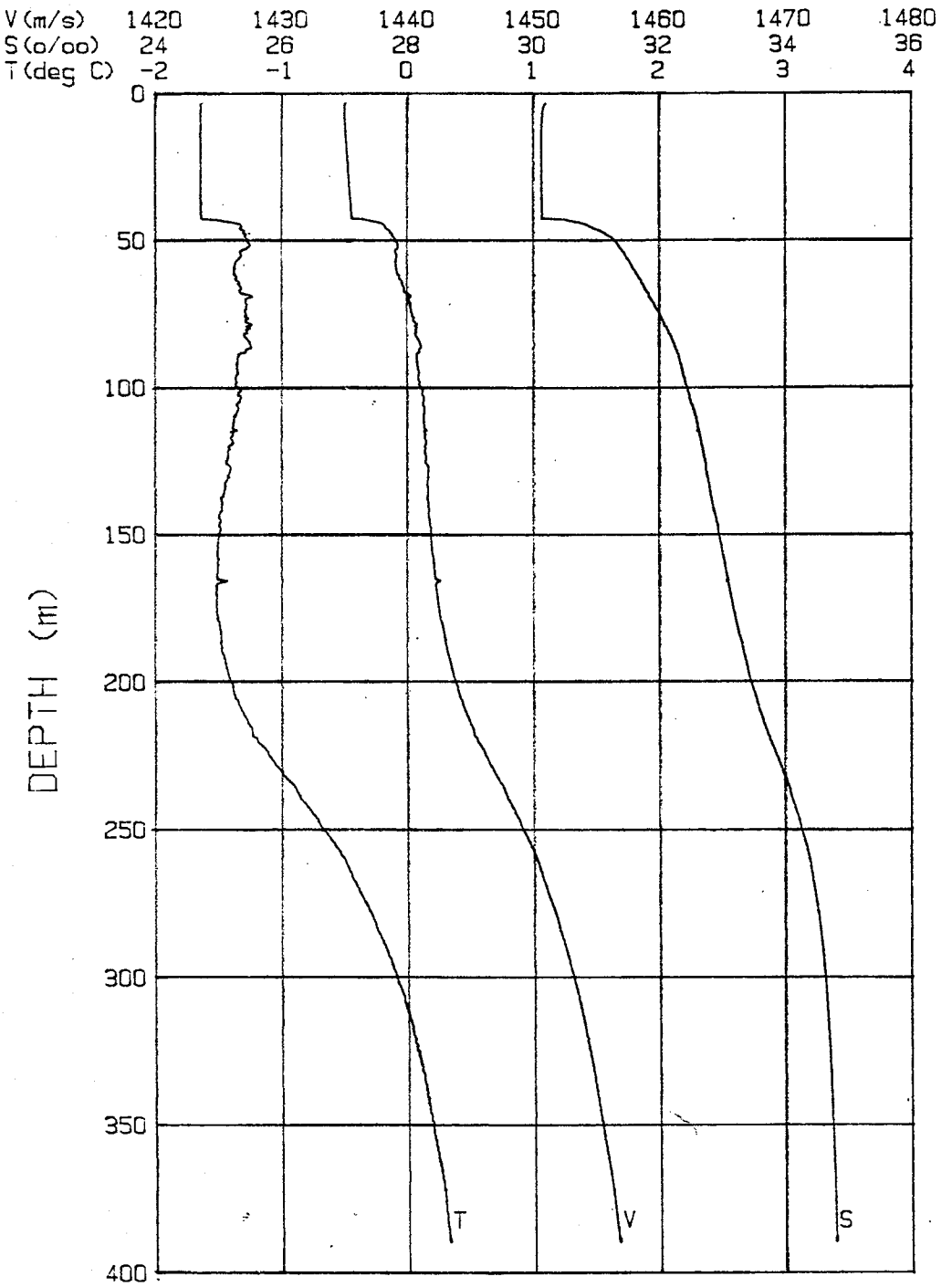
03-30-92 0627 CAST# 31 73-16.9 N 148-33.7 W
V(m/s) 1420 1430 1440 1450 1460 1470 1480
S(o/oo) 24 26 28 30 32 34 36
T(deg C) -2 -1 0 1 2 3 4
0
50
100
150
200
250
300
350
400
DEPTH (m)
T
V
S

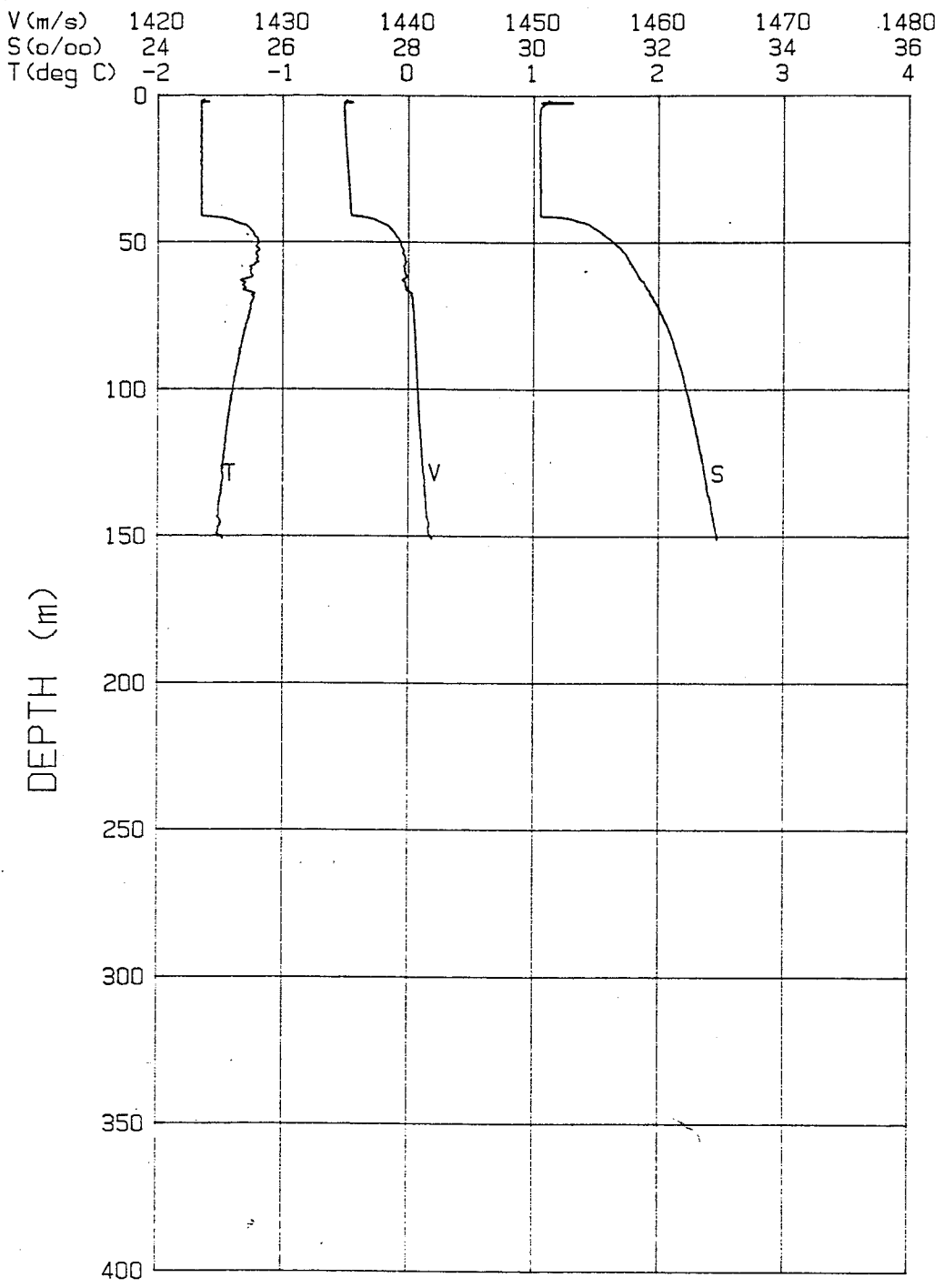
03-30-92 1745 CAST# 32
73-18.4 N 148-39.5 W
V(m/s) 1420 1430 1440 1450 1460 1470 1480
S(o/oo) 24 26 28 30 32 34 36
T(deg C) -2 -1 0 1 2 3 4
0
50
100
150
200
250
300
350
400
DEPTH (m)
T
V
S

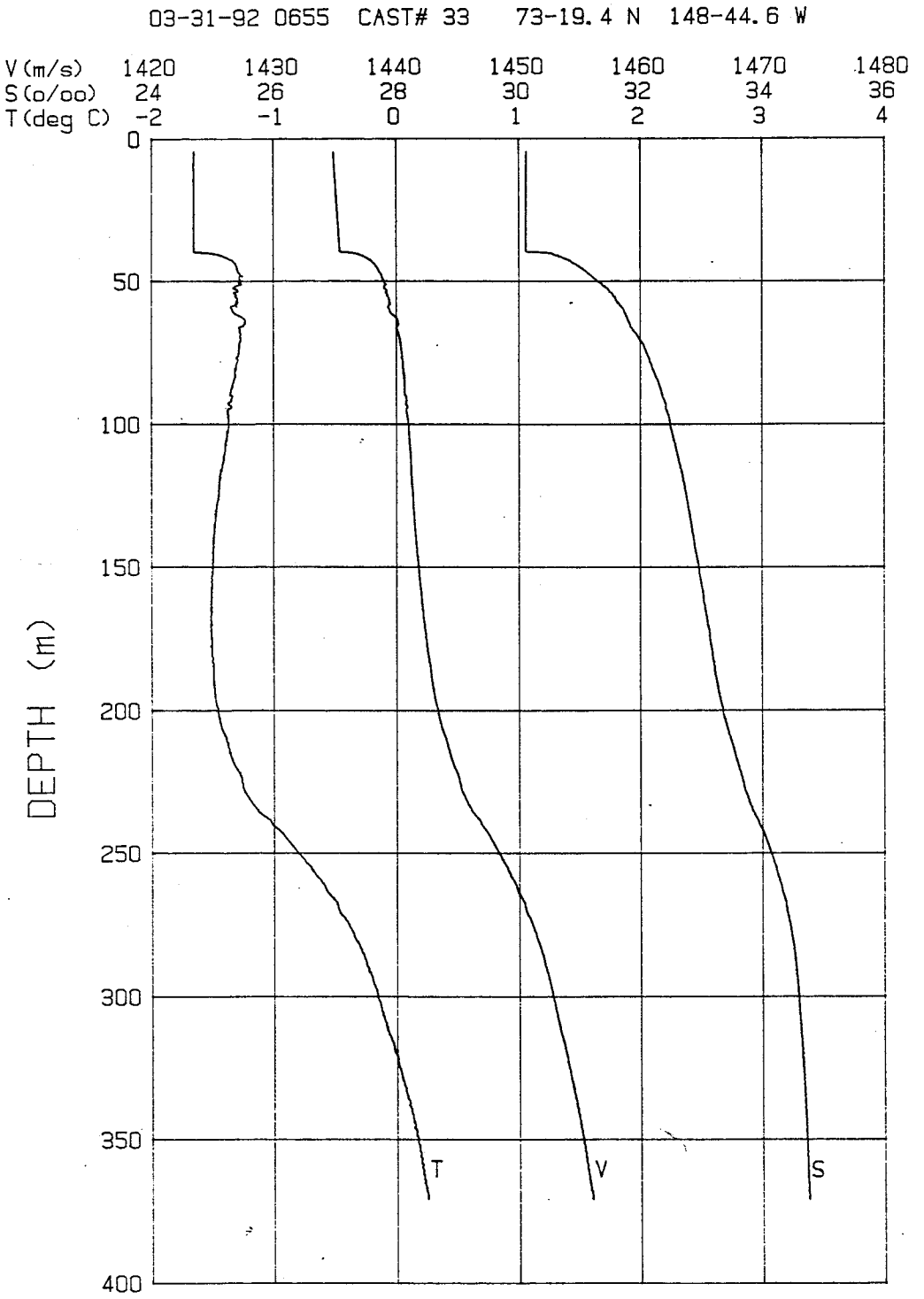
03-31-92 0655 CAST# 33 73-19.4 N 148-44.6 W
V(m/s) 1420 1430 1440 1450 1460 1470 1480
S(o/oo) 24 26 28 30 32 34 36
T(deg C) -2 -1 0 1 2 3 4
0
50
100
150
200
250
300
350
400
DEPTH (m)
T
V
S

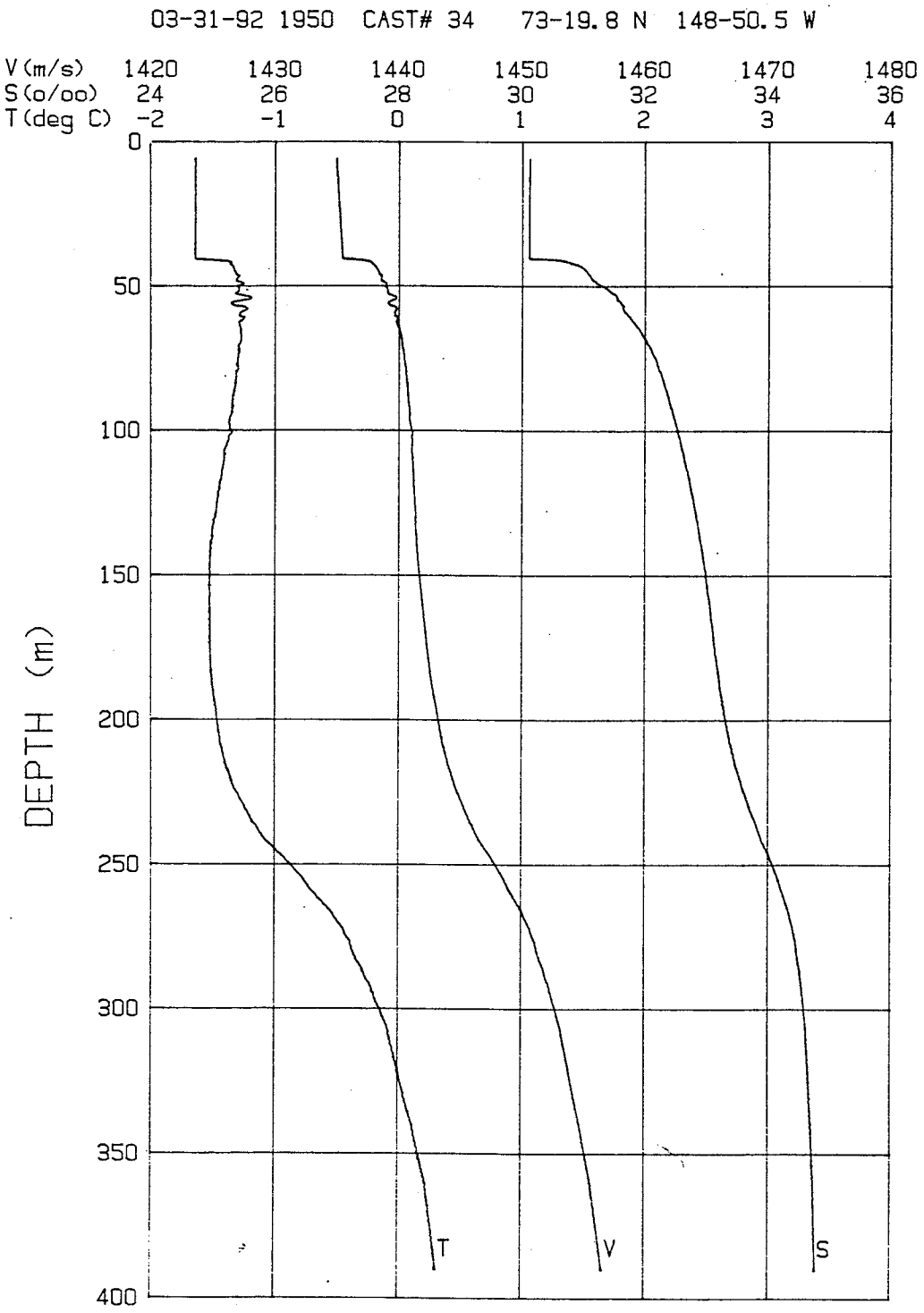
03-31-92 1950 CAST# 34 73-19.8 N 148-50.5 W
V(m/s) 1420 1430 1440 1450 1460 1470 1480
S(o/oo) 24 26 28 30 32 34 36
T(deg C) -2 -1 0 1 2 3 4
0
50
100
150
200
250
300
350
400
DEPTH (m)
T
V
S

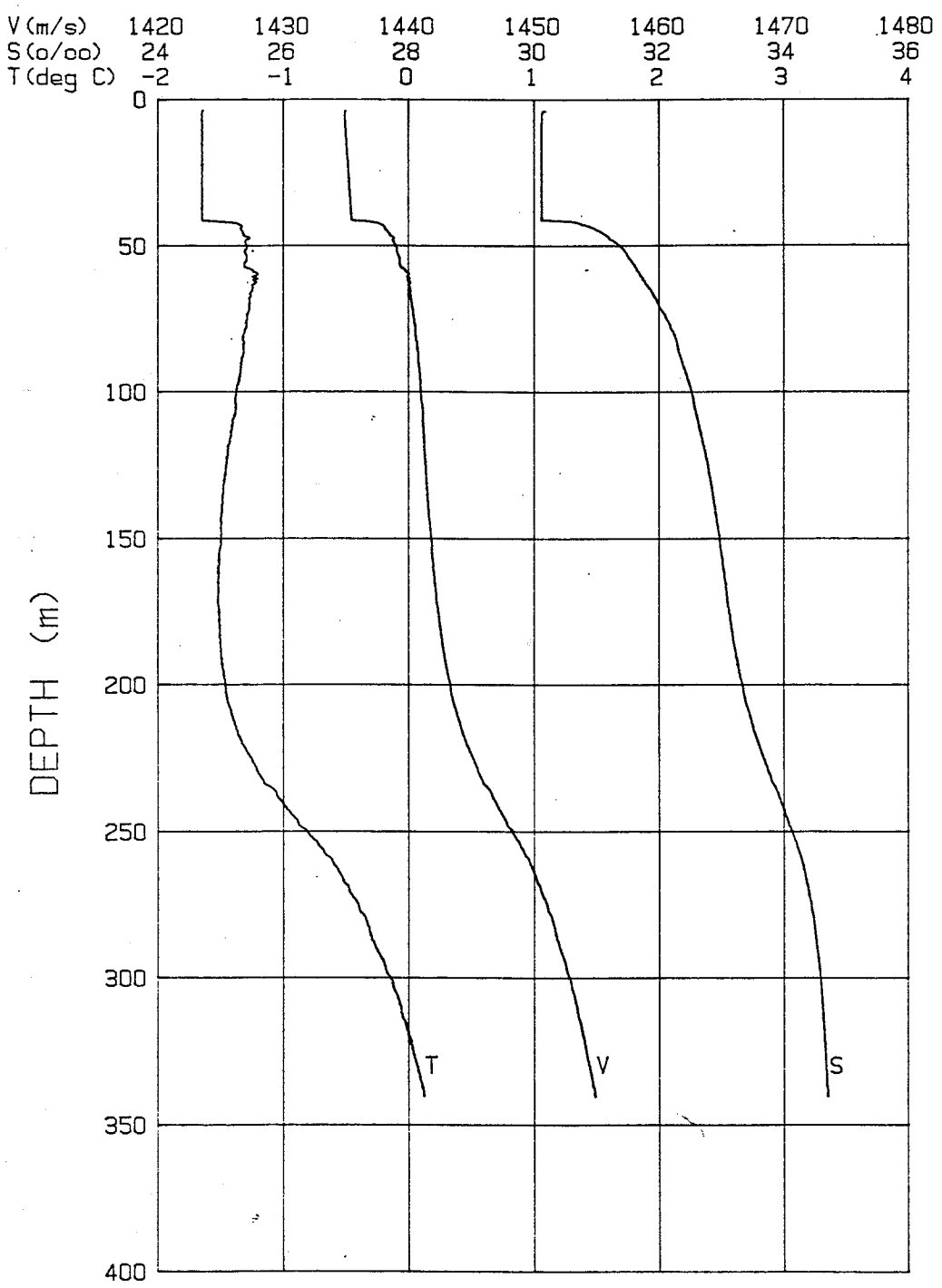
04-01-92 0732 CAST# 35 73-19.6 N 148-51.9 W
V(m/s) 1420 1430 1440 1450 1460 1470 1480
S(o/oo) 24 26 28 30 32 34 36
T(deg C) -2 -1 0 1 2 3 4
0
50
100
150
200
250
300
350
400
DEPTH (m)
T
V
S

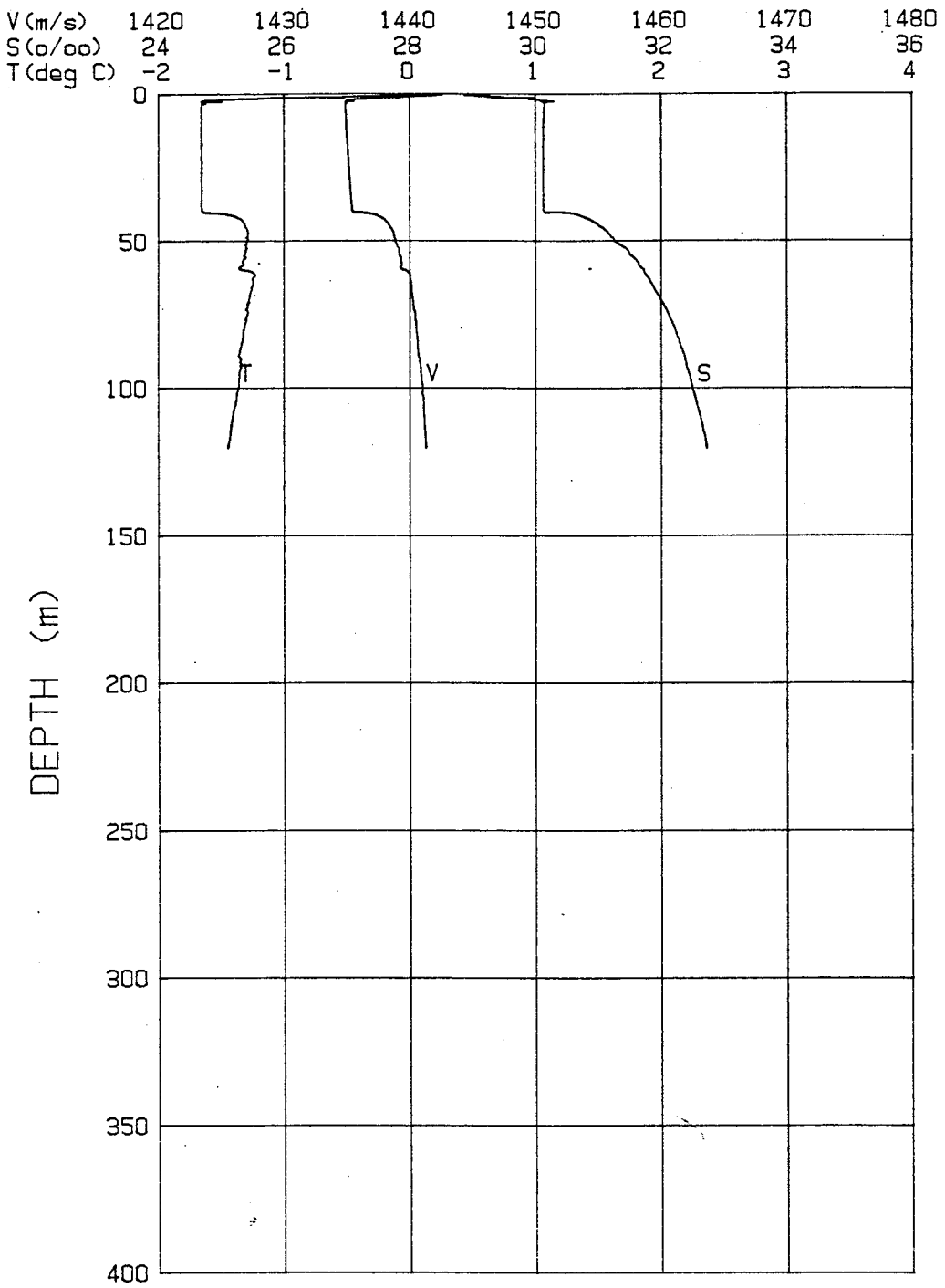
04-01-92 1452 CAST# 36
73-19.2 N 148-53.4 W
V(m/s) 1420 1430 1440 1450 1460 1470 1480
S(o/oo) 24 26 28 30 32 34 36
T(deg C) -2 -1 0 1 2 3 4
0
50
100
150
200
250
300
350
400
DEPTH (m)
T
V
S

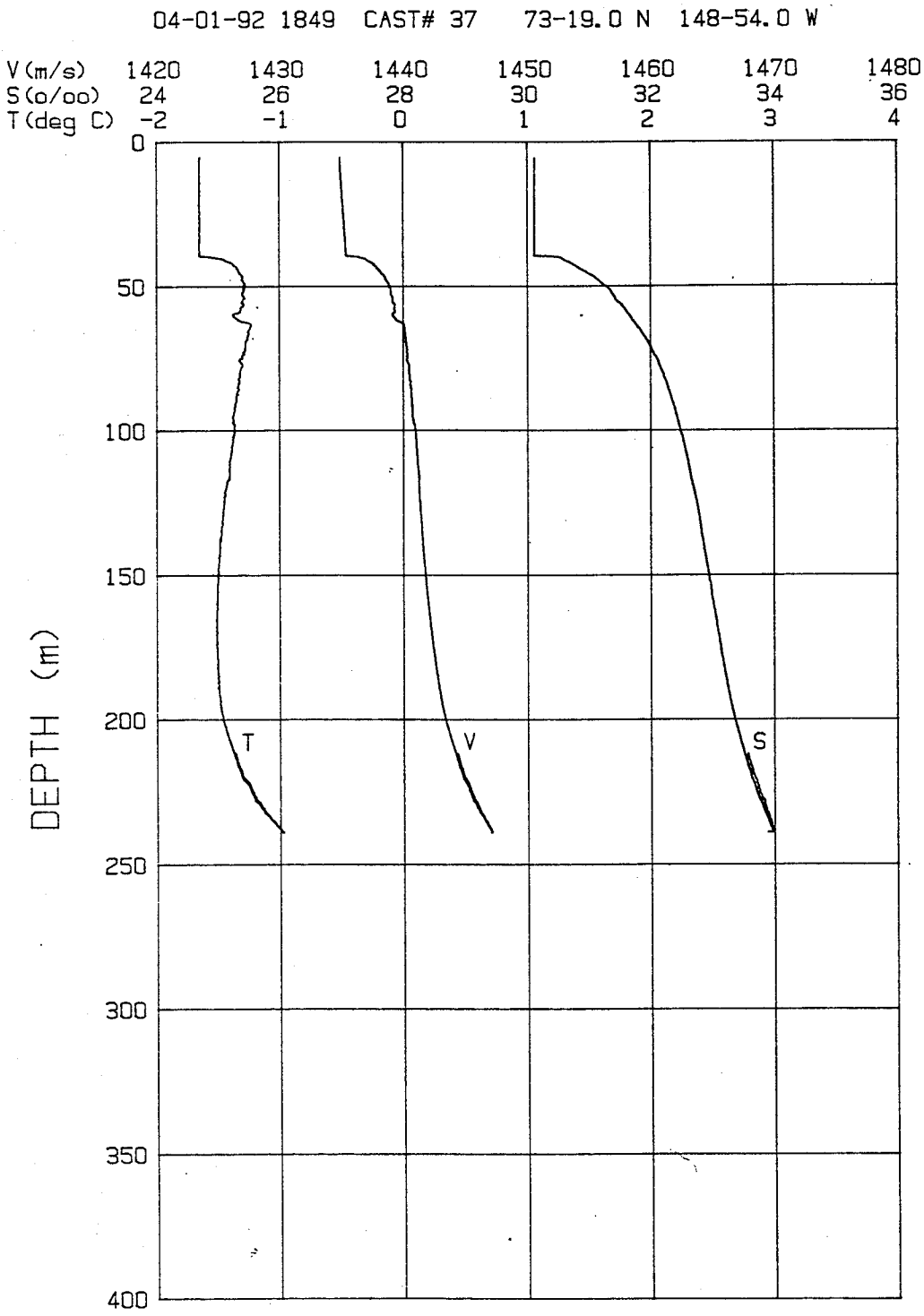
04-01-92 1849 CAST# 37 73-19.0 N 148-54.0 W
V(m/s) 1420 1430 1440 1450 1460 1470 1480
S(o/oo) 24 26 28 30 32 34 36
T(deg C) -2 -1 0 1 2 3 4
0
50
100
150
200
250
300
350
400
DEPTH (m)
T
V
S

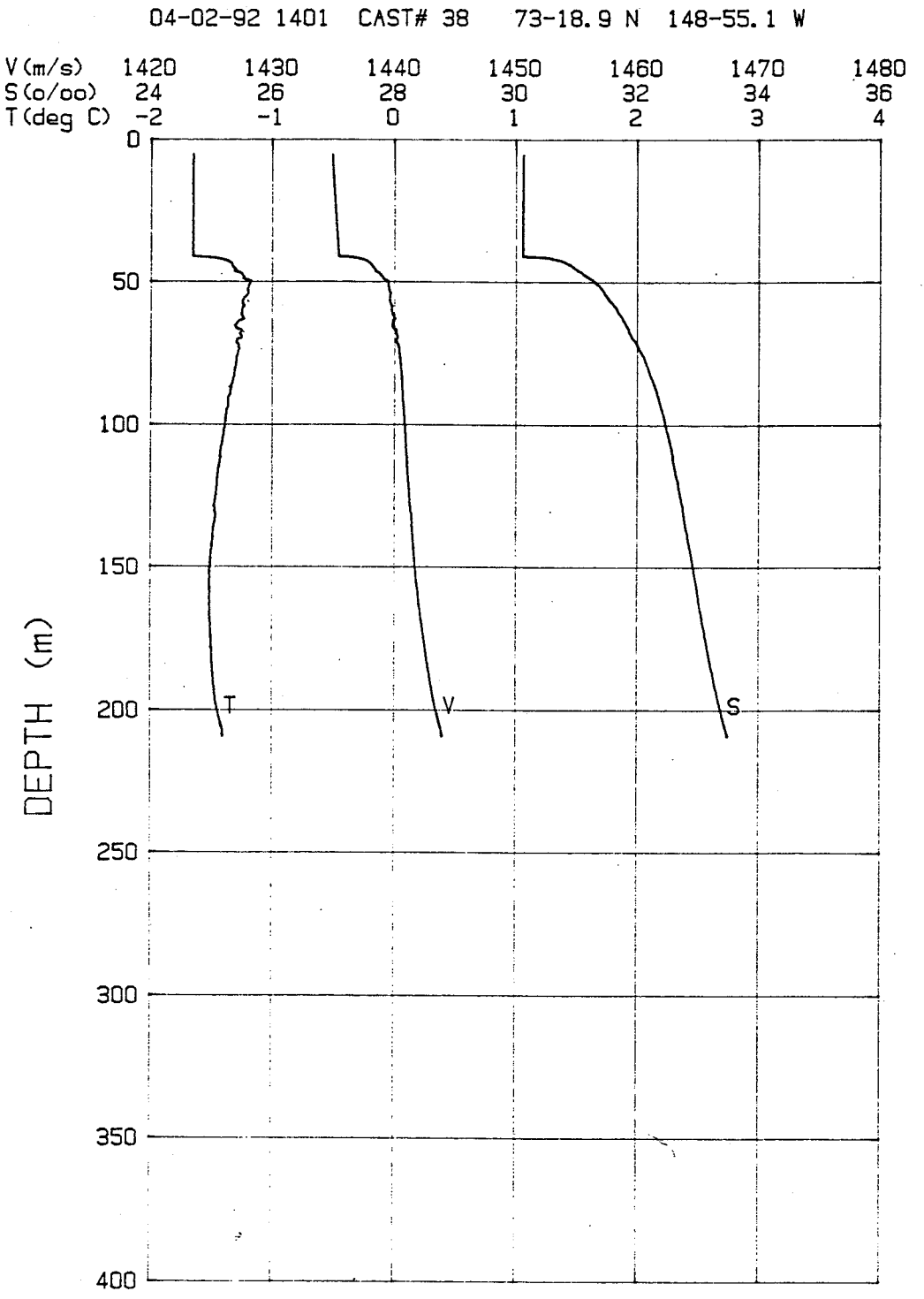
04-02-92 1401 CAST# 38 73-18.9 N 148-55.1 W
V(m/s) 1420 1430 1440 1450 1460 1470 1480
S(o/oo) 24 26 28 30 32 34 36
T(deg C) -2 -1 0 1 2 3 4
0
50
100
150
200
250
300
350
400
DEPTH (m)
T
V
S

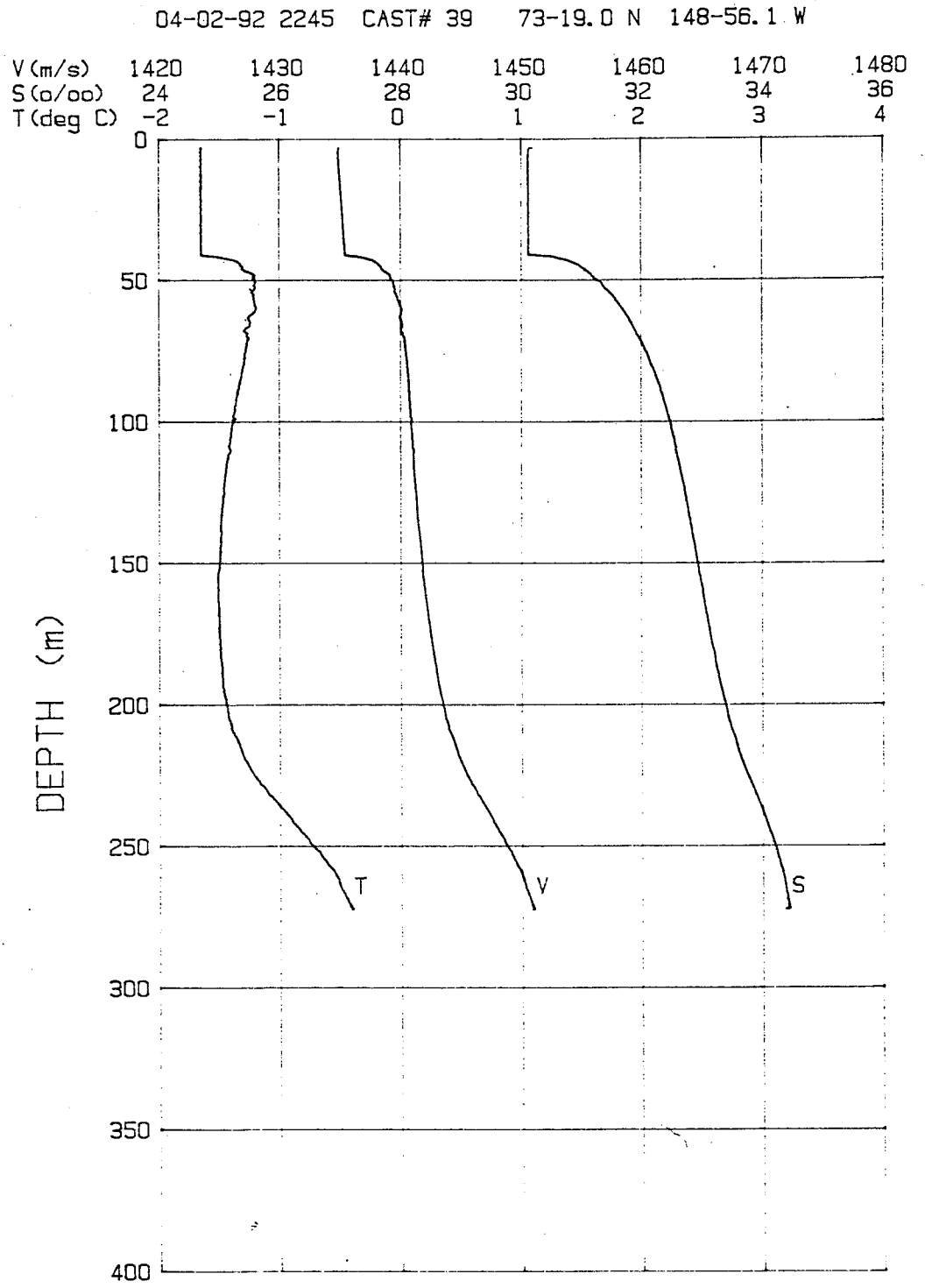
04-02-92 2245 CAST# 39 73-19.0 N 148-56.1 W
V(m/s) 1420 1430 1440 1450 1460 1470 1480
S(o/oo) 24 26 28 30 32 34 36
T(deg C) -2 -1 0 1 2 3 4
0
50
100
150
200
250
300
350
400
DEPTH (m)
T
V
S

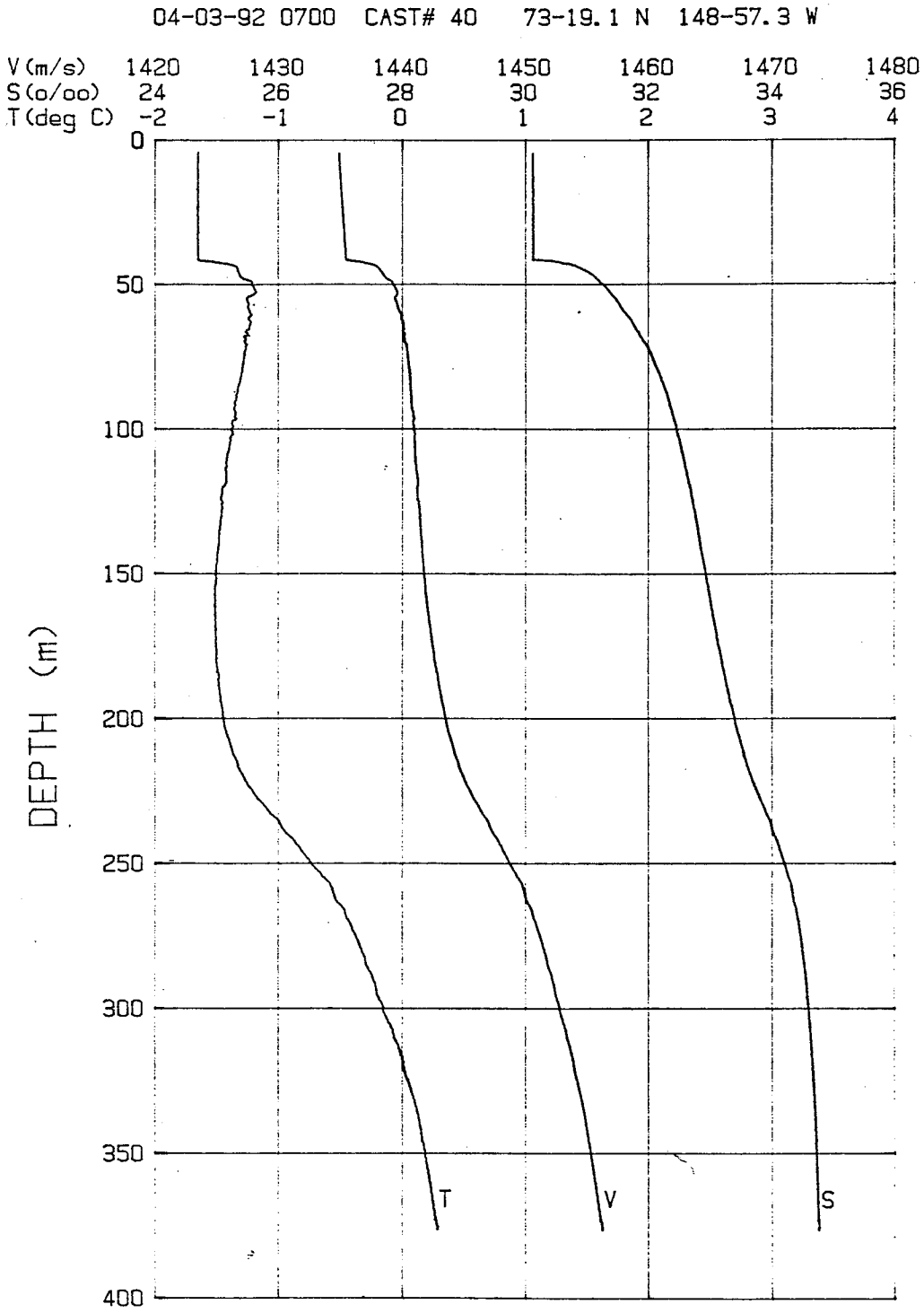
04-03-92 0700 CAST# 40 73-19.1 N 148-57.3 W
V(m/s) 1420 1430 1440 1450 1460 1470 1480
S(o/oo) 24 26 28 30 32 34 36
T(deg C) -2 -1 0 1 2 3 4
0
50
100
150
200
250
300
350
400
DEPTH (m)
T
V
S

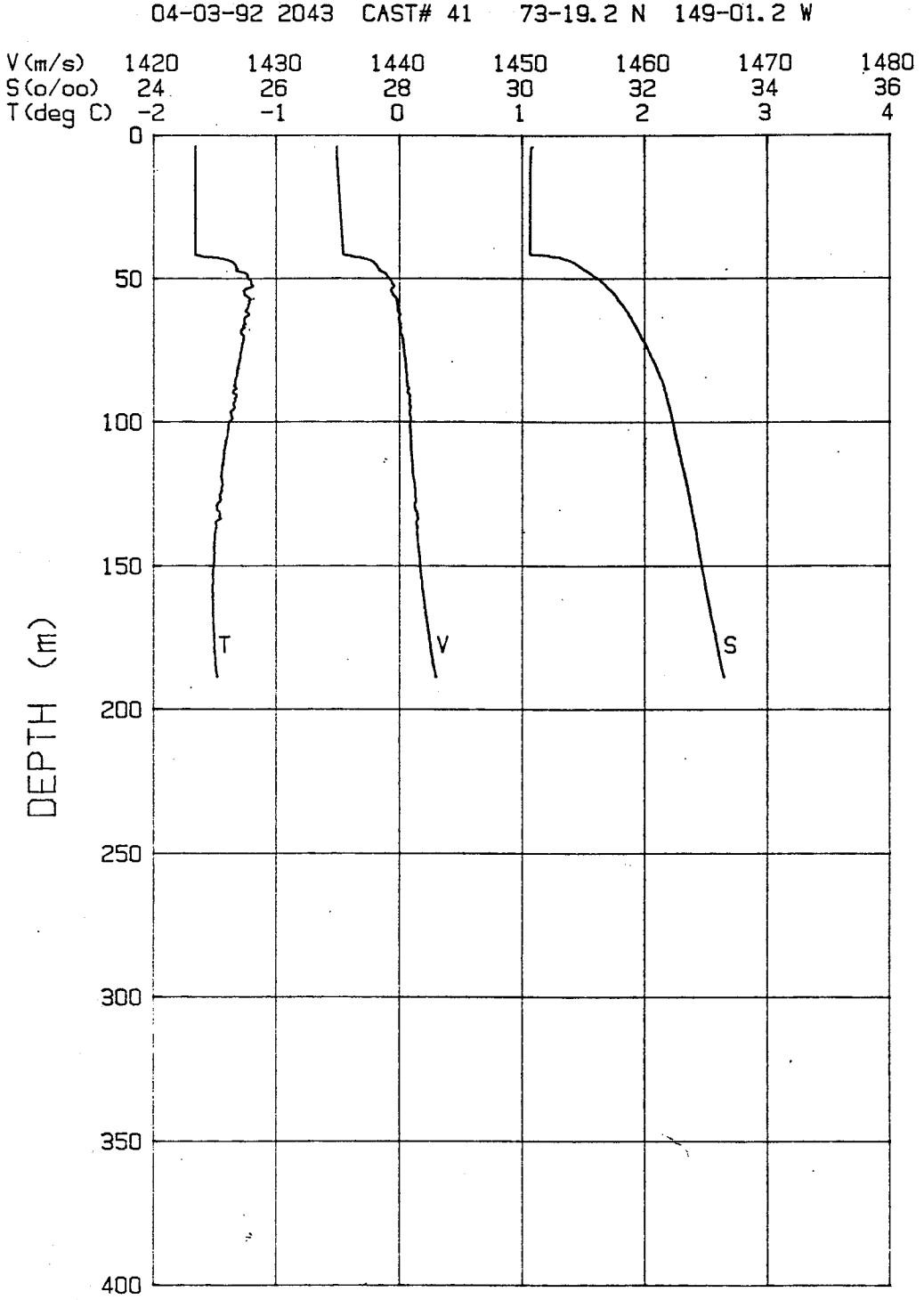
04-03-92 2043 CAST# 41 73-19.2 N 149-01.2 W
V(m/s) 1420 1430 1440 1450 1460 1470 1480
S(o/oo) 24 26 28 30 32 34 36
T(deg C) -2 -1 0 1 2 3 4
0
50
100
150
200
250
300
350
400
DEPTH (m)
T
V
S

APPENDIX C

Current Meter Data

Solid line is current relative to floe.
Dashed line is current relative to earth.
Number after cast indicates current meter.

Date	Local Time	Cast No.	Comments
3-21-92	1750	01a	
3-21-92	1750	01b	
3-23-92	1810	02a	Down
3-23-92	1825	02a	Up
3-23-92	1810	02b	Down
3-23-92	1825	02b	Up
3-25-92	1329	03b	
3-25-92	1330	03a	
3-25-92	1532	04b	Time series at 200 m
3-26-92	1344	05a	Time series at 350 m, concurrent with CTD cast #20
3-29-92	0803	07a	
3-30-92	0651	08a	
3-30-92	1329	09a	
3-30-92	1330	09b	
3-30-92	2226	10a	Time series at 46 m
3-30-92	2223	10b	Time series at 44 m

03-21-92 1750L CAST #01a

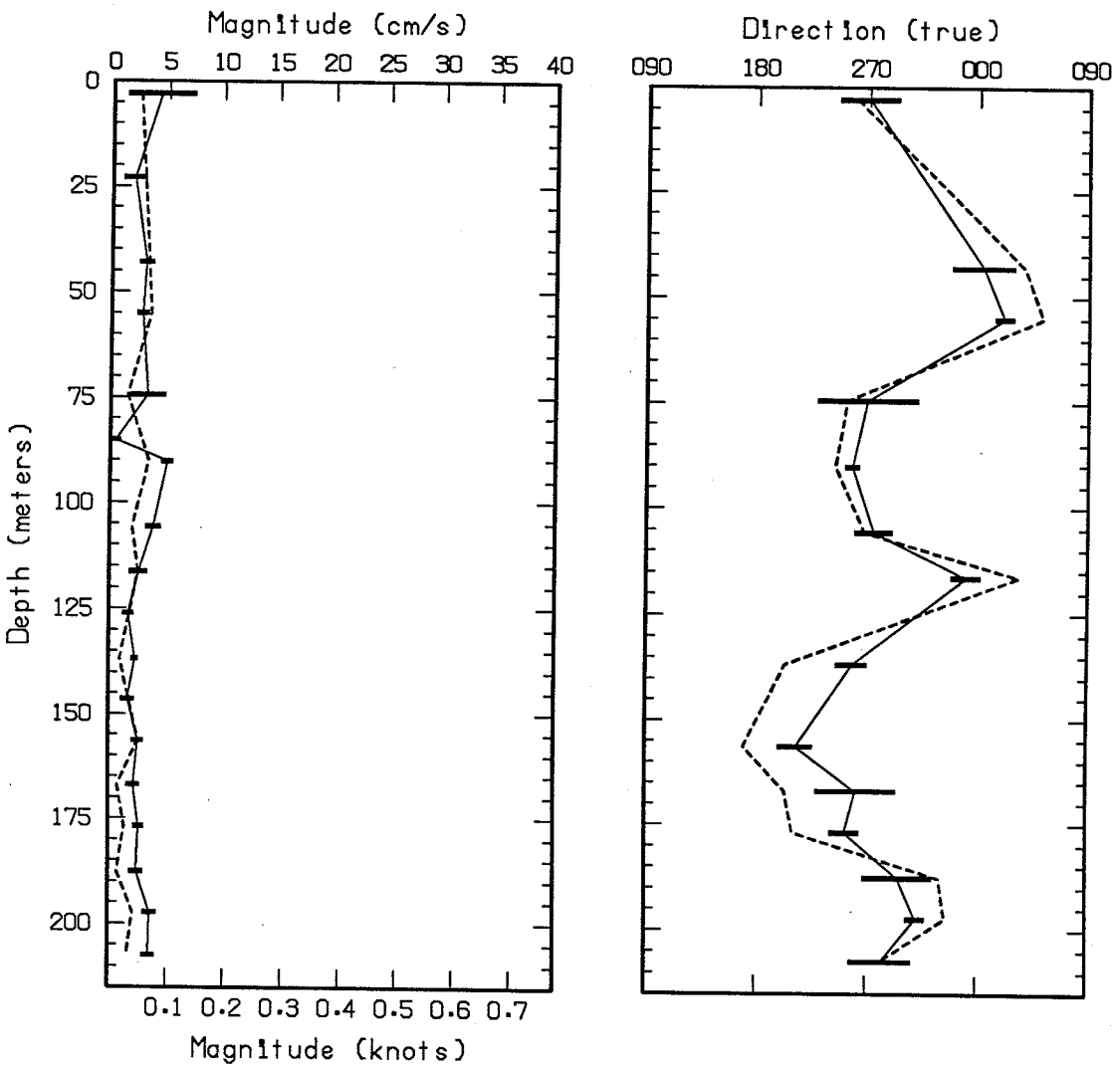

Magnetic bearing + 32 degrees = True bearing
True bearing of +Y axis = 72.2 degrees
Floe drift speed = 1.9 cm/s
Floe drift direction = 103 degrees true

03-21-92 1750L CAST #01b

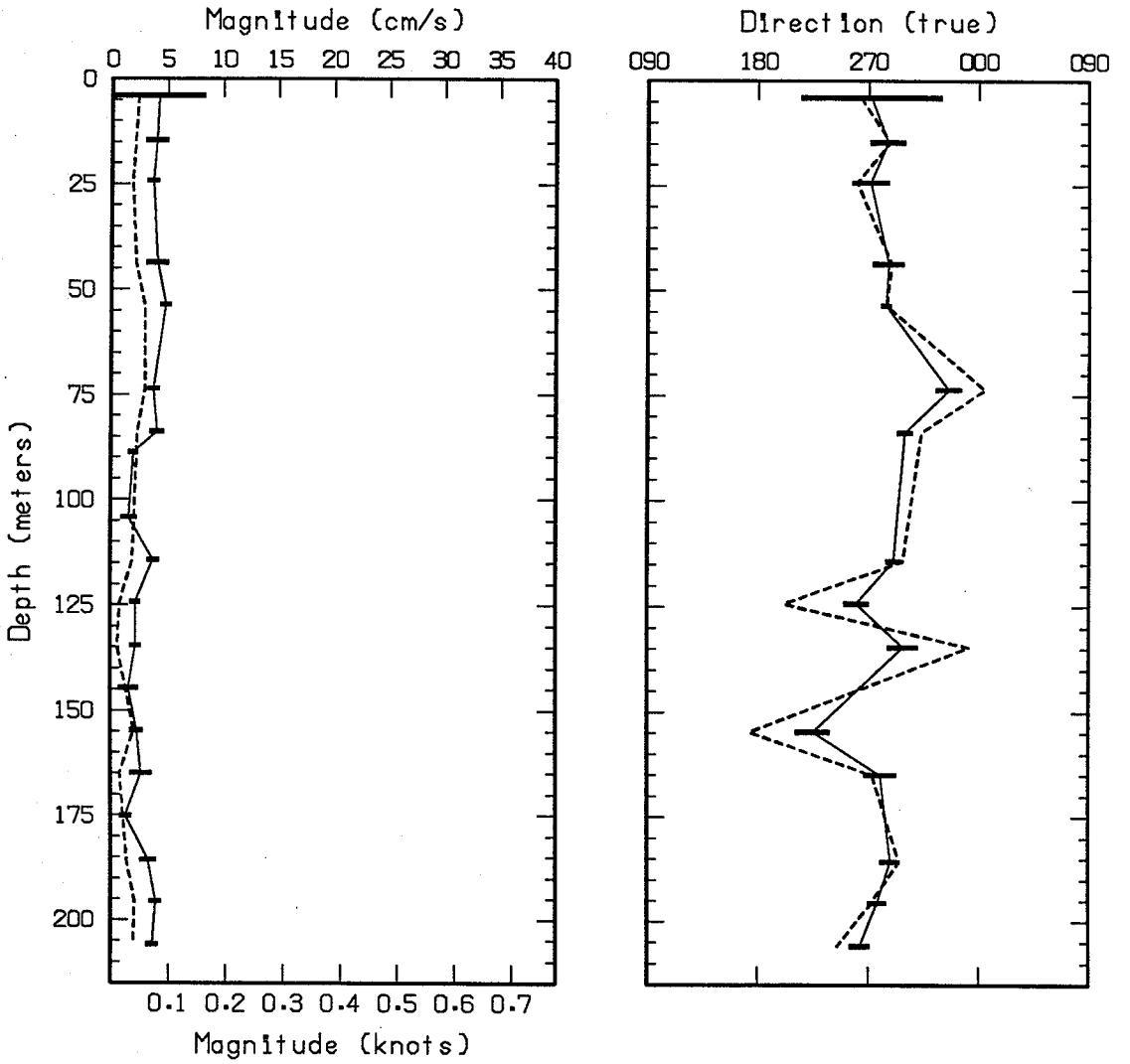

Magnetic bearing + 32 degrees = True bearing
True bearing of +Y axis = 72.2 degrees
Floe drift speed = 1.9 cm/s
Floe drift direction = 103 degrees true

03-23-92 1810L CAST #02a (down)

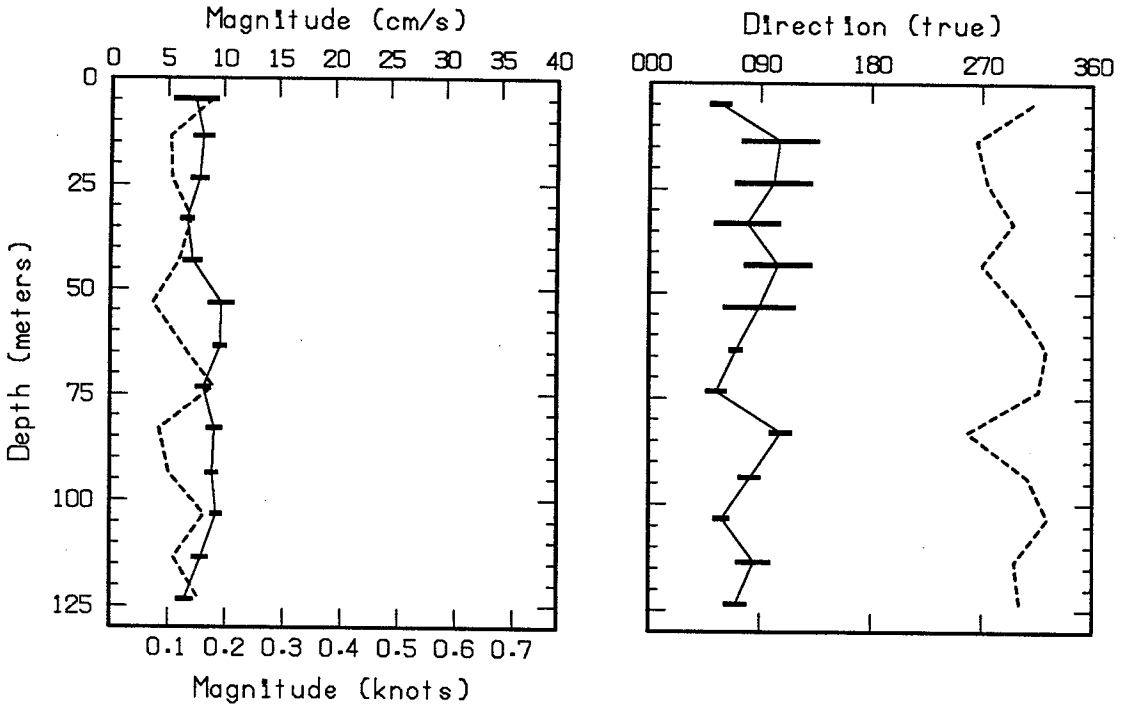

Magnetic bearing + 32 degrees = True bearing
True bearing of +Y axis = 72.2 degrees
Floe drift speed = 13.3 cm/s
Floe drift direction = 278 degrees true

03-23-92 1825L CAST #02a (up)

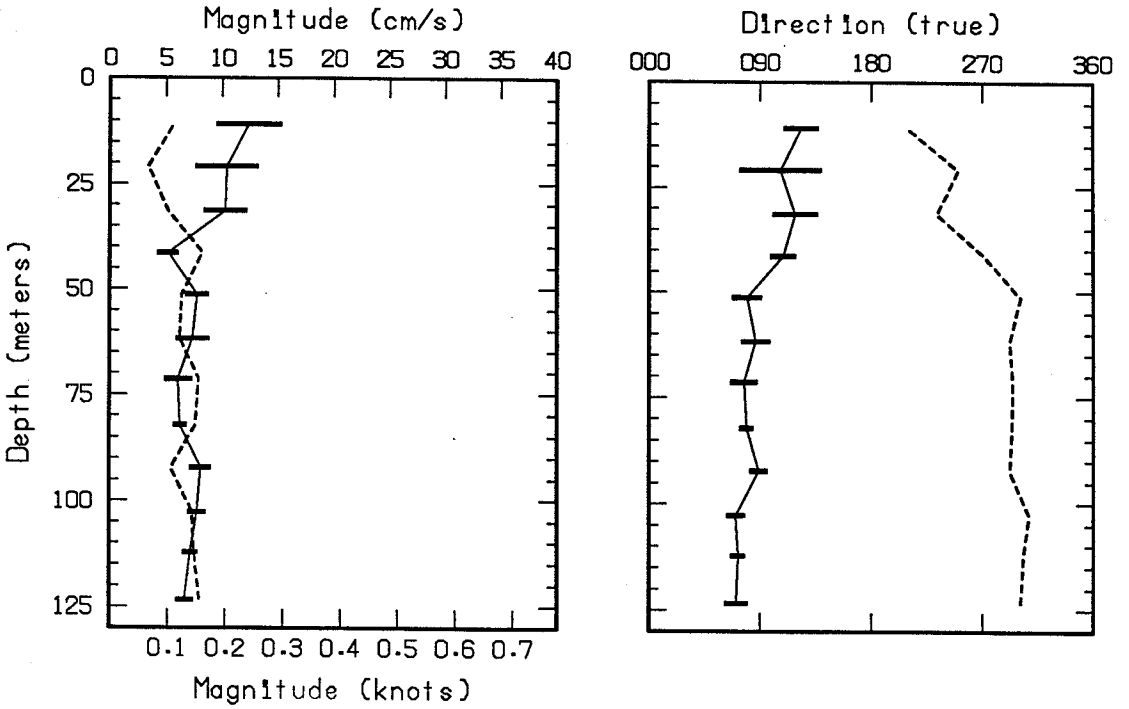

Magnetic bearing + 32 degrees = True bearing
True bearing of +Y axis = 72.2 degrees
Floe drift speed = 13.3 cm/s
Floe drift direction = 278 degrees true

03-23-92 1810L CAST #02b (down)

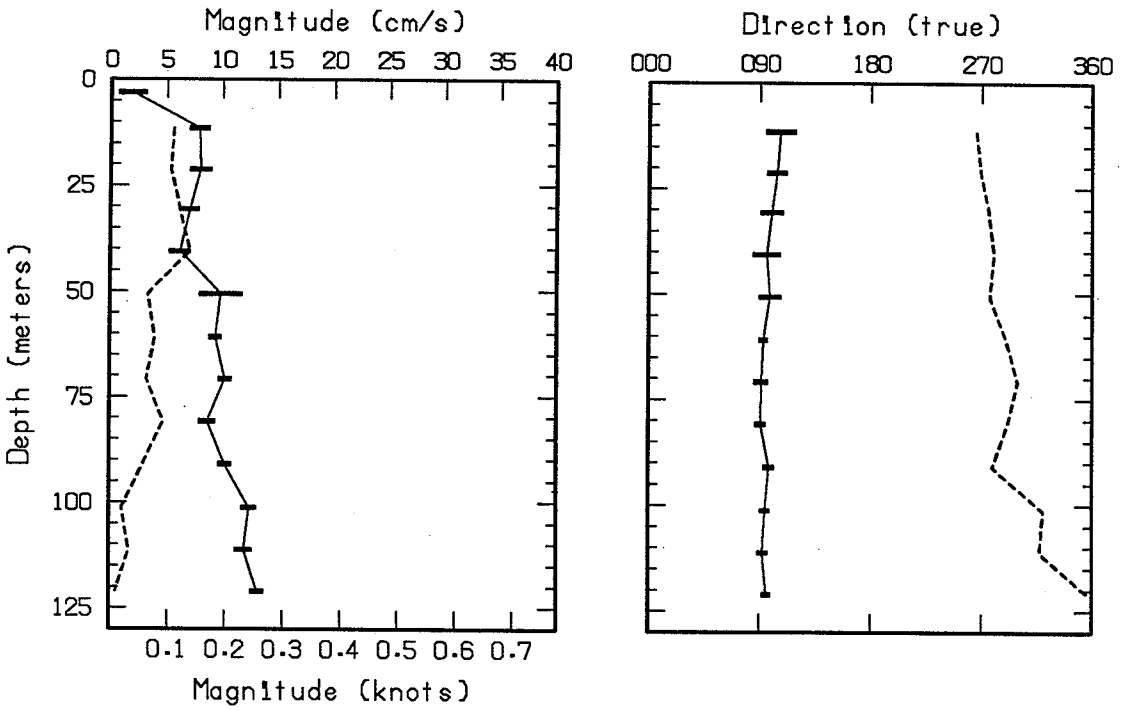

Magnetic bearing + 32 degrees = True bearing
True bearing of +Y axis = 72.2 degrees
Floe drift speed = 13.3 cm/s
Floe drift direction = 278 degrees true

03-23-92 1825L CAST #02b (up)

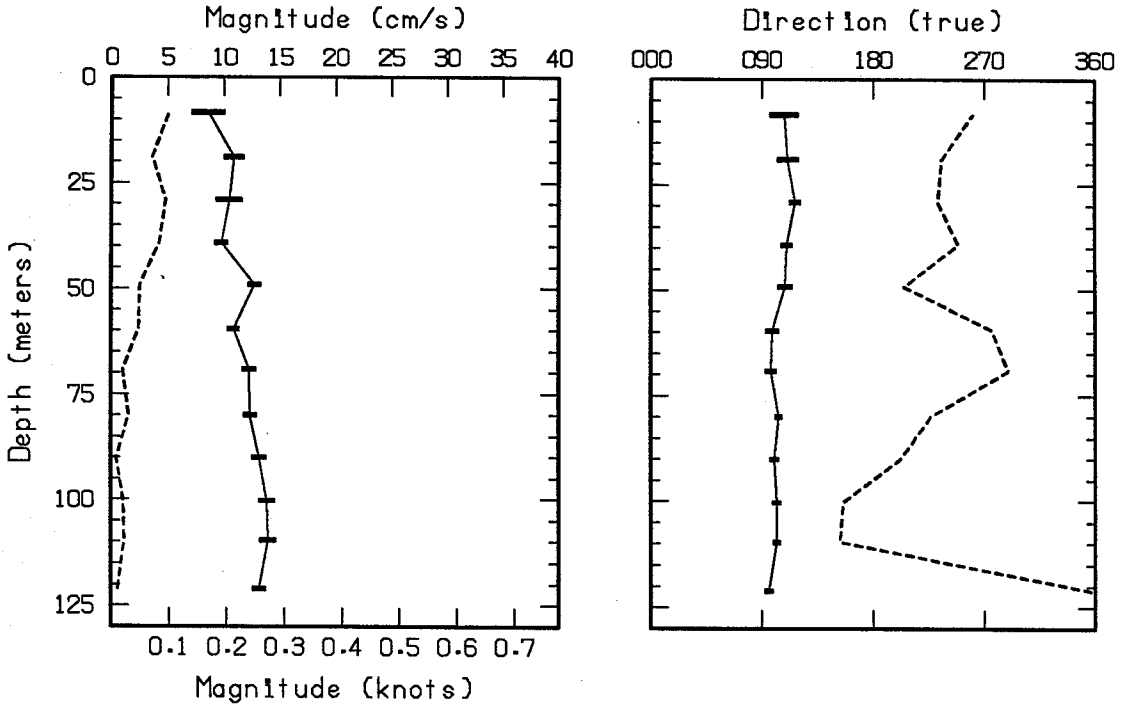

Magnetic bearing + 32 degrees = True bearing
True bearing of +Y axis = 72.2 degrees
Floe drift speed = 13.3 cm/s
Floe drift direction = 278 degrees true

03-25-92 1329L CAST #03b

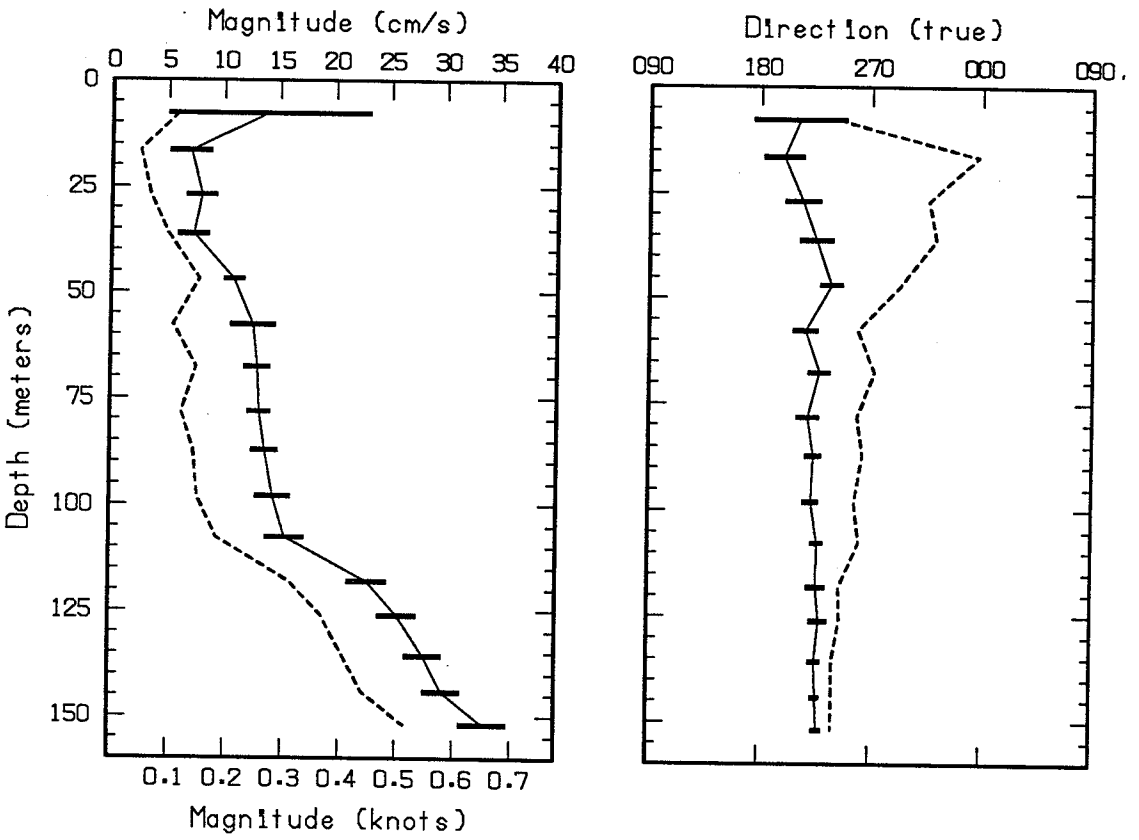

Magnetic bearing + 32 degrees = True bearing
True bearing of +Y axis = 72.2 degrees
Floe drift speed = 9.4 cm/s
Floe drift direction = 13 degrees true

03-25-92 1330L CAST #03a

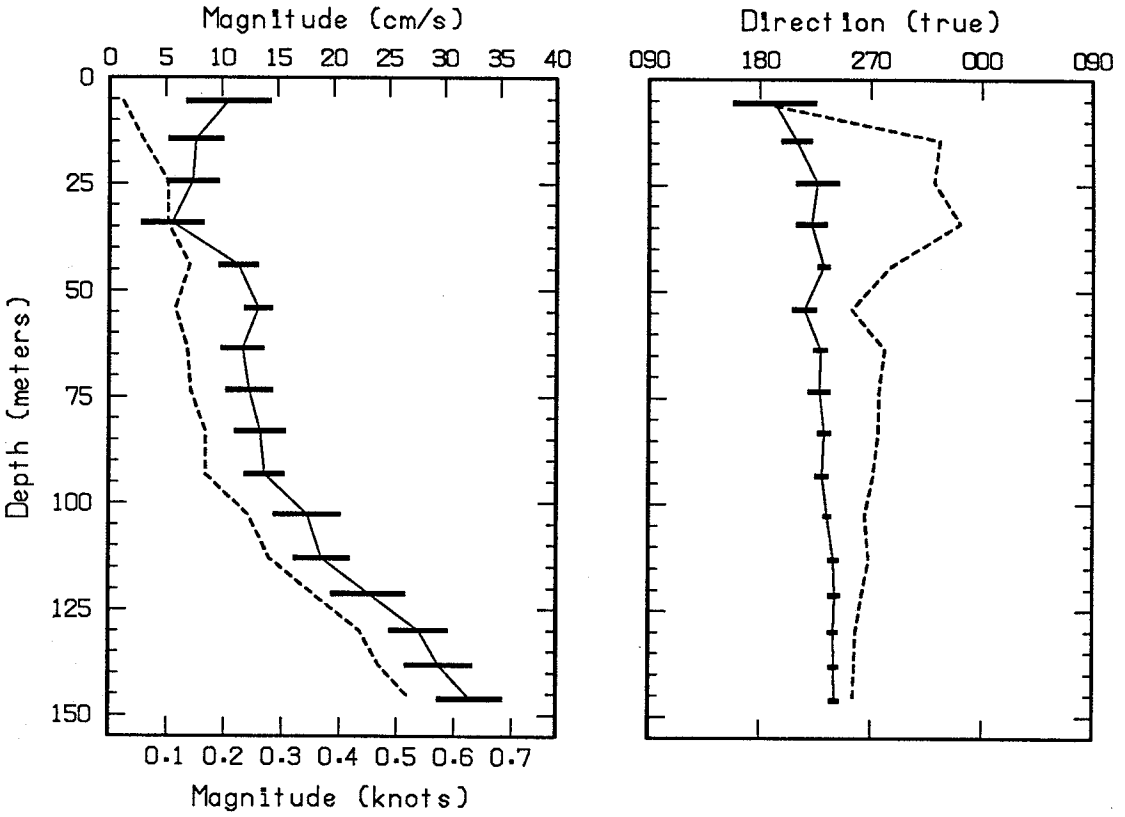

Magnetic bearing + 32 degrees = True bearing
True bearing of +Y axis = 72.2 degrees
Floe drift speed = 9.4 cm/s
Floe drift direction = 13 degrees true

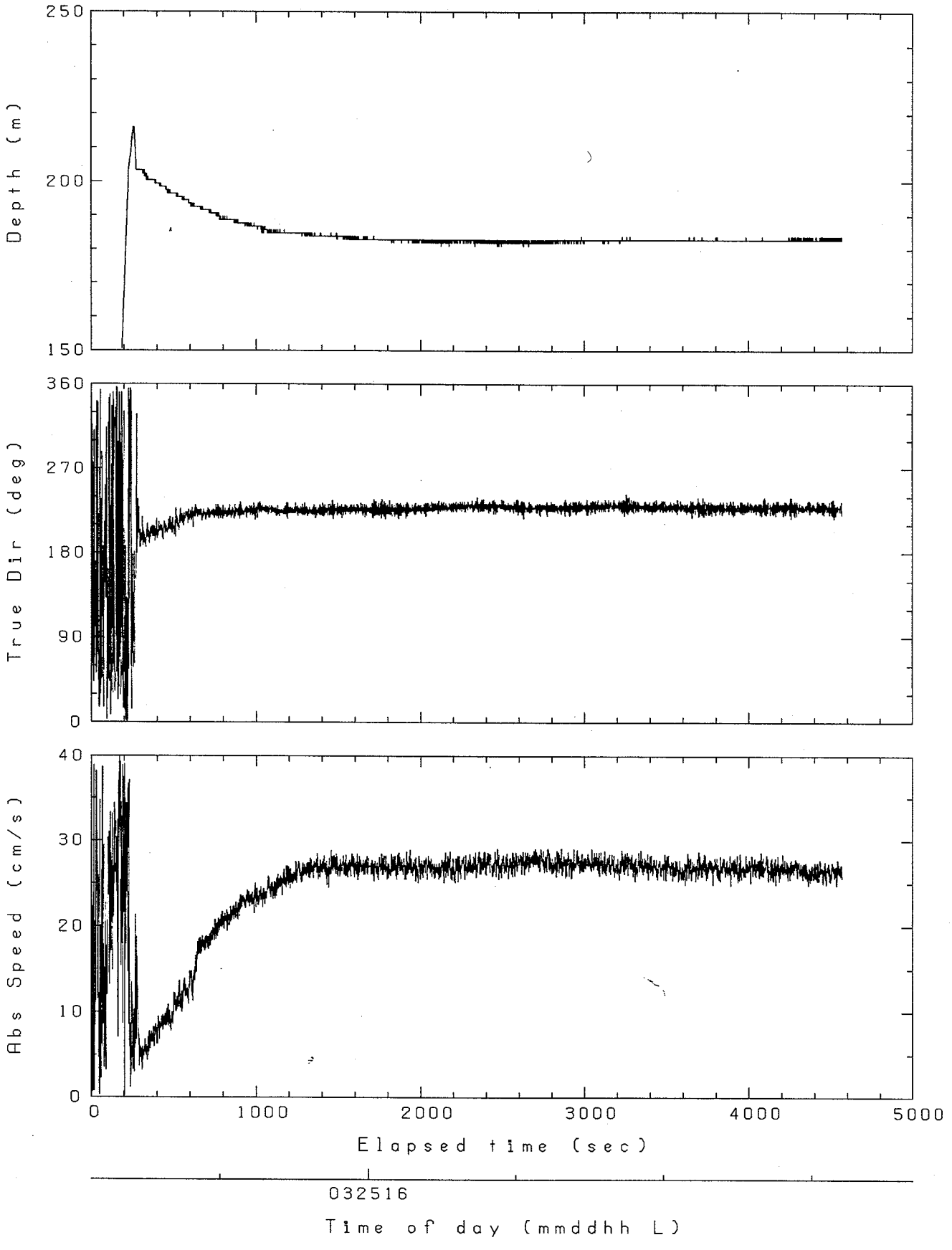

03251532.04b

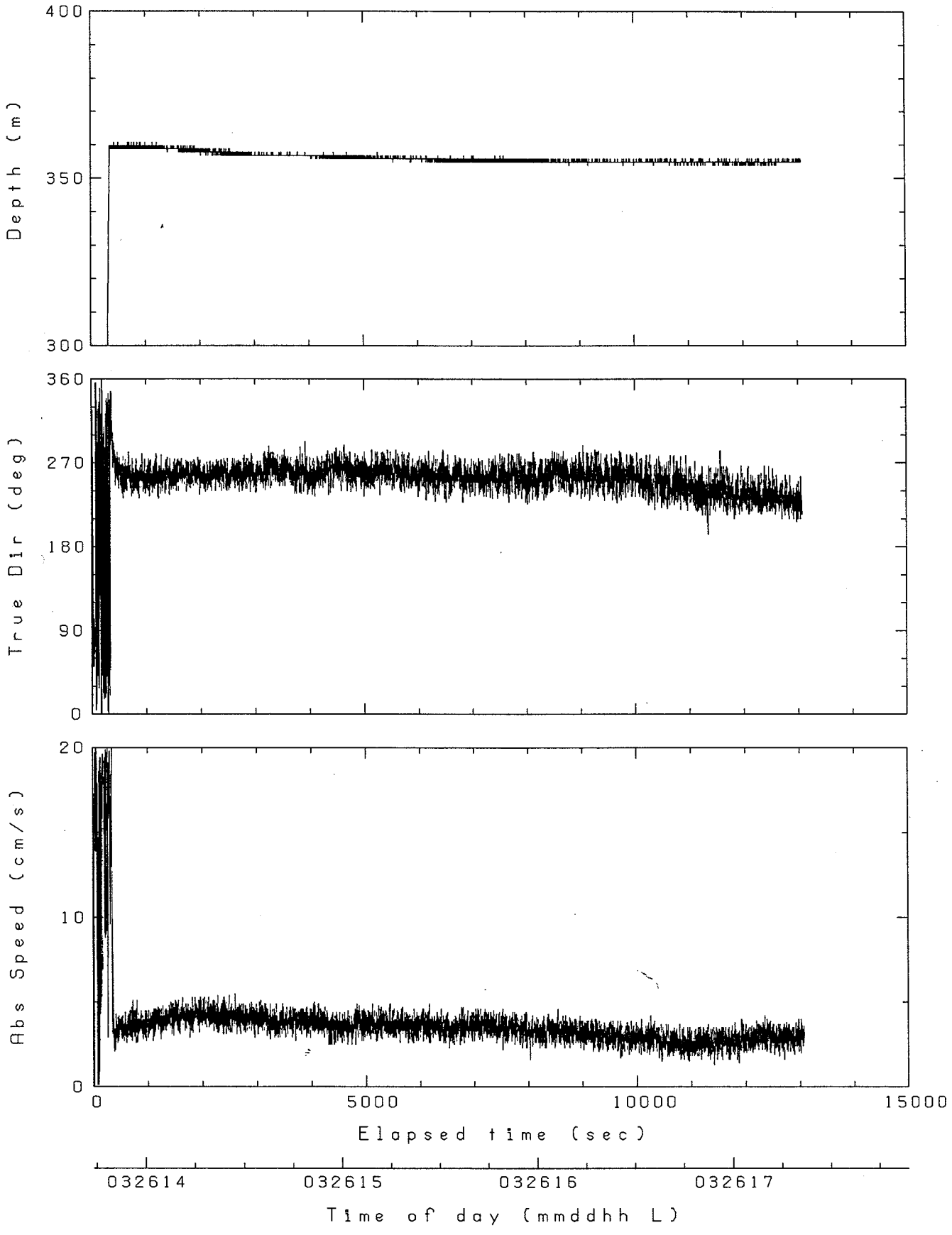

03261344.05a

03-29-92 0803L CAST #07a

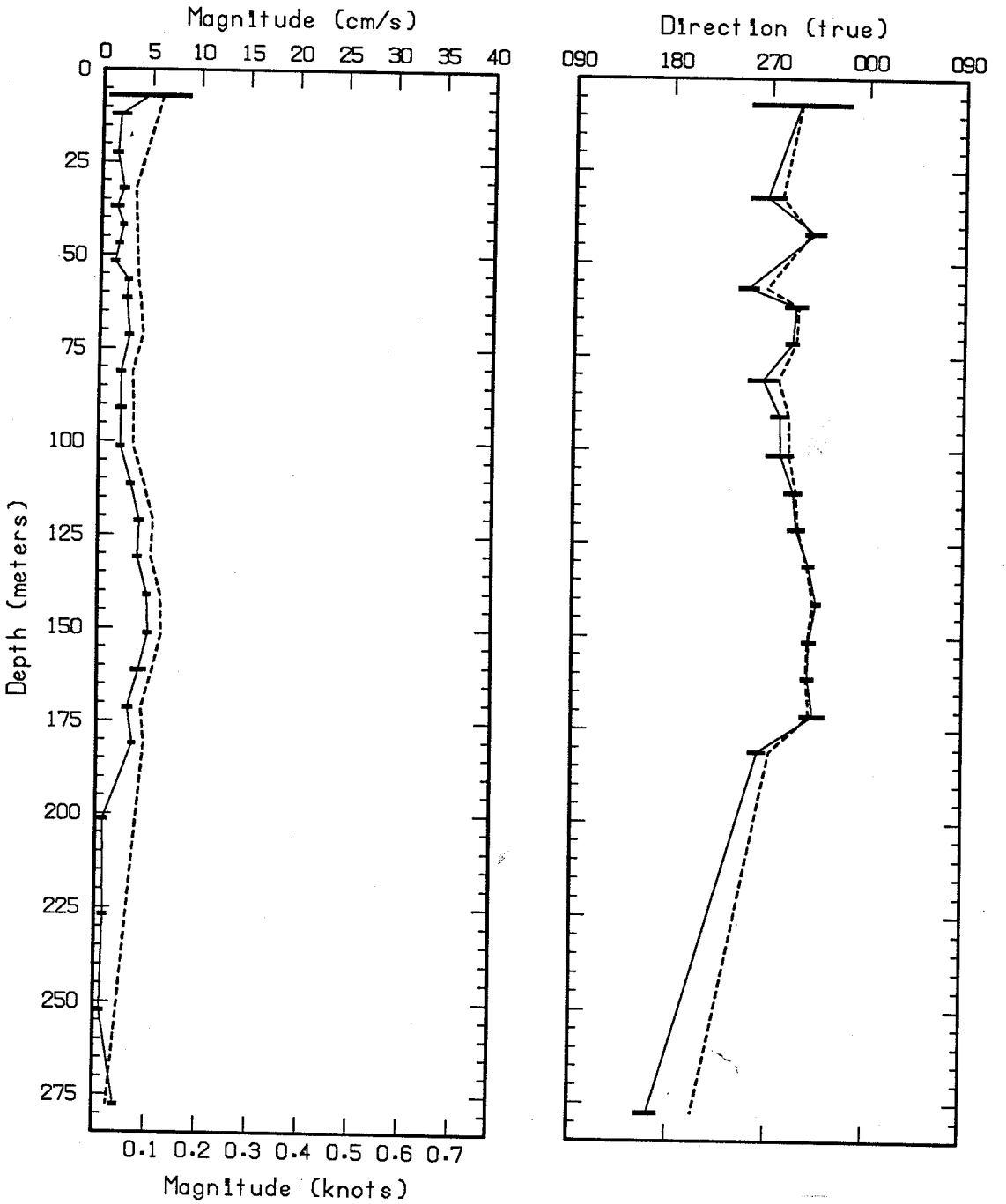

Magnetic bearing + 32 degrees = True bearing
True bearing of +Y axis = 72.2 degrees
Floe drift speed = 1.4 cm/s
Floe drift direction = 302 degrees true

03-30-92 0651L CAST #08a

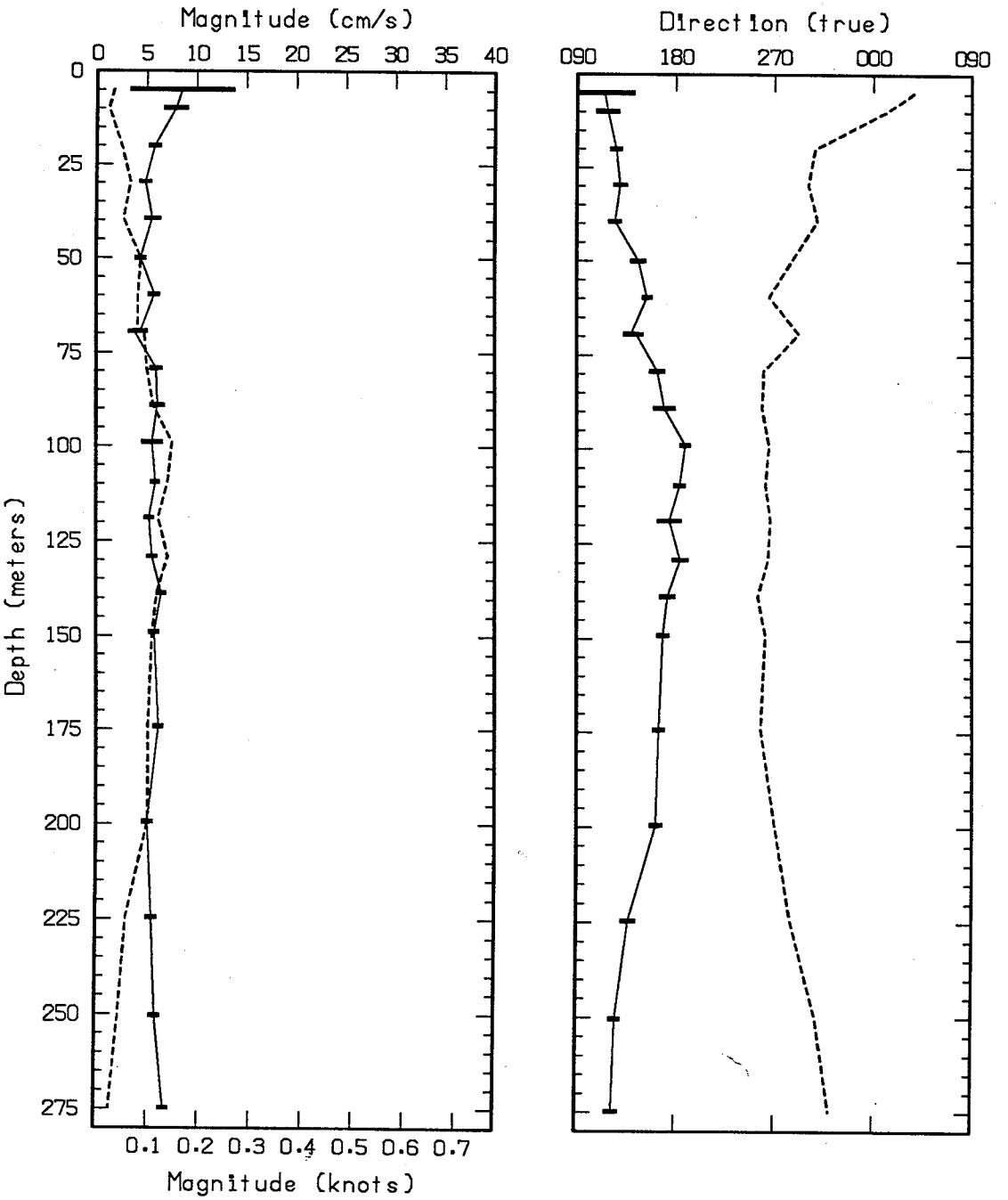

Magnetic bearing + 32 degrees = True bearing
True bearing of +Y axis = 72.2 degrees
Floe drift speed = 8.3 cm/s
Floe drift direction = 306 degrees true

03-30-92 1329L CAST #09a

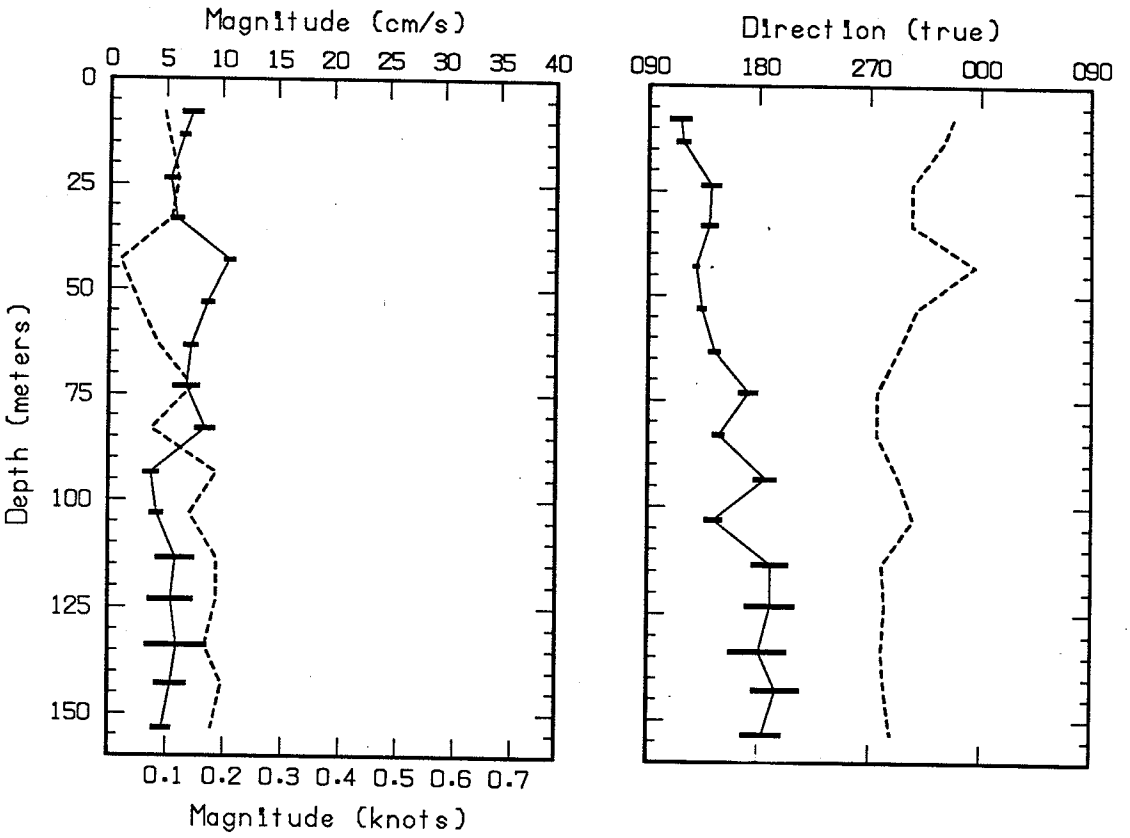

Magnetic bearing + 32 degrees = True bearing
True bearing of +Y axis = 72.2 degrees
Floe drift speed = 11.4 cm/s
Floe drift direction = 312 degrees true

03-30-92 1330L CAST #09b

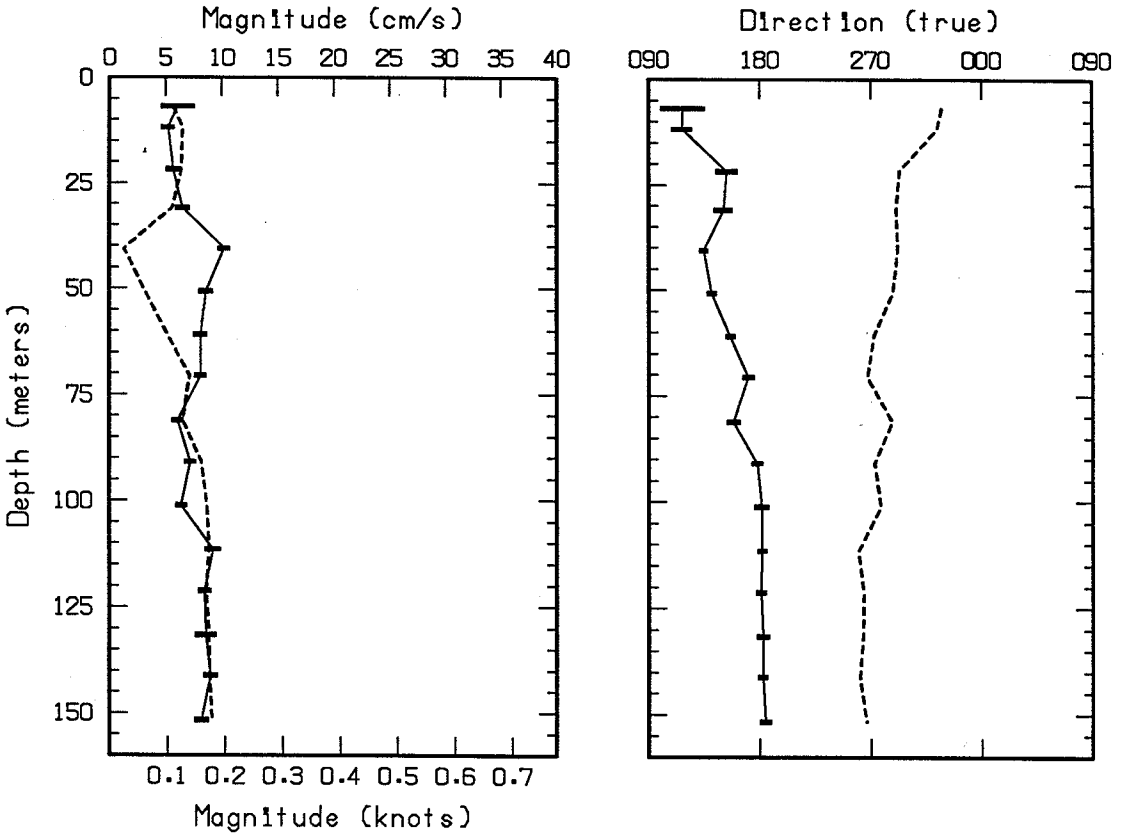

Magnetic bearing + 32 degrees = True bearing
True bearing of +Y axis = 72.2 degrees
Floe drift speed = 11.4 cm/s
Floe drift direction = 312 degrees true

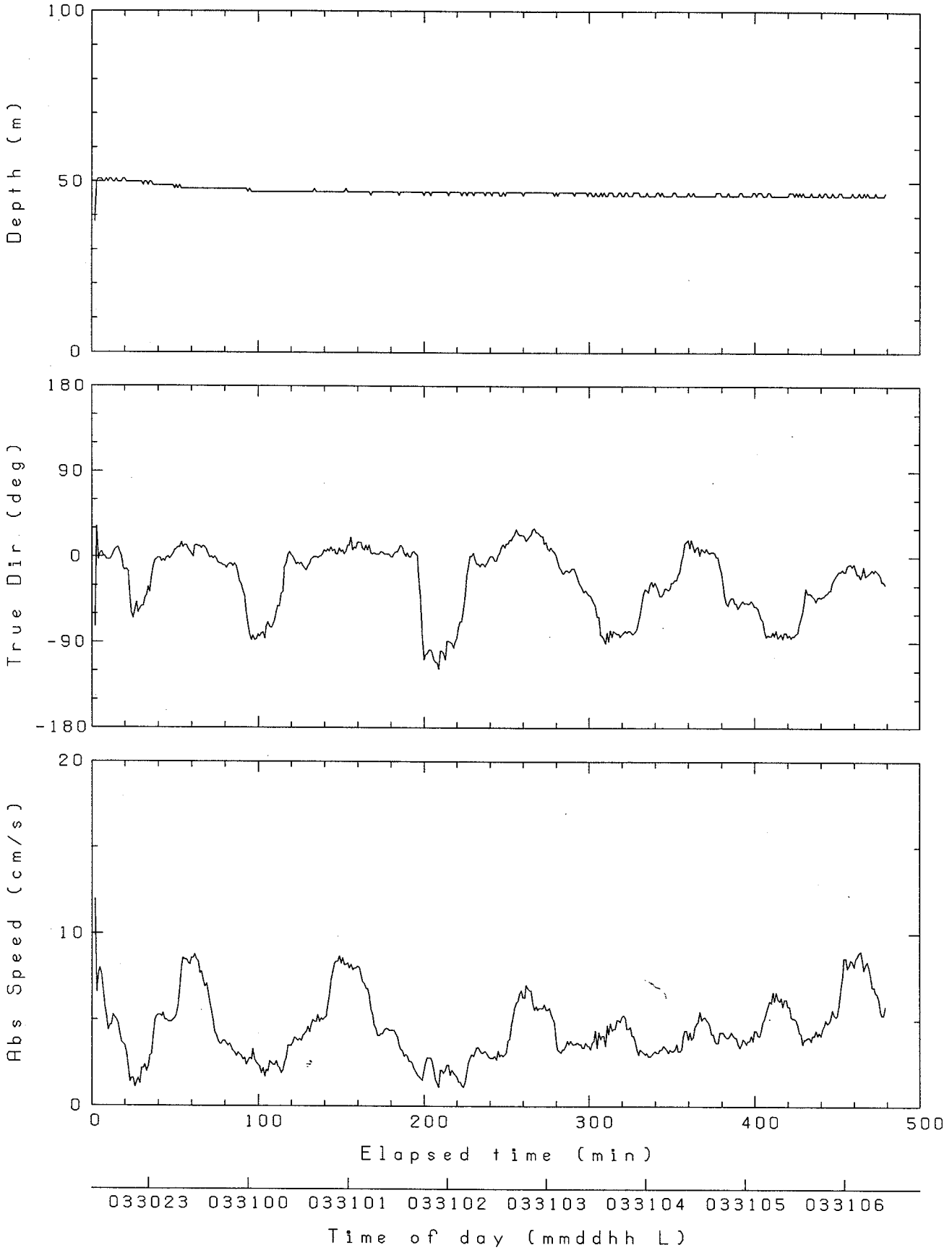

03302226.10a

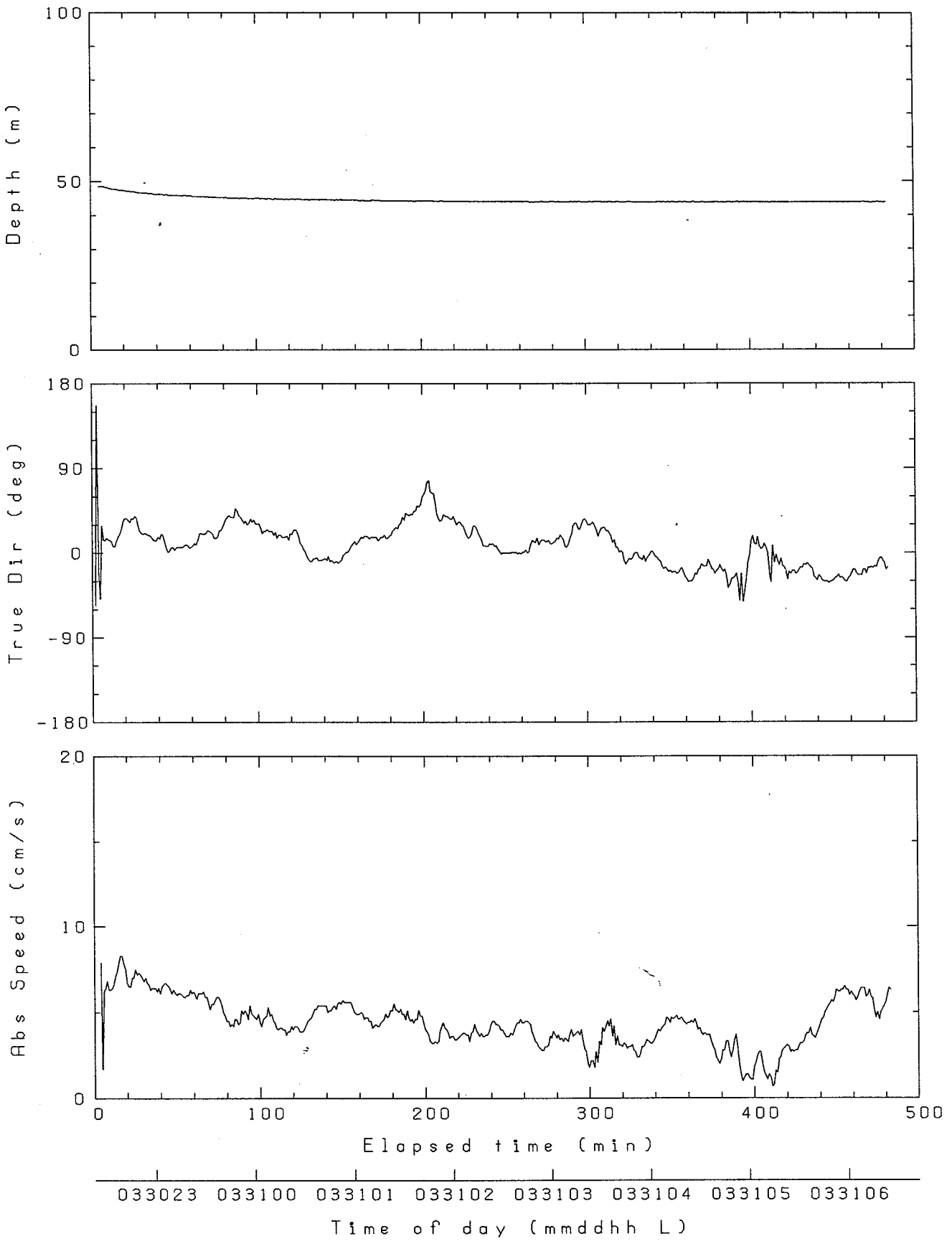

03302223.10b

APPENDIX D

Ambient Noise Level Plots

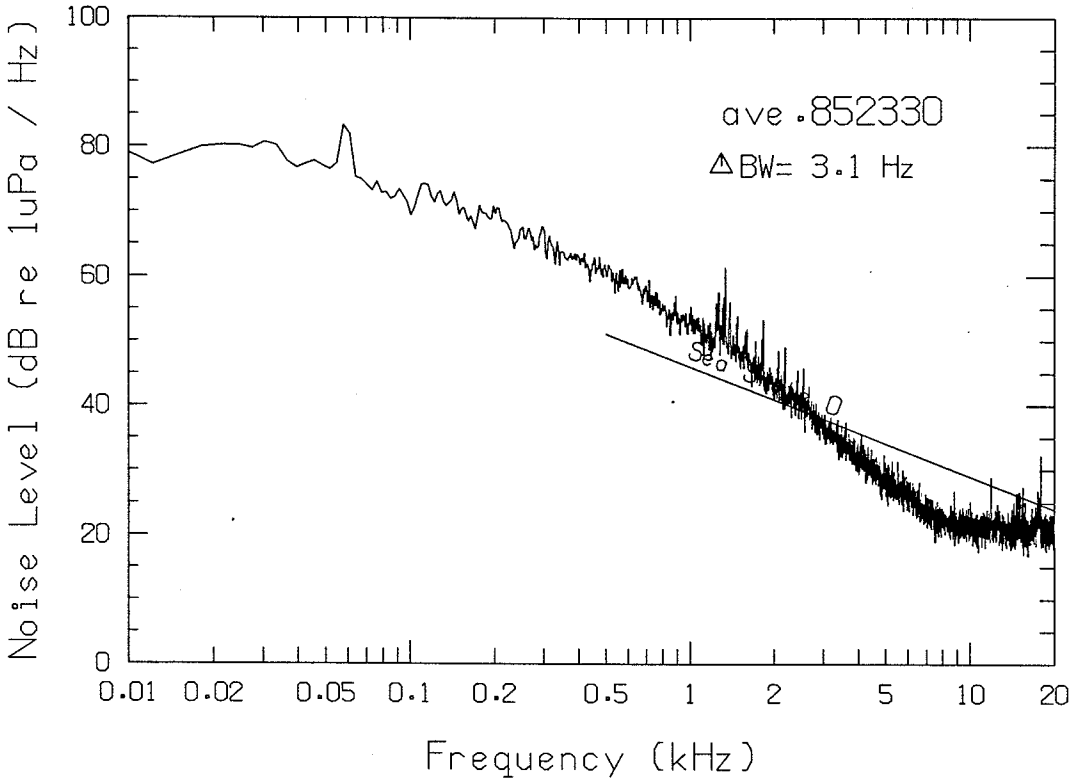
ave.852330
ΔBW= 3.1 Hz
Noise Level (dB re 1uPa / Hz)
Frequency (kHz)
100
80
60
40
20
0
0.01
0.02
0.05
0.1
0.2
0.5
1
2
5
10
20

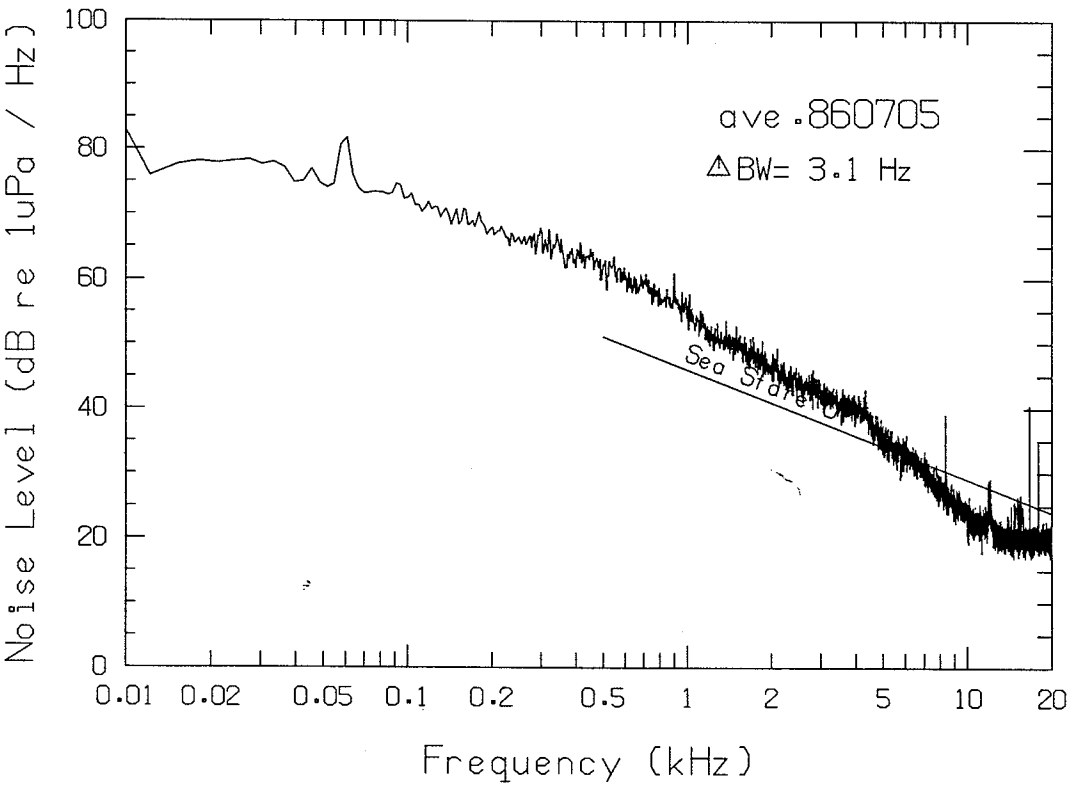
ave.860705
ΔBW= 3.1 Hz
Noise Level (dB re 1uPa / Hz)
Frequency (kHz)
100
80
60
40
20
0
0.01
0.02
0.05
0.1
0.2
0.5
1
2
5
10
20

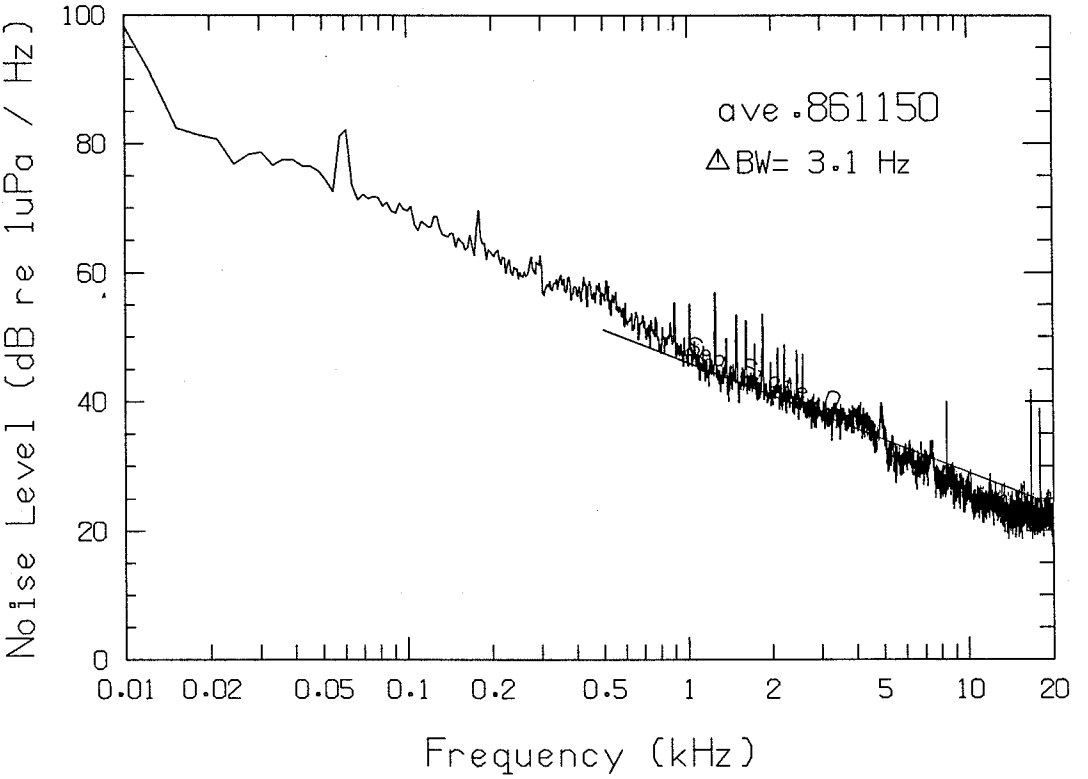
ave.861150
ΔBW= 3.1 Hz
Sea State 0
Noise Level (dB re 1uPa / Hz)
Frequency (kHz)
100
80
60
40
20
0
0.01
0.02
0.05
0.1
0.2
0.5
1
2
5
10
20

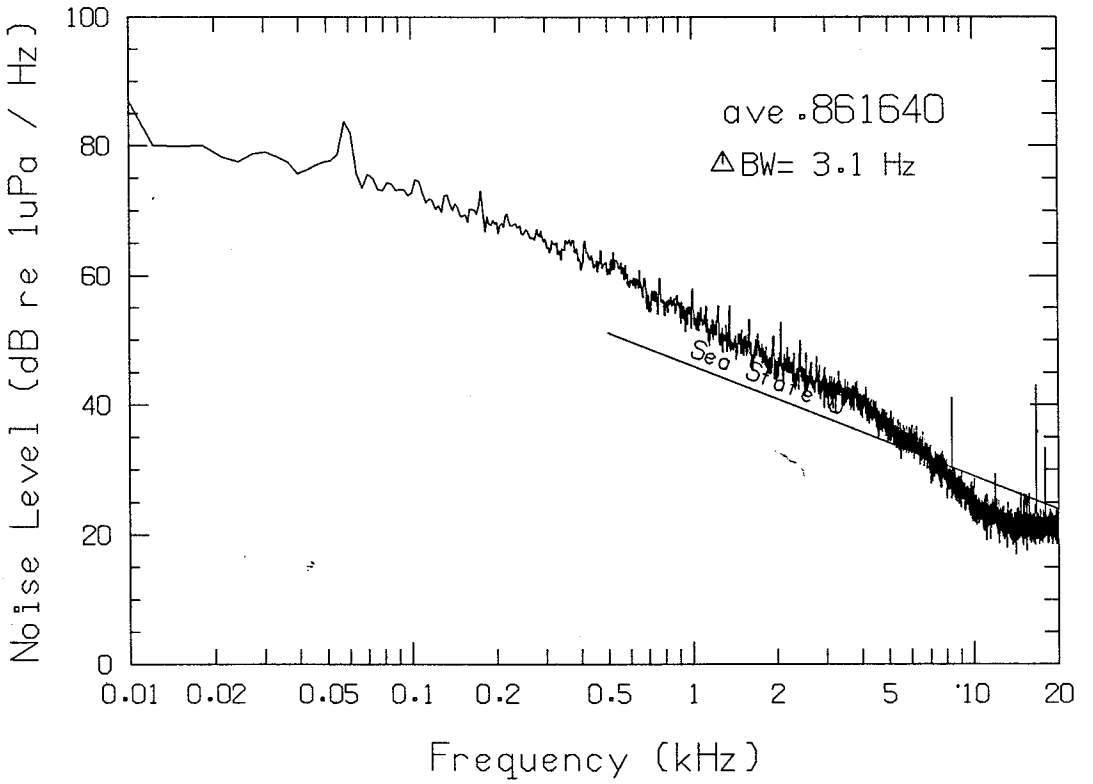
ave.861640
ΔBW= 3.1 Hz
Sea State 0
Noise Level (dB re 1uPa / Hz)
Frequency (kHz)
100
80
60
40
20
0
0.01
0.02
0.05
0.1
0.2
0.5
1
2
5
10
20

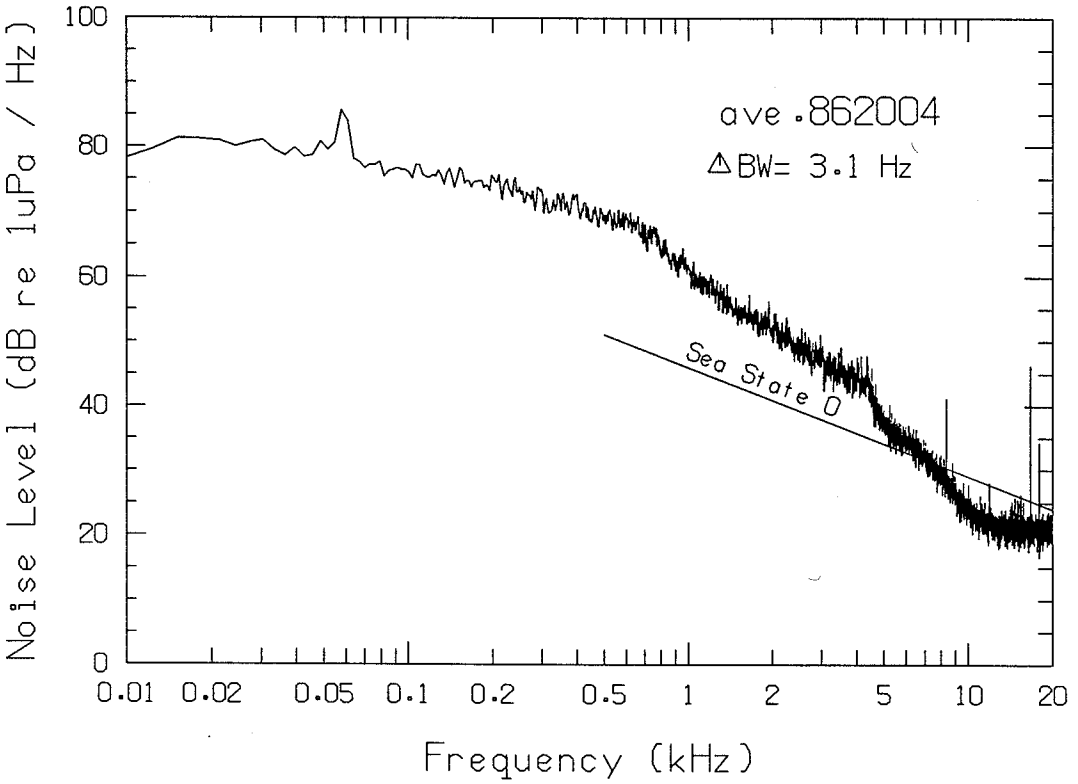
ave .862004
ΔBW= 3.1 Hz
Sea State 0
Noise Level (dB re 1uPa / Hz)
Frequency (kHz)
100
80
60
40
20
0
0.01
0.02
0.05
0.1
0.2
0.5
1
2
5
10
20

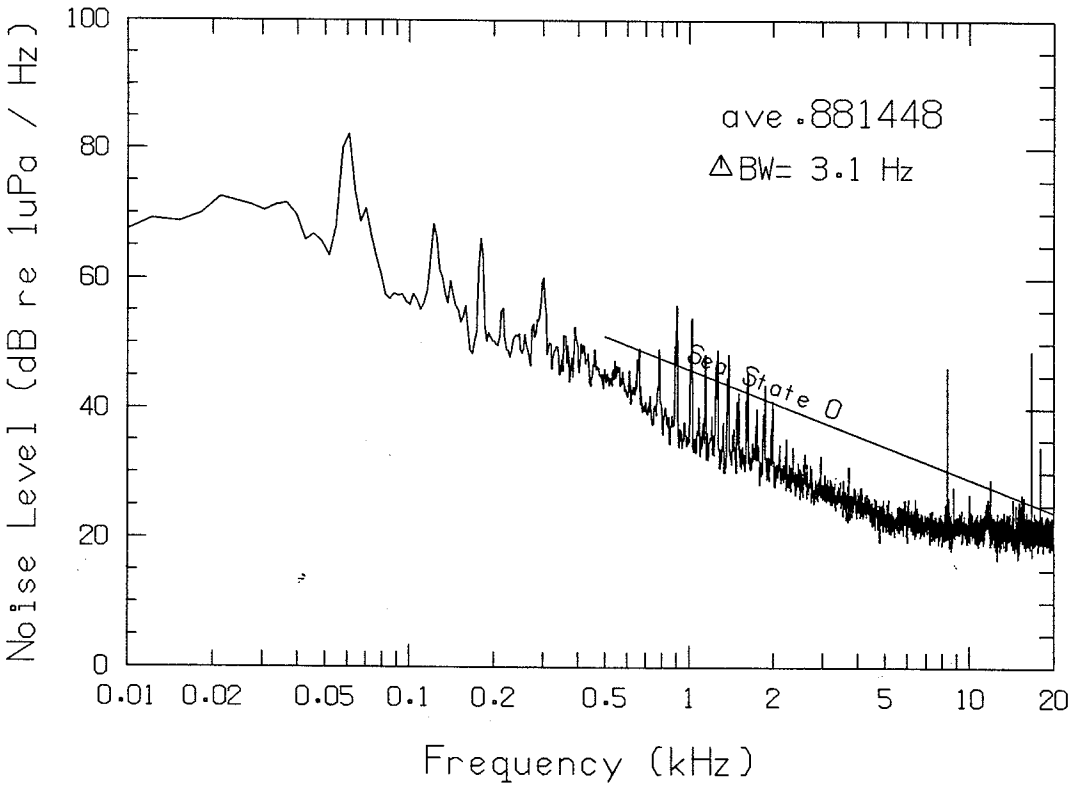
ave .881448
ΔBW= 3.1 Hz
Sea State 0
Noise Level (dB re 1uPa / Hz)
Frequency (kHz)
100
80
60
40
20
0
0.01
0.02
0.05
0.1
0.2
0.5
1
2
5
10
20

Distribution List for APL-UW TR9213

Office of the Chief of Naval Operations
Washington, DC 20350-2000

N872DL

Office of the Chief of Naval Research
800 N. Quincy St.
Arlington, VA 22217-5000

OCNR 1125AR (T. Curtin)

ONR Detachment
Stennis Space Center, MS 39529-7050

Code 124A2T (B. Wheatley)

Commanding Officer
Naval Polar Oceangraphy Center
Federal Bldg. #4
4301 Suitland Rd.
Washington, DC 20395-5180

Commander
Space and Naval Warfare Systems Command
Washington, DC 20363-5100

PMW 183-4 (G. Dreyer)

Commander
Naval Sea Systems Command
Washington, DC 20362

NSEA 06UR45 (H. Reichel)
PMO 402
PMO 406

Commander
Naval Undersea Warfare Center
Division Newport
Newport, RI 02840

Library
Code 22103 (C. Gardner)

Officer in Charge
New London Detachment
Naval Undersea Warfare Center
New London, CT 06320

Code 01Y (J. Donald)
Code 2113 (V. DiPalma)
Code 2122 (G. Kudlak)
Code 341 (C.G. Foster)

Commander
Naval Surface Warfare Center
White Oak Laboratory
Silver Spring, MD 20903-5000

Code R-43 (J. Scarzello)
Code U-13 (D. Keller)

Commander
Naval Command, Control and Ocean
Surveillance Center
Research and Development Division
San Diego, CA 92152-5019

Library
Code 541 (J. Newton)
Code 844 ((B. Sotirin)

Commander
Naval Undersea Warfare Center
Arctic Submarine Laboratory
San Diego, CA 92152-5019

Code 96 (CAPT B.B. Scott) (3 copies)
Code 963 (D. Bentley)

Commanding Officer
Naval Civil Engineering Laboratory
Port Hueneme, CA 93043-5003

Library

Director
Naval Research Laboratory
4555 Overlook Ave. SW
Washington, DC 20375

Code 5550 (E. Kennedy)

Commander
Naval Surface Warfare Center
Dahlgren Division
Coastal Systems Station
Panama City, FL 32407

Library

Commanding Officer
Naval Oceanographic Office
Stennis Space Center, MS 39522-5001

Code OAR (C. O'Neill)
Code OPS (M. Car)

Naval Research Laboratory Detachment
Stennis Space Center, MS 39529-5004

Code 240 (D. Ramsdale)
Code 242 (R. Meredith)

Commander
Naval Air Warfare Center
Aircraft Division
Warminster, PA 18974

Code 3031 (A. Horbach)

Commander
Naval Surface Warfare Center
Carderock Division
Bethesda, MD 20084-5000

Code 1720 (J. Baylis)
Code 1908 (S. Awwad)

Commanding Officer
Naval Submarine School
Box 70
Naval Submarine Base New London
Groton, CT 06340

Superintendent
Naval Postgraduate School
Monterey, CA 93943-5100

Library

Commander Submarine Force
U.S. Atlantic Fleet
Norfolk, VA 23511

Code 019 (D.T. Lewis)

Commander Submarine Force
U.S. Pacific Fleet
Pearl Harbor, HI 96860

N21
N3051 (B. Campbell)

Commander
Submarine Development Squadron TWELVE
Box 70
Naval Submarine Base New London
Groton, CT 06349-5200

N201 (CDR G.C. Thomas)

Commander Patrol Wing FIVE
NAS Brunswick
Brunswick, ME 04011

N3 (LCDR B. Prindle)

Director
Applied Research Laboratories
University of Texas at Austin
PO Box 8029
Austin, TX 78713-8029

Dr. J. Huckaby

Director
Applied Research Laboratory
The Pennsylvania State University
State College, PA 16801

F. Symons, Jr.
J. Kisenwether

Chief, British Naval Staff
PO Box 4855
Washington, DC 20008

CAPT F. Hiscock

U.S. Army Cold Regions Research &
Engineering Laboratory
72 Lyme Rd.
Hanover, NH 03755

W.B. Tucker

APL-UW

K. Aagaard
A. Brookes
W. Felton
E. Gough
F. Karig
J. Luby
R. Stein
T. Wen
K. Williams

REPORT DOCUMENTATION PAGE

Form Approved OMB No. 0704-0188

1a. REPORT SECURITY CLASSIFICATION Unclassified	1b. RESTRICTIVE MARKINGS
2a. SECURITY CLASSIFICATION AUTHORITY	3. DISTRIBUTION/AVAILABILITY OF REPORT Approved for public release. Distribution is unlimited.
2b. DECLASSIFICATION/DOWNGRADING SCHEDULE	
4. PERFORMING ORGANIZATION REPORT NUMBER(S) APL-UW TR 9213	5. MONITORING ORGANIZATION REPORT NUMBER(S)
6a. NAME OF PERFORMING ORGANIZATION Applied Physics Laboratory University of Washington 6b. OFFICE SYMBOL (*If applicable*)	7a. NAME OF MONITORING ORGANIZATION Arctic Submarine Laboratory Naval Undersea Warfare Center
6c. ADDRESS (*City, State, and ZIP Code*) 1013 N.E. 40th Street Seattle, WA 98105-6698	7b. ADDRESS (*City, State, and ZIP Code*) San Diego, CA 92152-5019
8a. NAME OF FUNDING/SPONSORING ORGANIZATION Various 8b. OFFICE SYMBOL (*If applicable*)	9. PROCUREMENT INSTRUMENT IDENTIFICATION NUMBER SPAWARSYSCOM N00039-91-C-0072
8c. ADDRESS (*City, State, and ZIP Code*)	10. SOURCE OF FUNDING NUMBERS PROGRAM ELEMENT NO. / PROJECT NO. / TASK NO. / WORK UNIT ACCESSION NO.

11. TITLE (*Include Security Classification*)
Environmental Measurements in the Beaufort Sea, Spring 1992

12. PERSONAL AUTHOR(S)
T. Wen, F. Karig, and W. Felton

13a. TYPE OF REPORT	13b. TIME COVERED	14. DATE OF REPORT (*Year, Month, Day*)	15. PAGE COUNT
Technical	FROM 3/92 TO 4/92	September 1992	93

16. SUPPLEMENTARY NOTATION
All the data presented are stored in digital format and available for further analysis.

17. COSATI CODES			18. SUBJECT TERMS (*Continue on reverse if necessary and identify by block number*)		
FIELD	GROUP	SUB-GROUP			
68	03		Arctic	Sea ice properties	Weather
			Beaufort Sea	Floe drift	Ambient noise
20	01		Currents	STD profiles	

19. ABSTRACT (*Continue on reverse if necessary and identify by block number*)

This report presents environmental and underwater ambient noise data obtained by the Applied Physics Laboratory of the University of Washington (APL-UW) and the Arctic Submarine Laboratory of the Naval Undersea Warfare Center (ASL/NUWC) at APLIS 92, an ice camp established in the Beaufort Sea in spring 1992 to support Navy-sponsored tests and research during ICEX1-92. The purpose of the report is to provide field data to ice camp participants, so data analysis is limited here. The data were collected to document the meteorological and oceanographic conditions that existed during camp activities. The main data sets are weather, floe drift, STD profiles, currents, ice properties, and underwater ambient noise.

20. DISTRIBUTION/AVAILABILITY OF ABSTRACT ☐ UNCLASSIFIED/UNLIMITED ☒ SAME AS RPT. ☐ DTIC USERS	21. ABSTRACT SECURITY CLASSIFICATION Unclassified
22a. NAME OF RESPONSIBLE INDIVIDUAL Capt. B.B. Scott	22b. TELEPHONE (*Include Area Code*) (619) 553-0190 22c. OFFICE SYMBOL Code 96